

Toward a better quantification of orientations and magnitudes of past crustal stresses : insights from calcite twinning paleopiezometry and comparison with present-day stresses

Professor Olivier LACOMBE

Why to characterize stresses in the crust ?

The motivation arises :

from applied geological purposes, such as geological hazards, engineering activities and resource exploration;

and

from fundamental geological purposes, such as understanding the mechanical behaviour of geological materials and deciphering various tectonic mechanisms, from those related to plate motions at a large scale to those causing jointing and faulting or even microstructures at a smaller scale.

Despite an increasing number of in situ stress measurements, magnitudes of crustal stresses remain poorly constrained...

Twinning of minerals depends on the magnitude of the shear stress which has been applied to them.

One can make use of this property to evaluate the magnitudes of stresses which have been supported by a rock during its history.

An access to paleostress magnitudes in the upper crust : Calcite twinning paleopiezometry

In the upper part of the crust, brittle deformation of carbonate rocks is accompanied by pressure-solution, porosity reduction and crystalline deformation.

Deformation of calcite grains reflects the brittle-to-ductile transition.

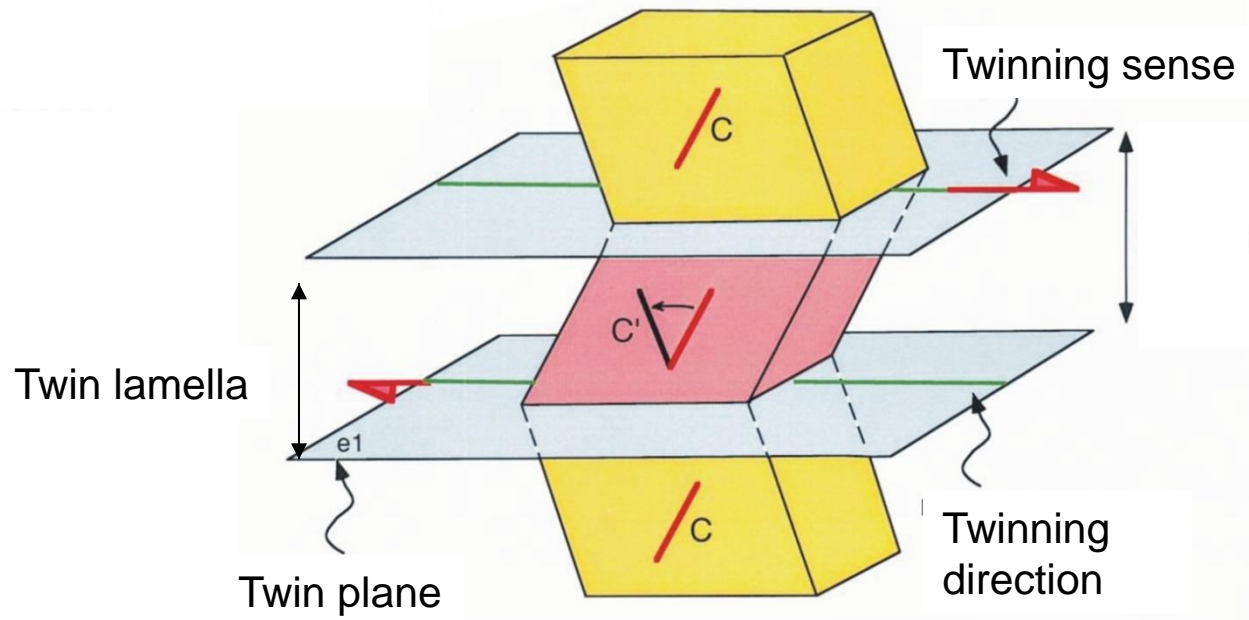
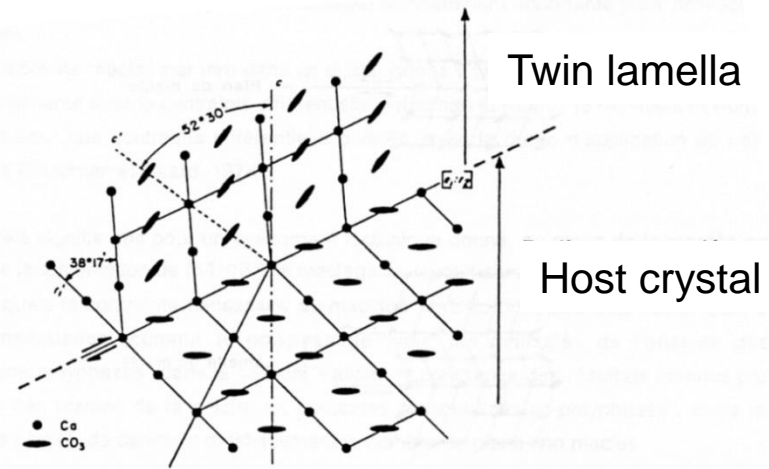
This low-temperature (0-300°) plasticity corresponds to the prevalence of e-twinning {10-12}, which is more easily activated at low temperature than other gliding systems, so that in most deformed limestones, e-twins are the dominant microstructures in calcite crystals.

How to constrain both orientations
and magnitudes of past stresses :

calcite twinning paleopiezometry

Geometry and significance of calcite twins

Twinning ~ simple shearing in a particular sense and direction along e-planes {01-12}



A twin is a polycrystalline association formed by the juxtaposition of two homogeneous parts, or more, of a single crystalline species, oriented one with respect each other following well-specified laws.

This very general law is applicable to growth twins and mechanical twins, among others.

The composition plane along which twinning occurs is a plane of high atomic density that separates the twinned portion of the crystal from the host (untwinned) part. The twin plane is the plane that belongs to both portions : it is the equivalent of the shear plane if one considers that a twin lamella results from simple shearing of the crystal.

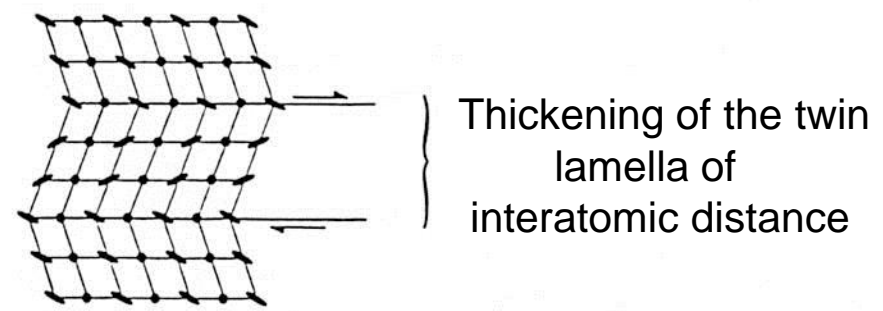
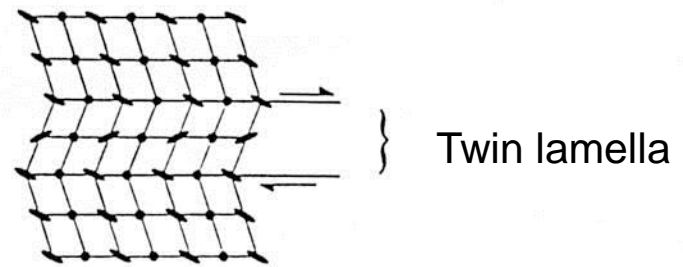
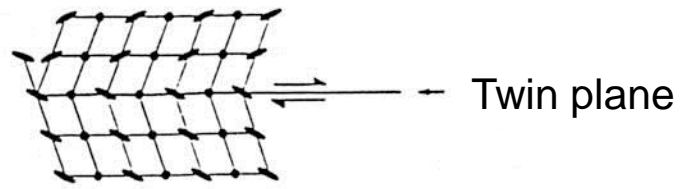
The twinning direction is the « gliding » direction : this is the line that connects an atom before twinning to the same atom after twinning; it belongs to the twin plane.

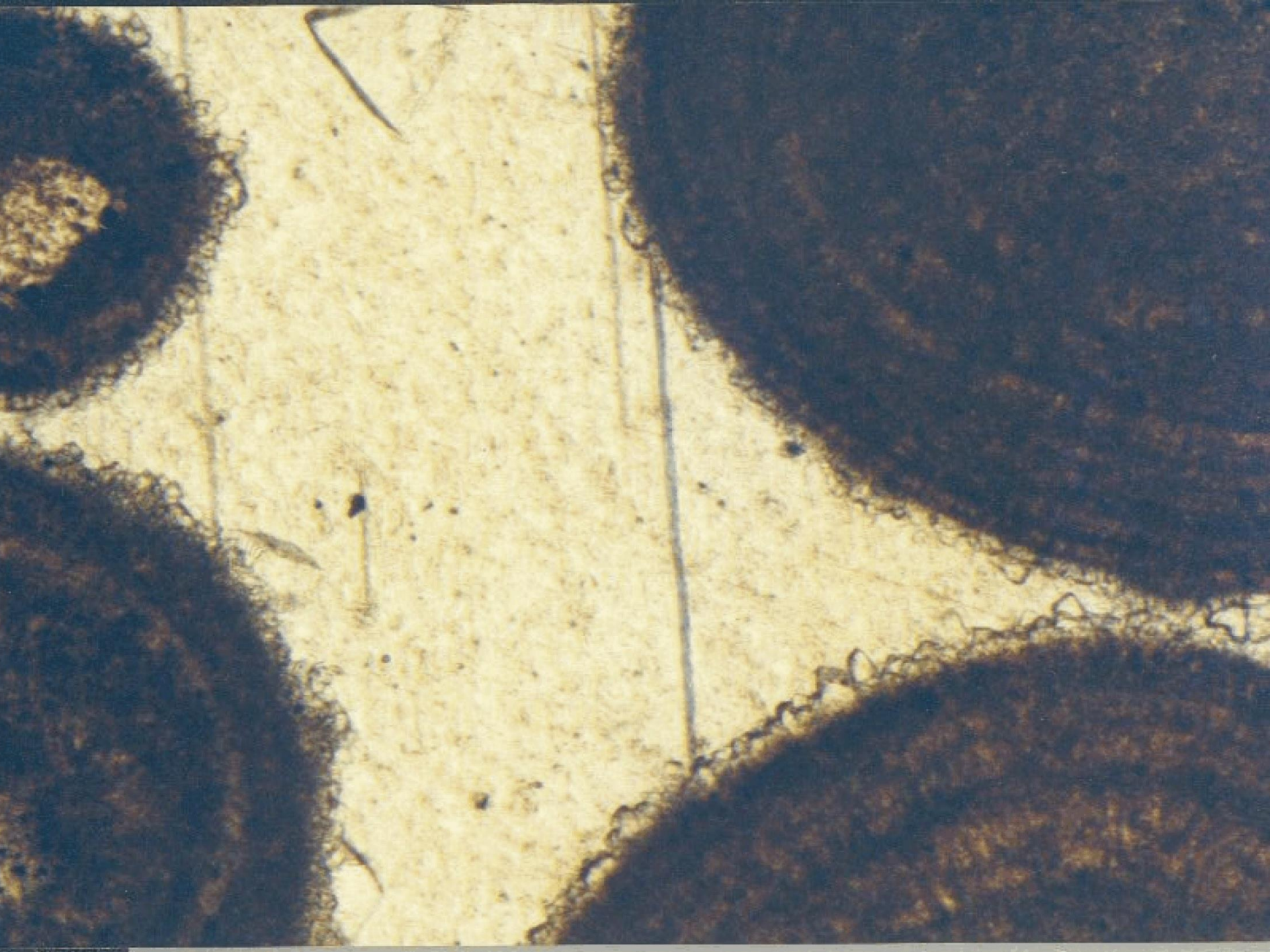
The orientation of the twinned portion of the crystal can be deduced from the orientation of the host crystal by a rotation that accounts for the geometry of the lattice. However, this rotation is virtual and by no means corresponds to the physical mechanism of twinning.

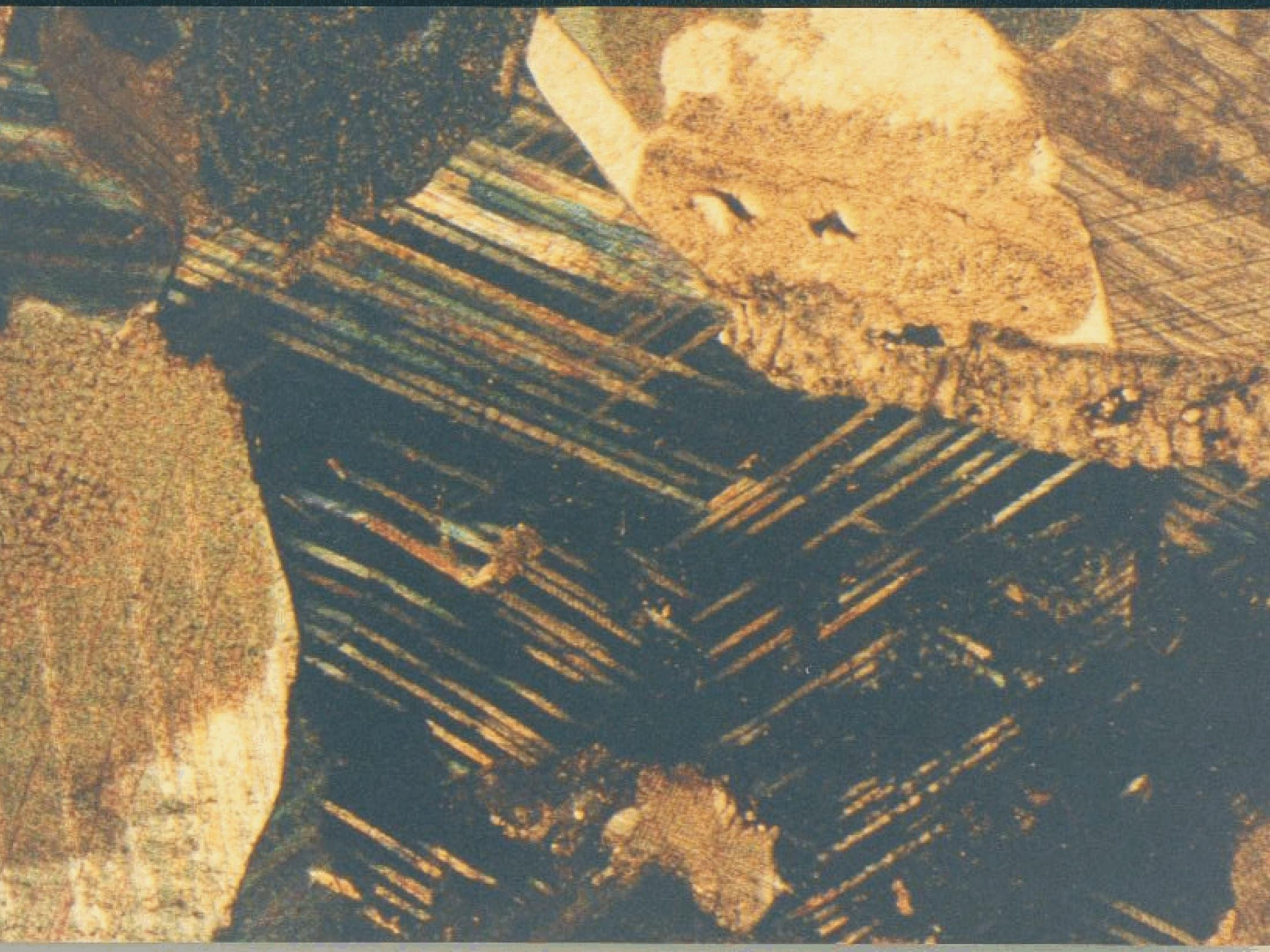
« Translation gliding » (r , f in calcite for example) reflects the macroscopic motion of an edge dislocation along the gliding plane; the host crystal is « simply sheared ».

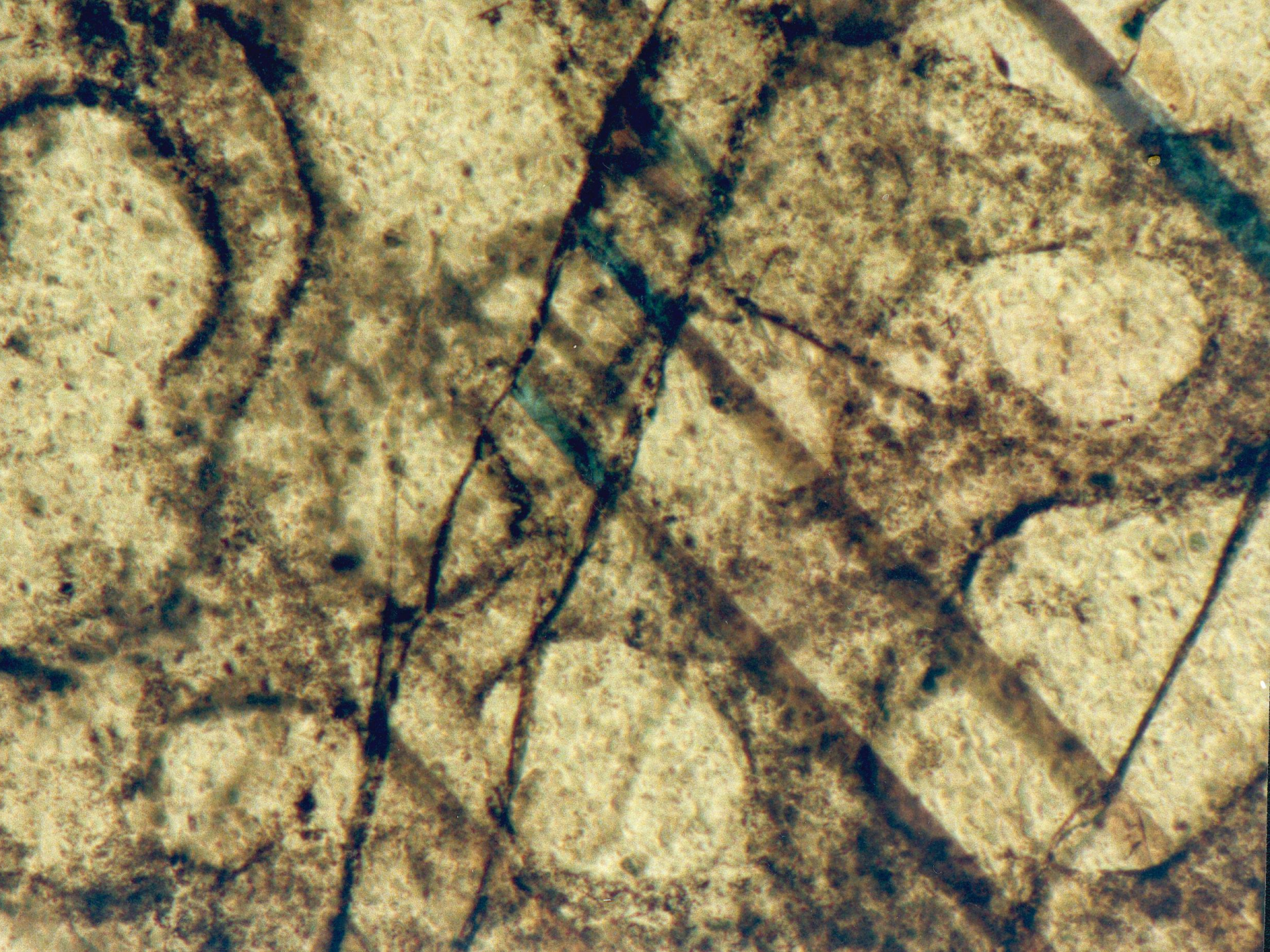
« Twinning » (e in calcite) can also be described as geometrically analogue of simple shearing of the crystal lattice along the twin plane, but it differs from gliding because :

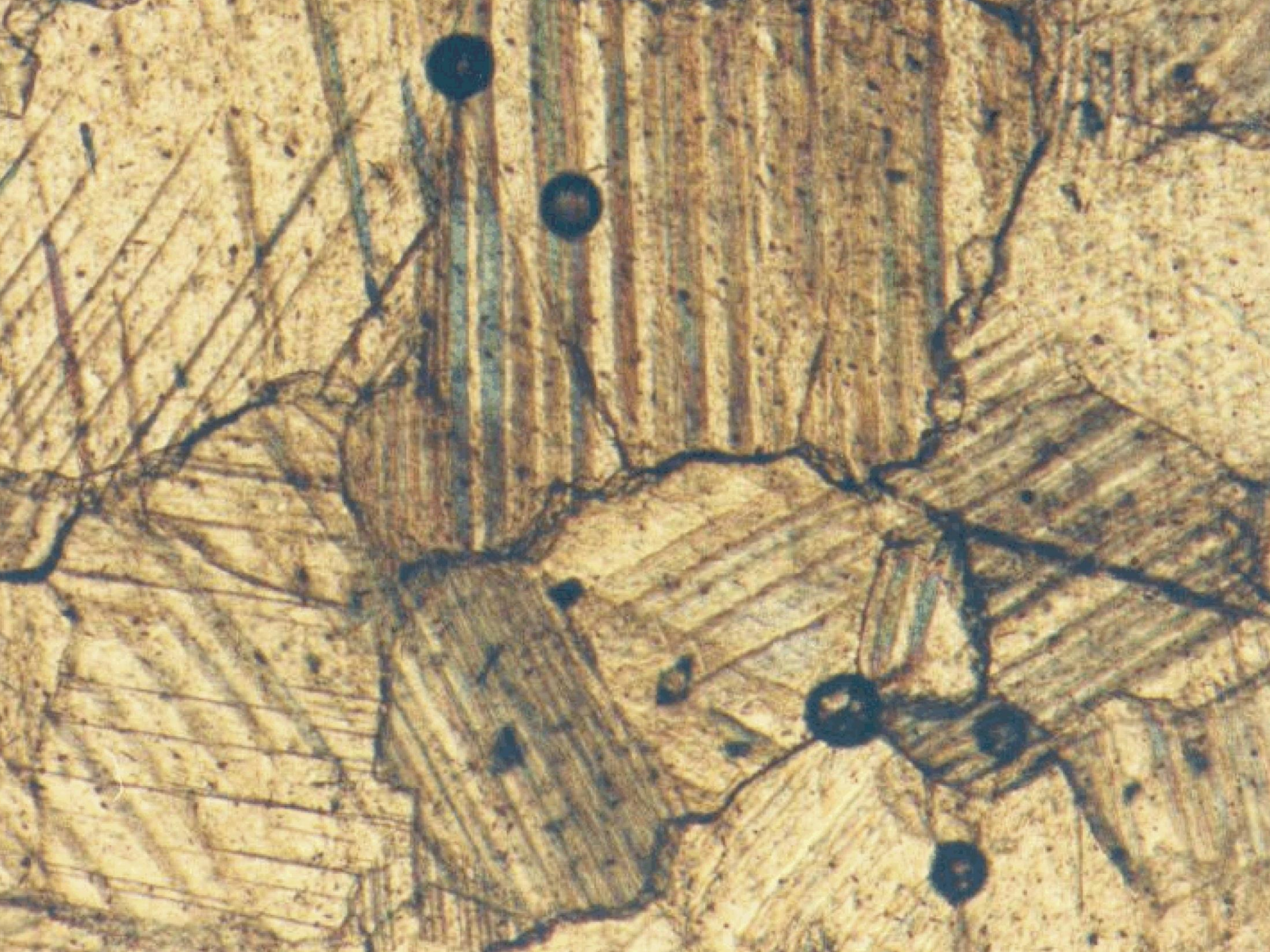
- (1) Twinning is "homogeneous", i.e., each plane of the lattice is displaced by the same quantity with respect to the « above » plane
- (2) The twinned portion is the mirrored part of the host crystal across the twin plane, which reflects the motion of a screw dislocation across the crystal lattice. In addition, the amount of strain accommodated by twinning is constant for a given twinning law.

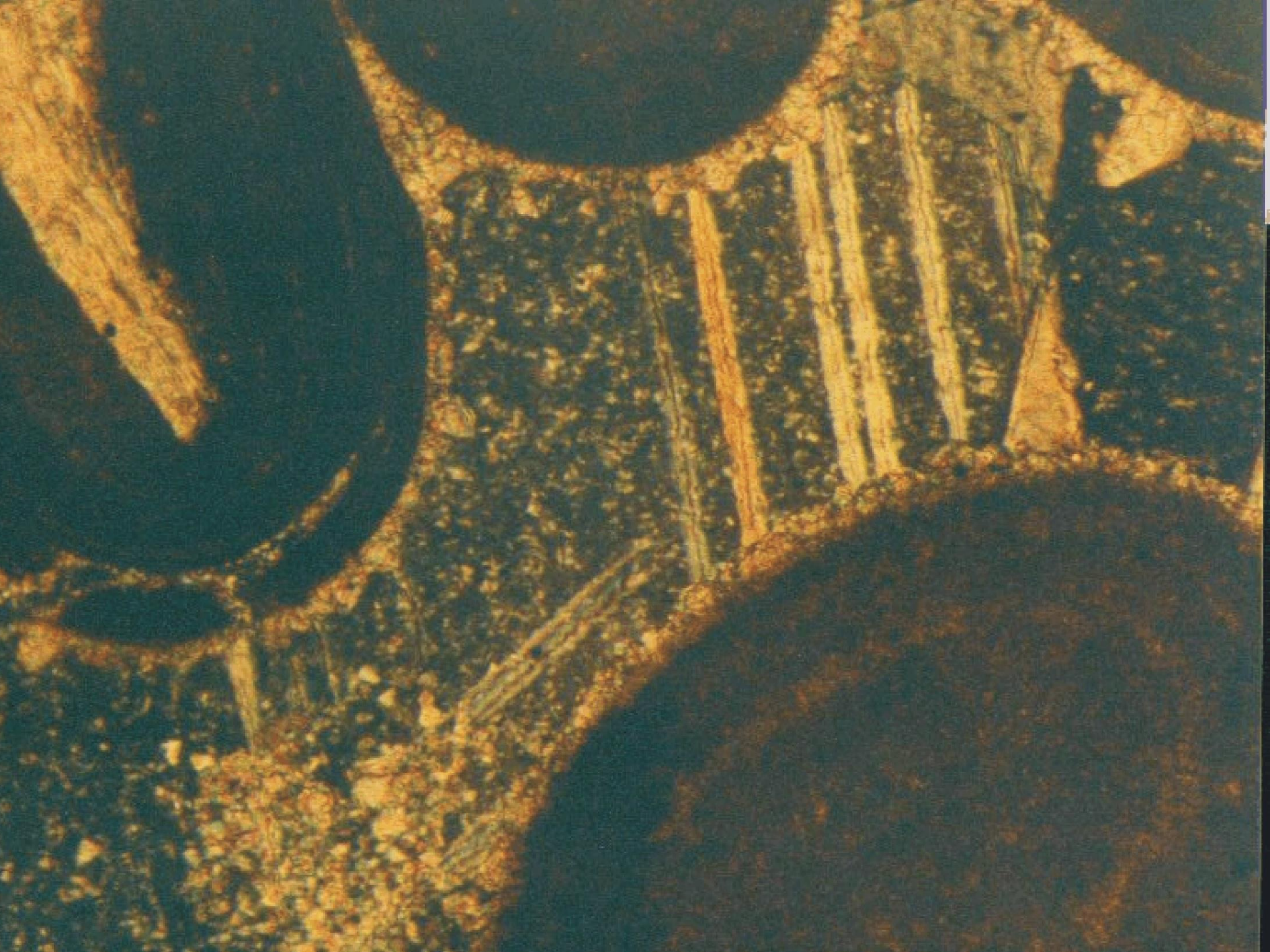


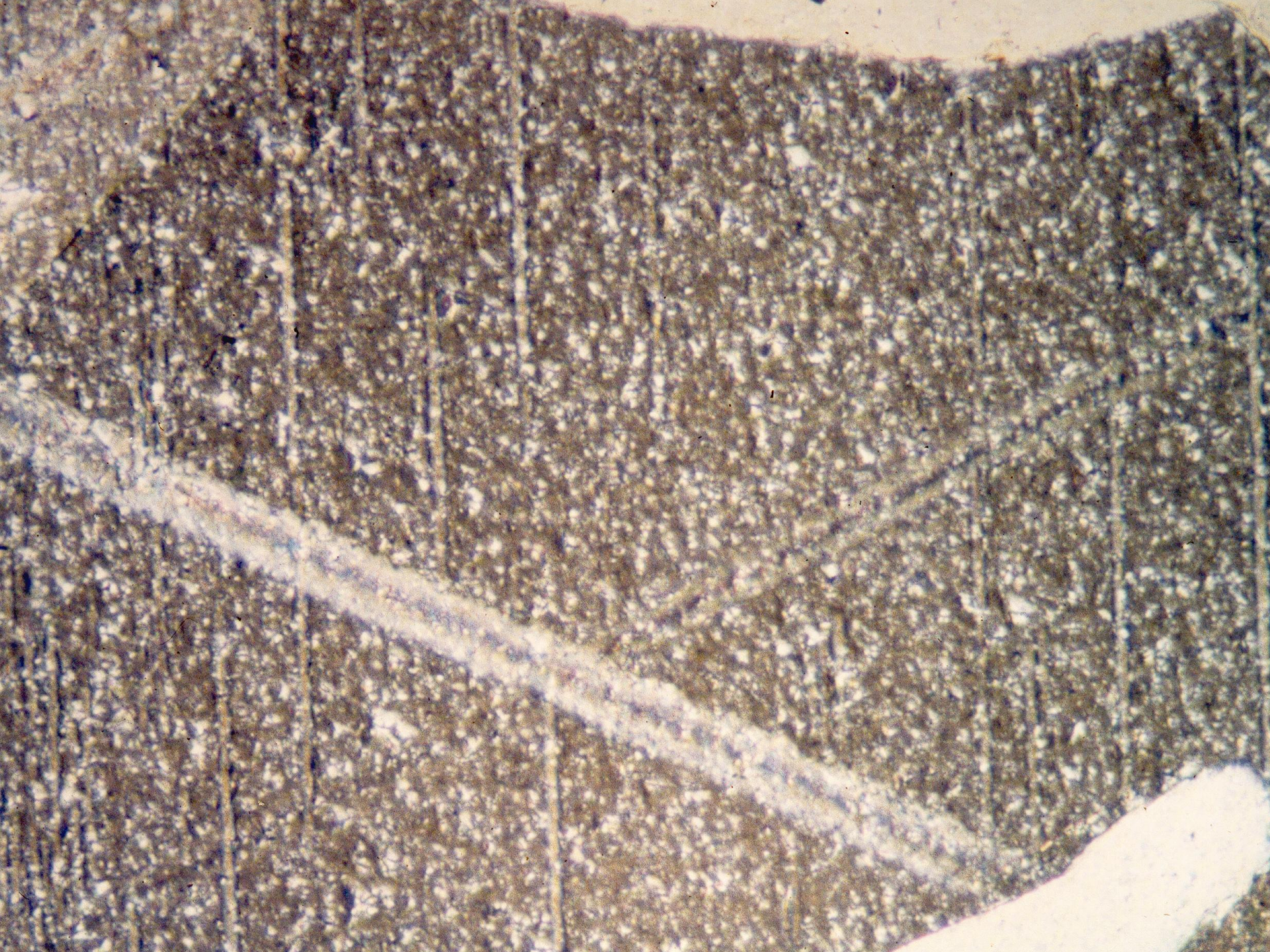


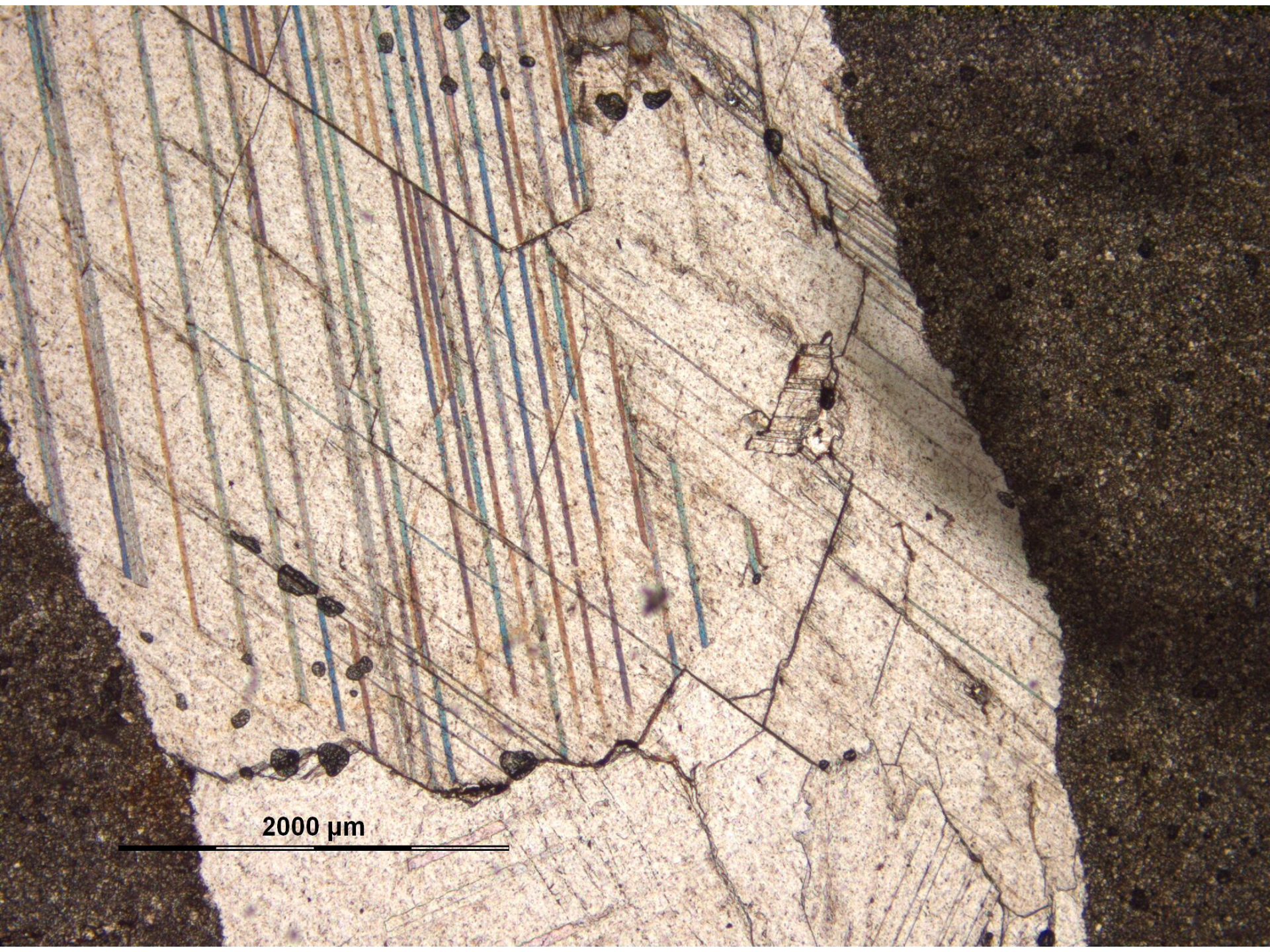




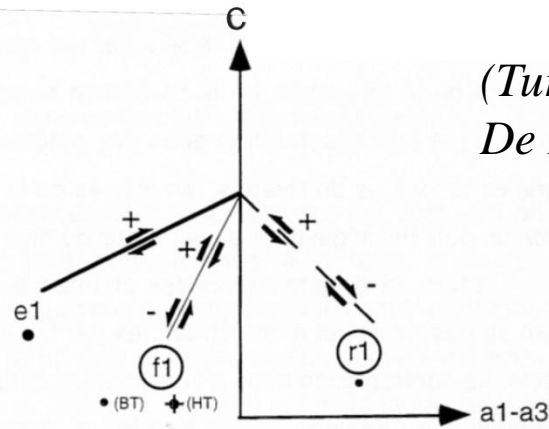
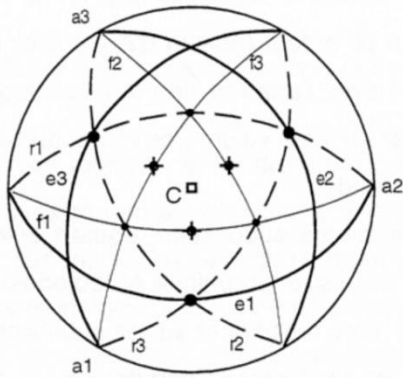






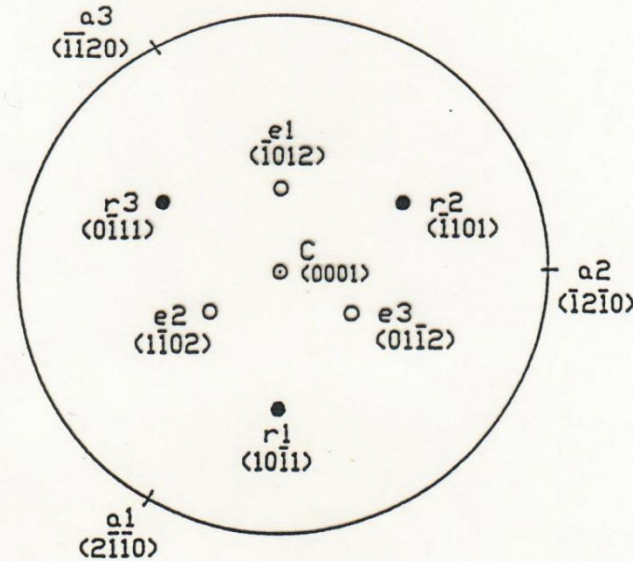
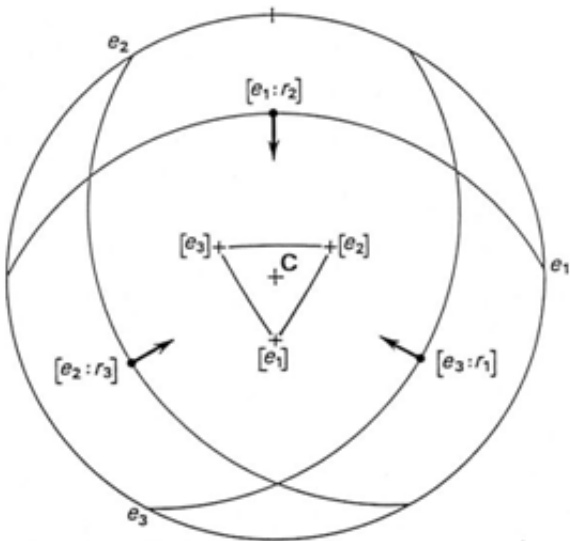


2000 μm

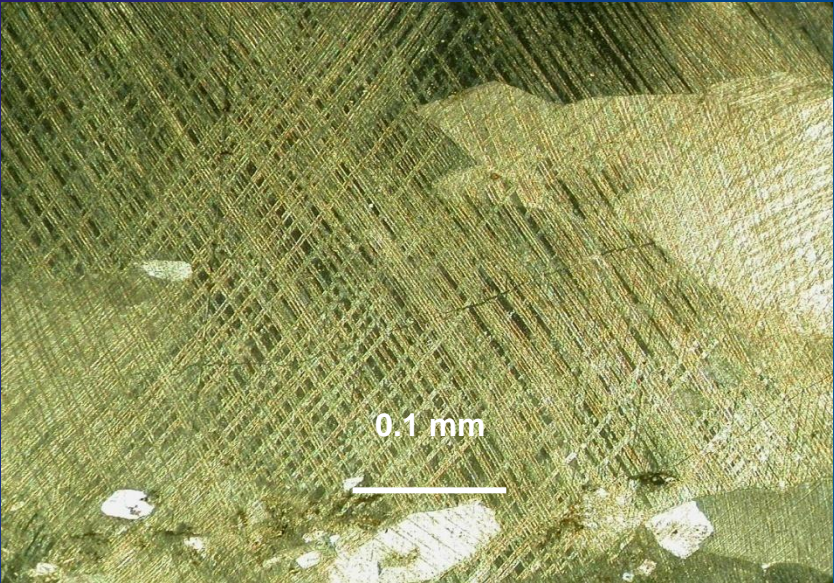
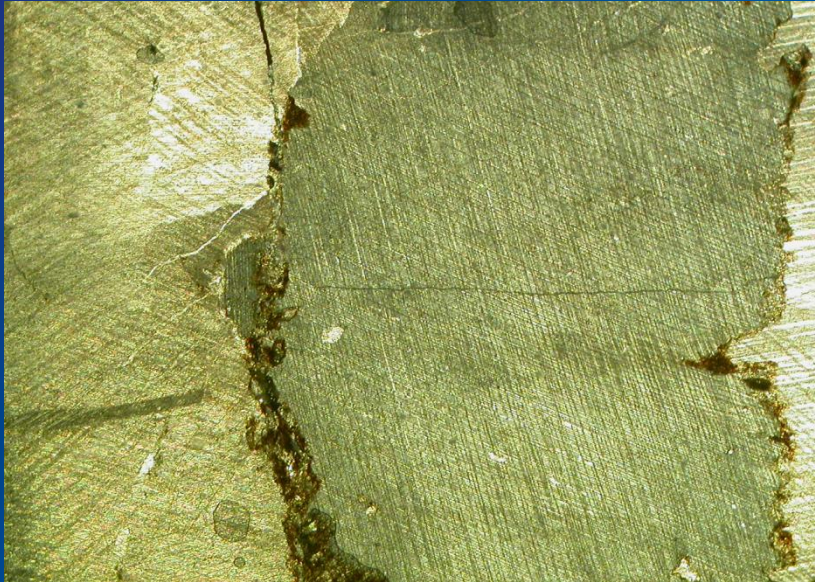
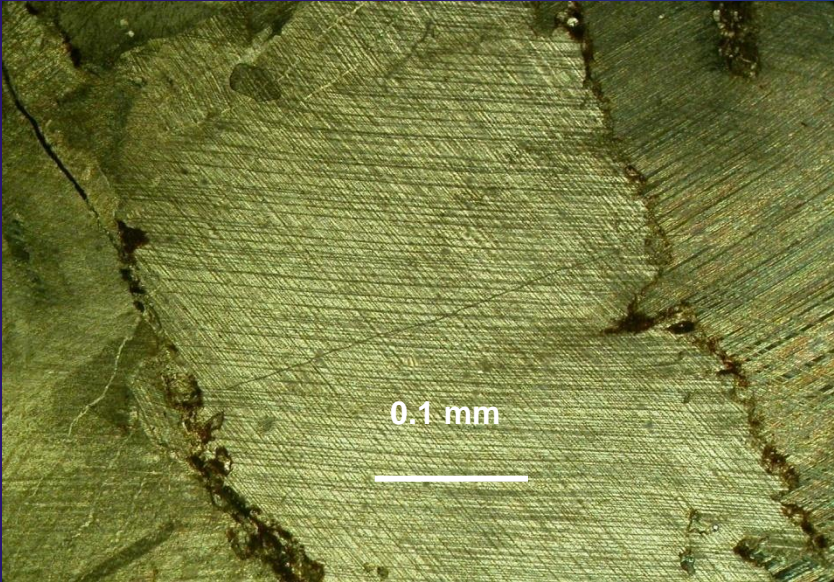


(Turner and Weiss, 1976;
De Bresser et al., 1997)

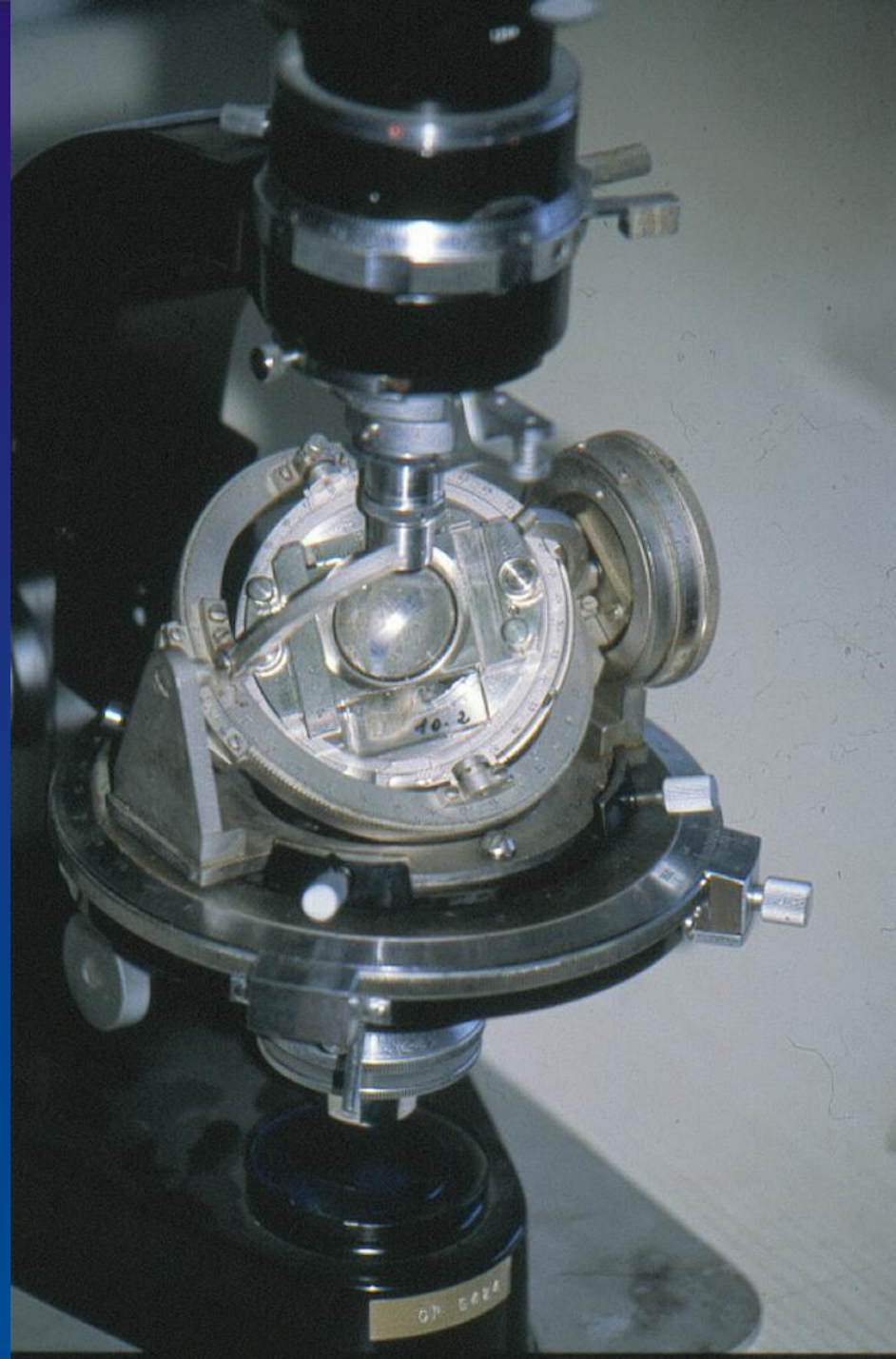
e-twinning and r, f-gilding systems in calcite

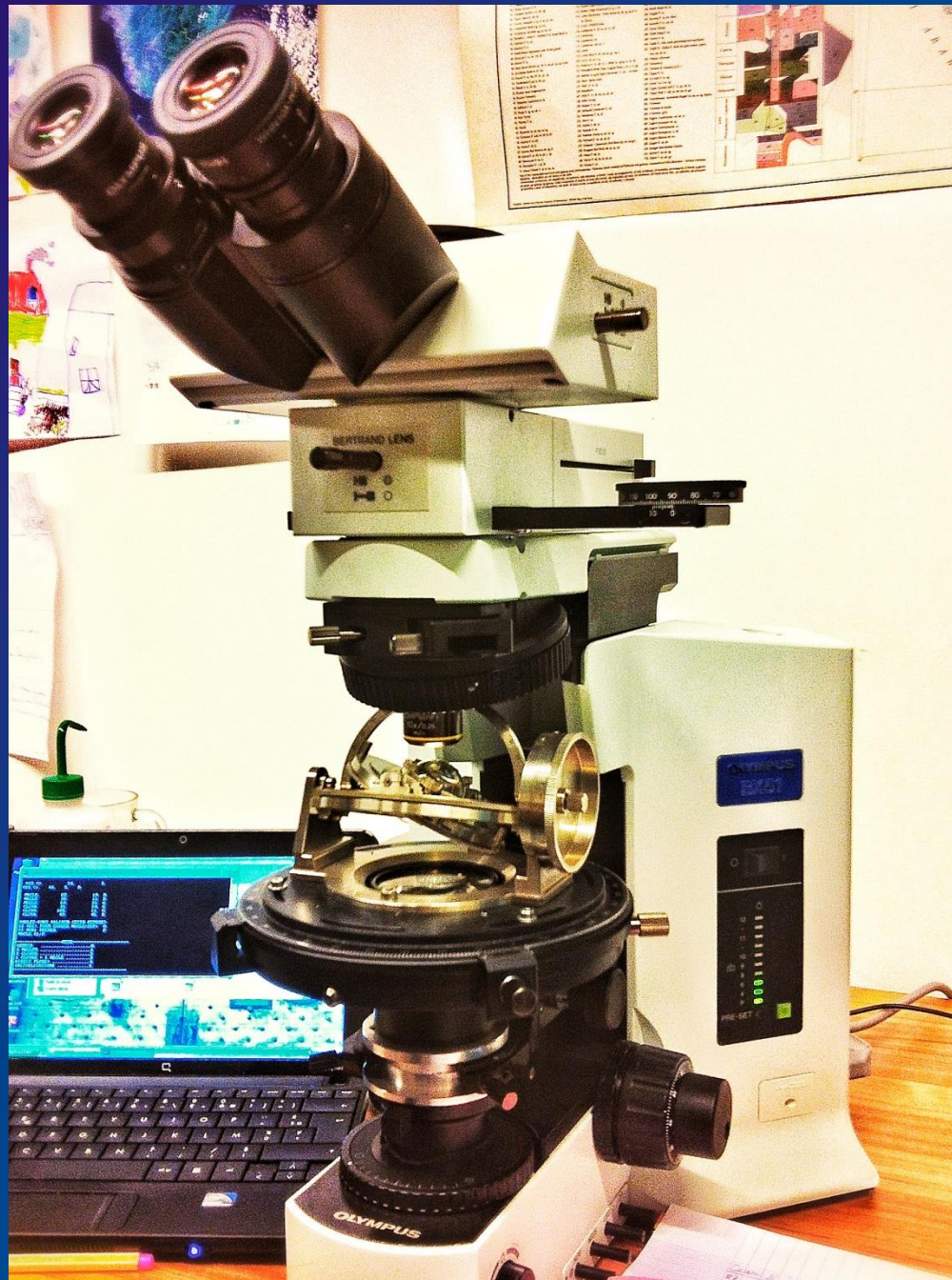


C, e_i	$= 26,5^\circ$
e_i, e_j	$= 44,5^\circ$
e_i, r_i	$= 71,5^\circ$
e_i, r_j	$= 37,5^\circ$
r_i, r_j	$= 75^\circ$
C, r_i	$= 44,5^\circ$









CRYSTAL

YES

Twinned

NO

Visible twin lamellae

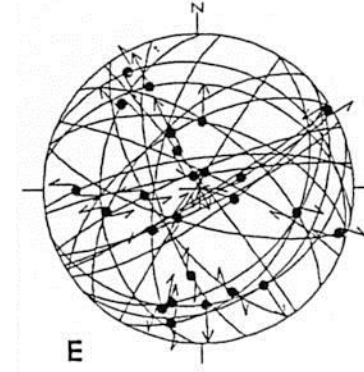
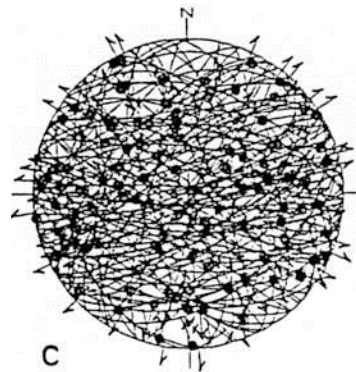
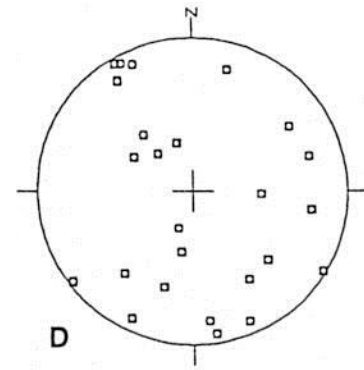
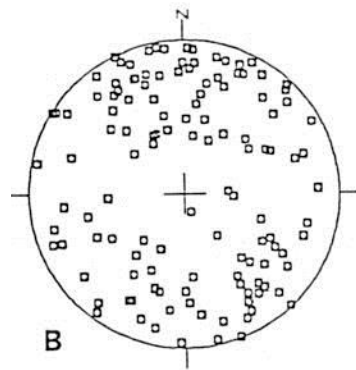
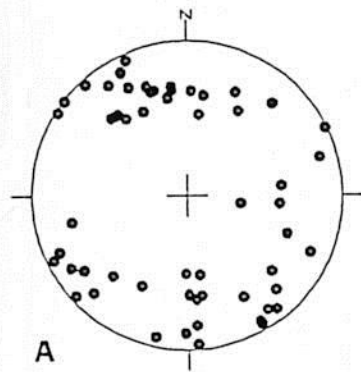
Non visible twin lamellae

Direct measurement

Indirect measurement

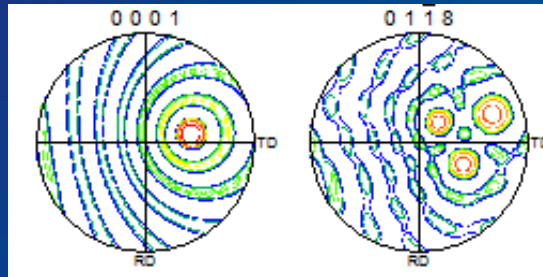
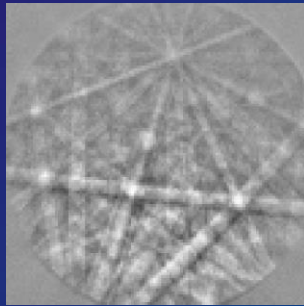
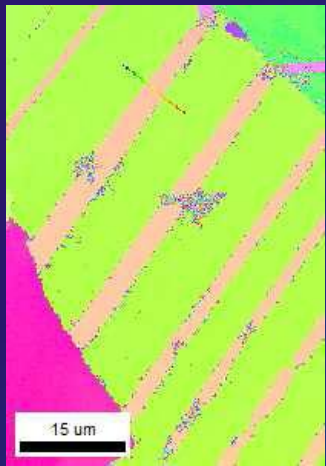
Spatial orientations of about 270 planes,
twinned and untwinned

The data...

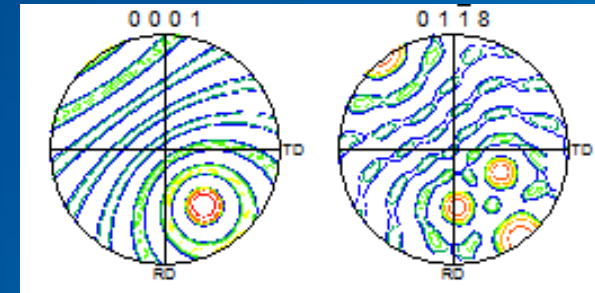


Among the on-going improvements

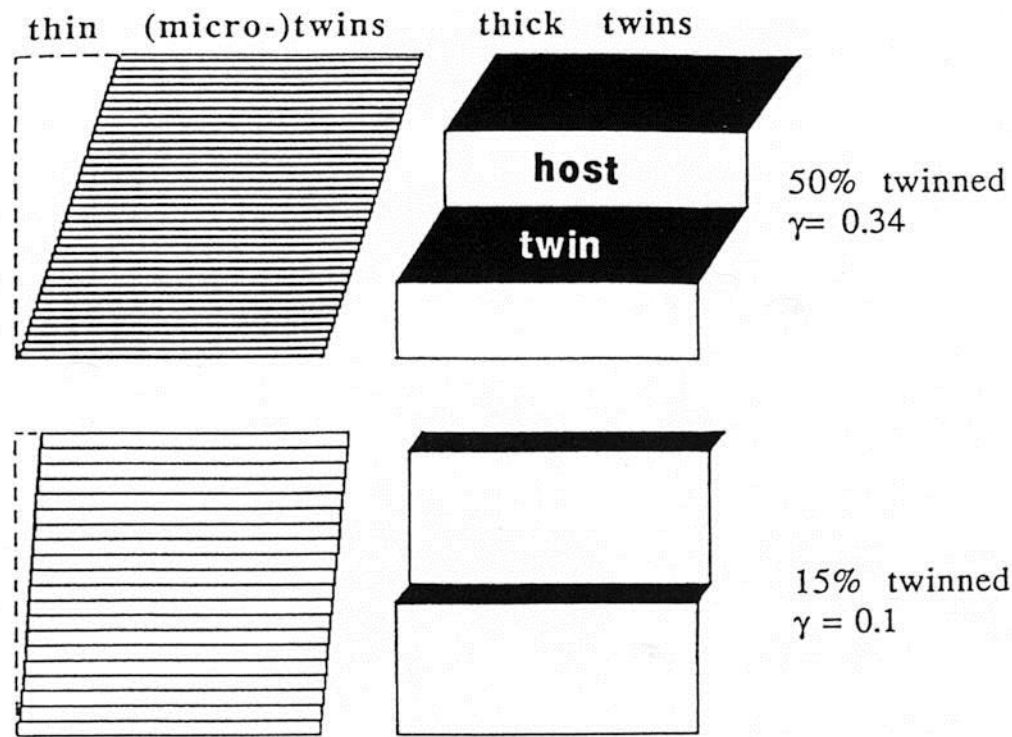
Automatic data acquisition using EBSD



Host crystal

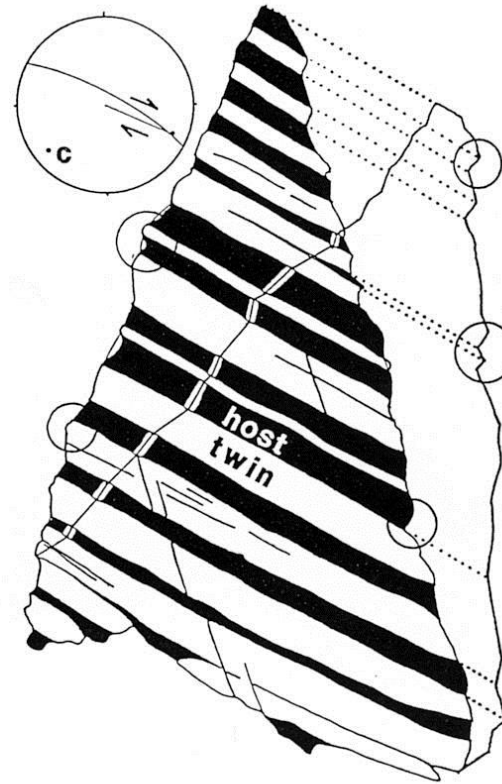


Twin lamella



Schematic diagram illustrating the difference between thin and thick twins, twin density (number of twins per mm) and percentage volume fraction of twin lamellae. In both cases, exactly the same amount of shearing by 15% ($\gamma=0.1$) and 50% ($\gamma=0.34$) twinning respectively is distributed either relatively homogeneously into many thin twins or just a few thick ones - the latter case is leading to very inhomogeneous deformation and causes larger steps in the grain boundary.

(Burkhard, 1993)

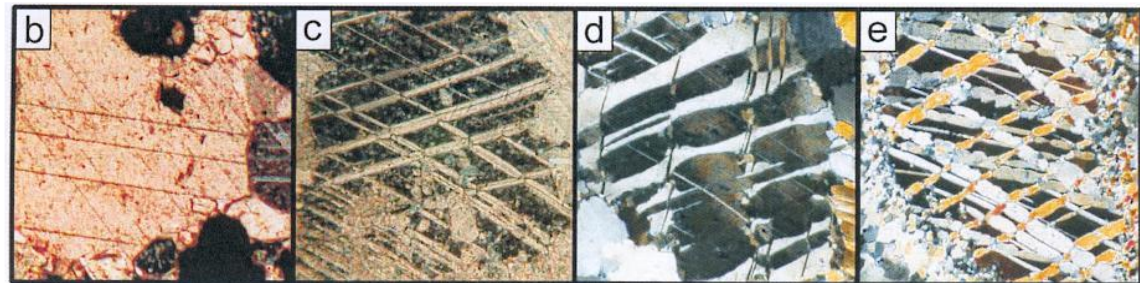


(Burkhard, 1993)

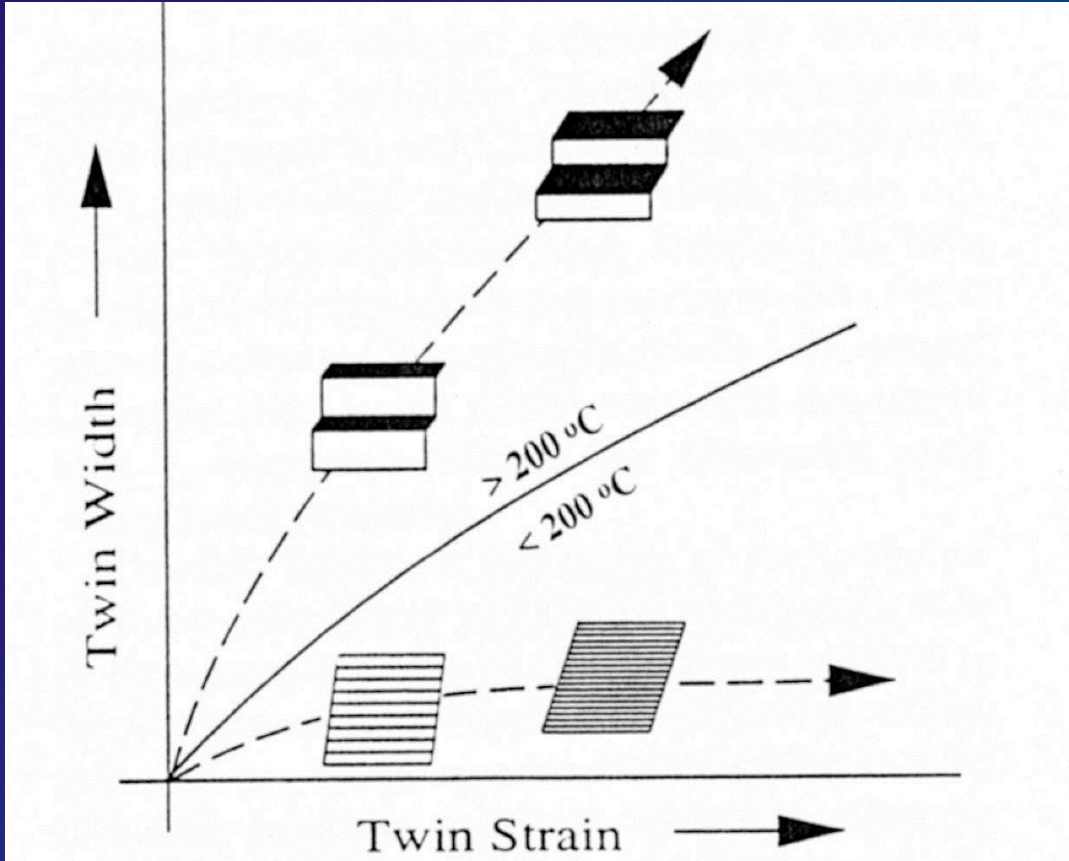
Natural example of a calcite grain, considerably deformed by twinning on a single set of thick twins (drawn after microphotograph). Twins (white) are identified as such by their slight lense shaped constriction toward the grain boundary. The calcite grain is graphically retrodeformed into its presumed original shape. Very angular steps in both actual and retrodeformed grain boundary are circled. Such steps are a consequence of twinning deformation and their impingement (on the left hand side) requires pressure solution/crystallisation deformation along the grain boundary in order to prevent the formation of voids. Stereogram in the upper left hand corner shows the crystallographic orientation of c-axis of host, e-lamellae (great circle) and inferred shear direction.

	type I	type II	type III	type IV
Geometry	-thin	-thick ($\gg 1\mu\text{m}$)	-curved twins	-thick, patchy
Description	-straight -rational	-straight -slightly lens-shaped -rational	-twins in twins -irrational -completely twinned	-sutured boundaries -trails of tiny grains -irrational
Interpretations	-little deformation -little cover -low temperature -(post-metamorphic) -(late tectonic)	-considerable def. -completely twinned grains are possible -syn- or post- metamorphic	-large deformation. -intracrystalline def. mechanisms e.g. (r- & f-glide) -syn-metamorphic deformation.	-large deformation -recrystallization (grain boundary migration) -pre- or syn- metamorphic
Temperature	< 200°C	150-300°C	> 200°C	>250°C

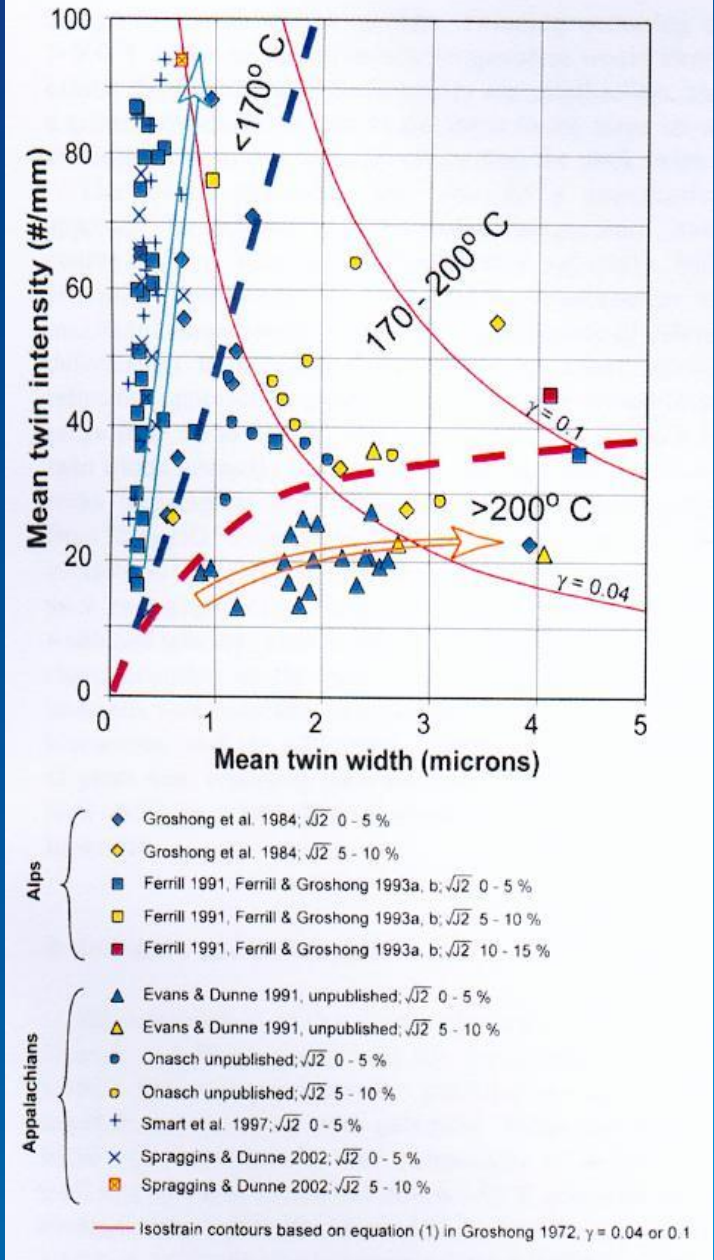

Increasing temperature



(Burkhard, 1993;
Ferrill et al., 2004)



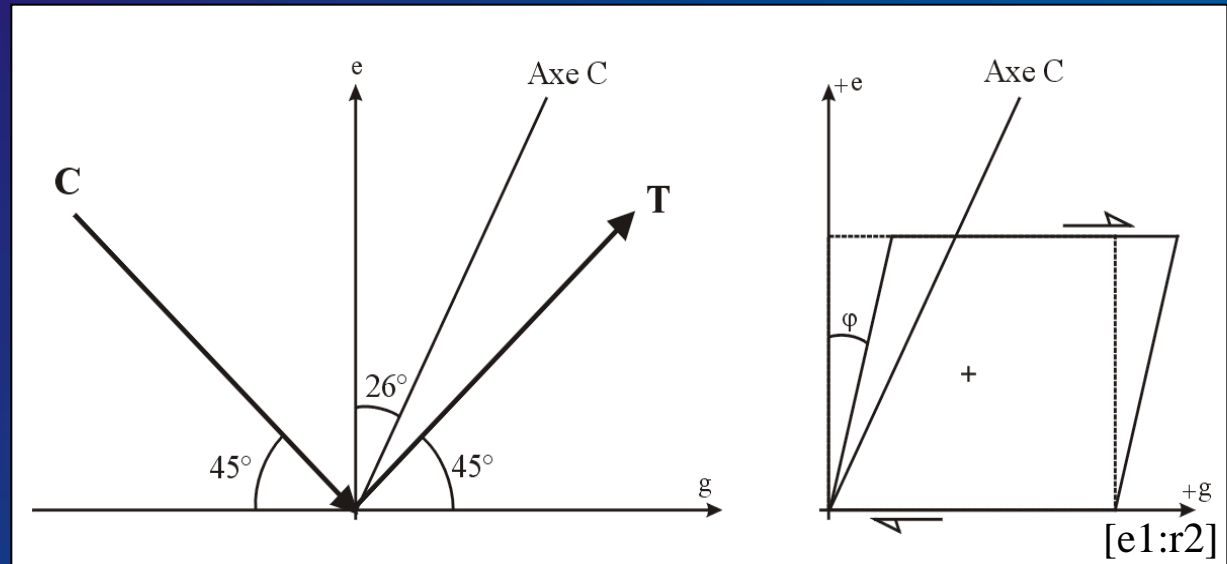
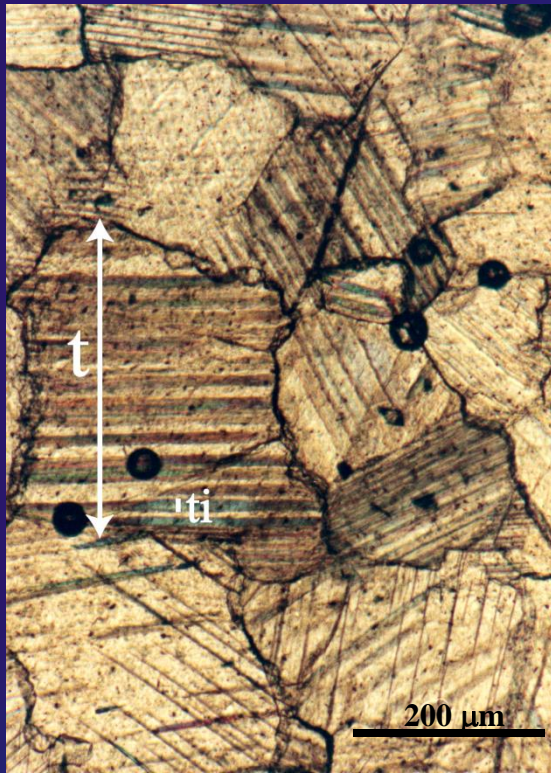
(Ferrill, 1998)



(Ferrill et al., 2004)

**Stress and strain analysis of calcite twinning :
The 'historical' techniques**

Groshong (1974, 1984) : determination of the strain tensor by twinning



$$\Gamma_{eg} = \frac{1}{2} \cdot \tan \varphi = \frac{0.347}{t} \cdot \sum_{i=1}^n t_i$$

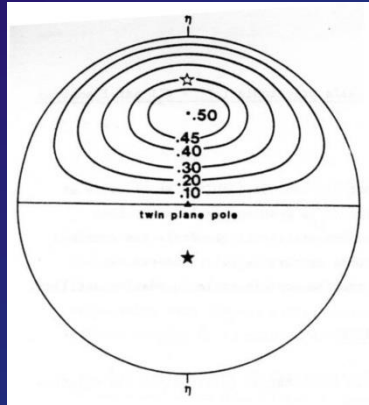
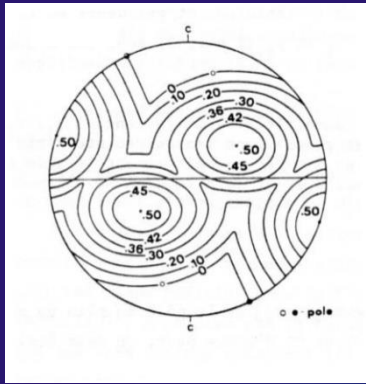
Deformation
by shearing
for a twin set

$\Gamma_{eg} = (lelg - neng) \epsilon_x + (memg - neng) \epsilon_y + (lemg + melg) \Gamma_{xy} + (men_g + nemg) \Gamma_{yz} + (nelg + leng) \Gamma_{zx}$,
with ϵ_x , ϵ_y , Γ_{yz} , Γ_{xy} and Γ_{zx} being the components of the strain tensor in (x,y,z) and le , me , ne
and lg , mg , ng the direction cosines of e and g in (x,y,z). $\epsilon_z = -(\epsilon_x + \epsilon_y)$ assuming $\Delta V = 0$

Limitations :

- time consuming
- finite strain tensor by twinning only
- significance of finite strain tensor in case of polyphase tectonics ?

Jamison and Spang (1976) :
determination of differential stress magnitudes



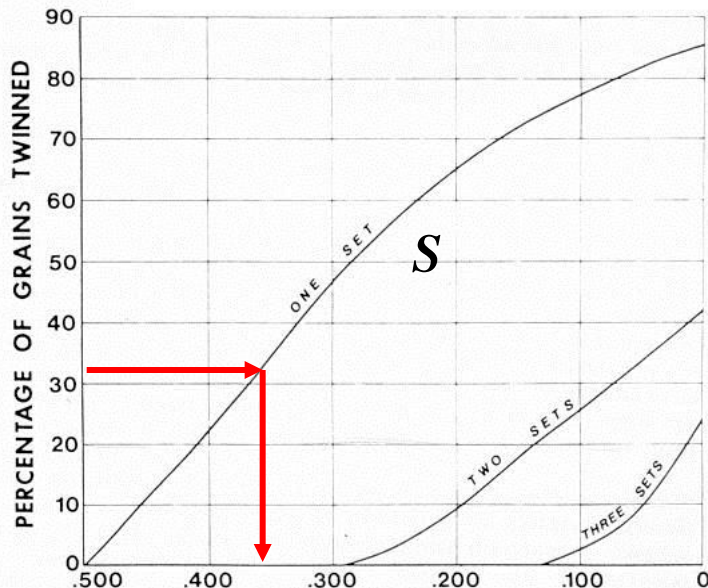
$$\tau_s = \Delta\sigma \cdot S$$



if τ_c is known, $\Delta\sigma$

In a sample with no preferred crystallographic orientation, the percentages of grains twinned on 0, 1, 2 or 3 twin planes are functions of the applied differential stress ($\sigma_1 - \sigma_3$) value.

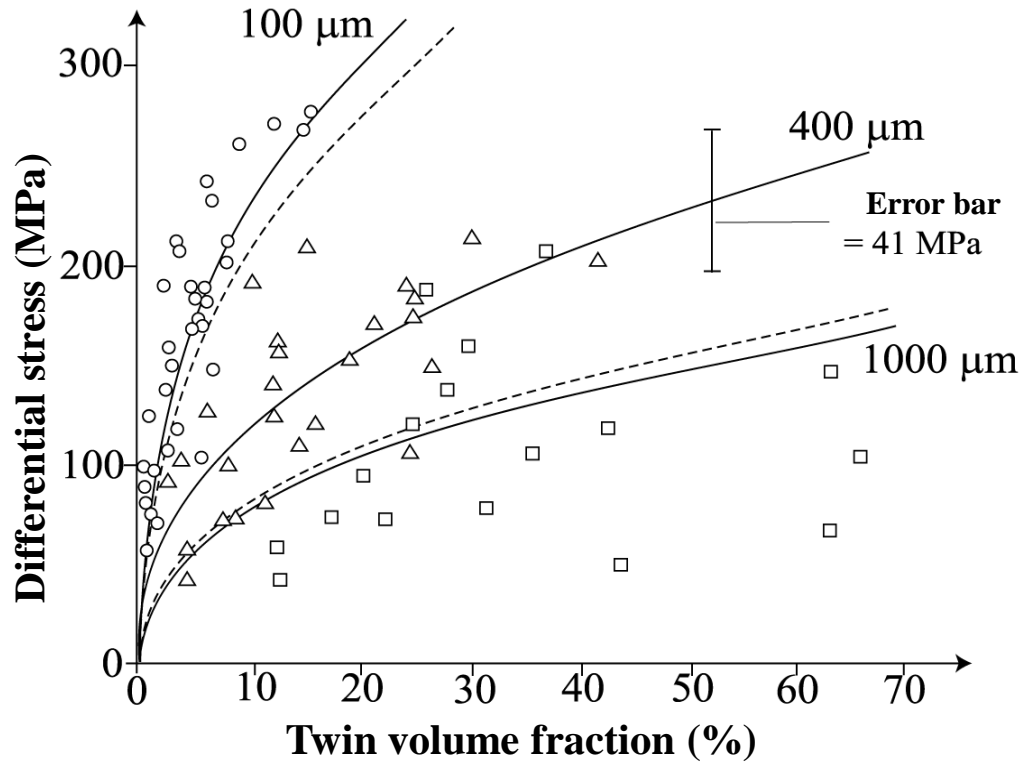
Experimentally calibrated



Limitations :

- uniaxial stress
- critical resolved shear stress for twinning = constant $\tau_c = 10$ MPa
- takes into account neither grain size nor mutual compatibility of twin systems
- significance of 'bulk' maximum differential stresses in case of polyphase tectonics ?

Rowe and Rutter (1990) : determination of differential stress magnitudes



Twin volume fraction,
 V

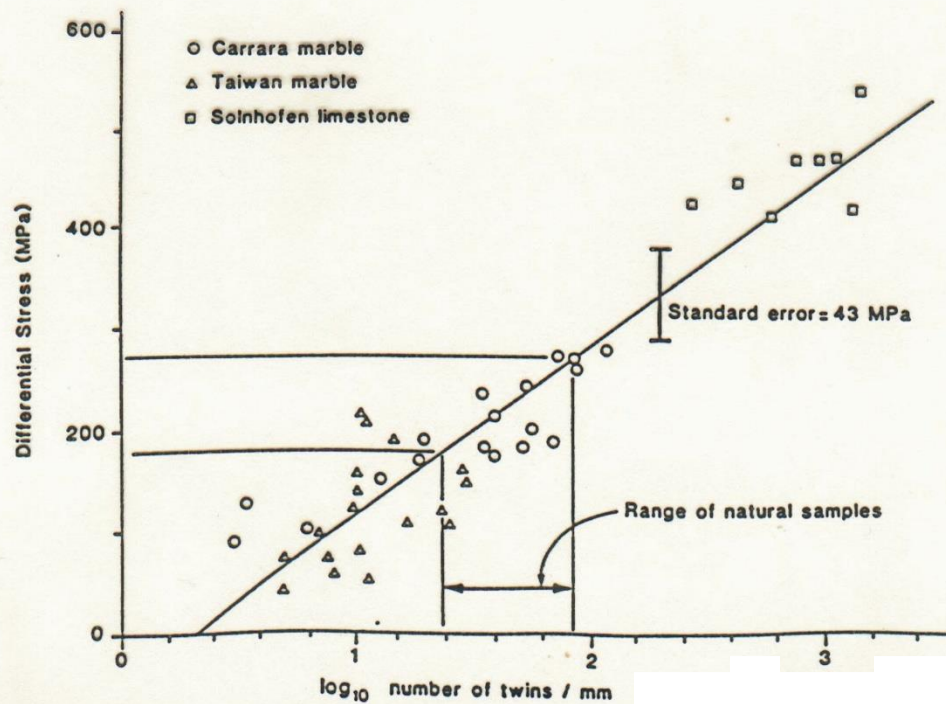
○ Grain size 100 μm
△ Grain size 400 μm
□ Grain size 1000 μm

*% volume
of twinned portion*

$$\log \sigma = 2,72 + 0,40 \cdot (\log V - \log d)$$

Rowe and Rutter (1990) : determination of differential stress magnitudes

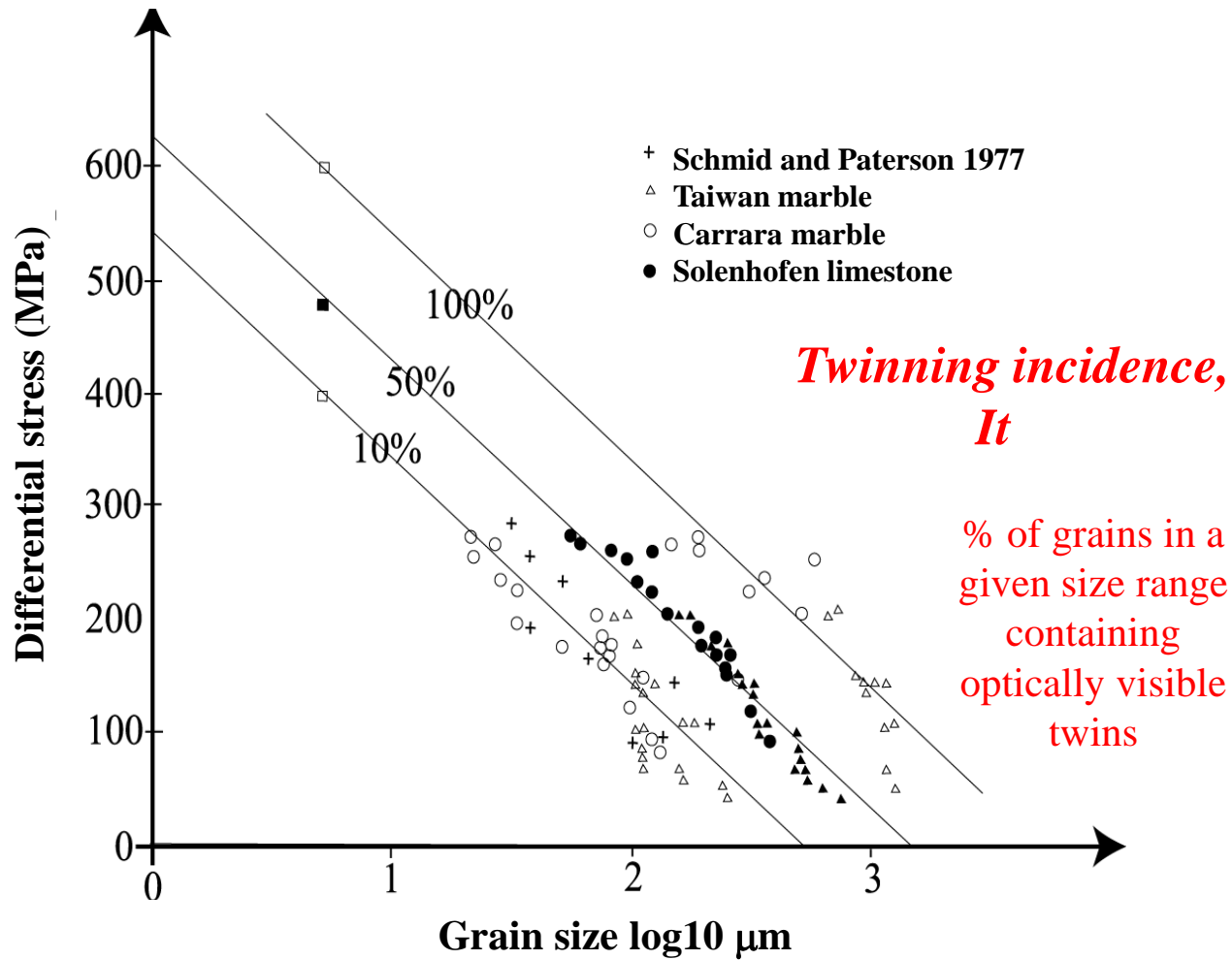
Twin density, D



$$\sigma = -52,0 + 171,1 \cdot \log D$$

Independent on grain size

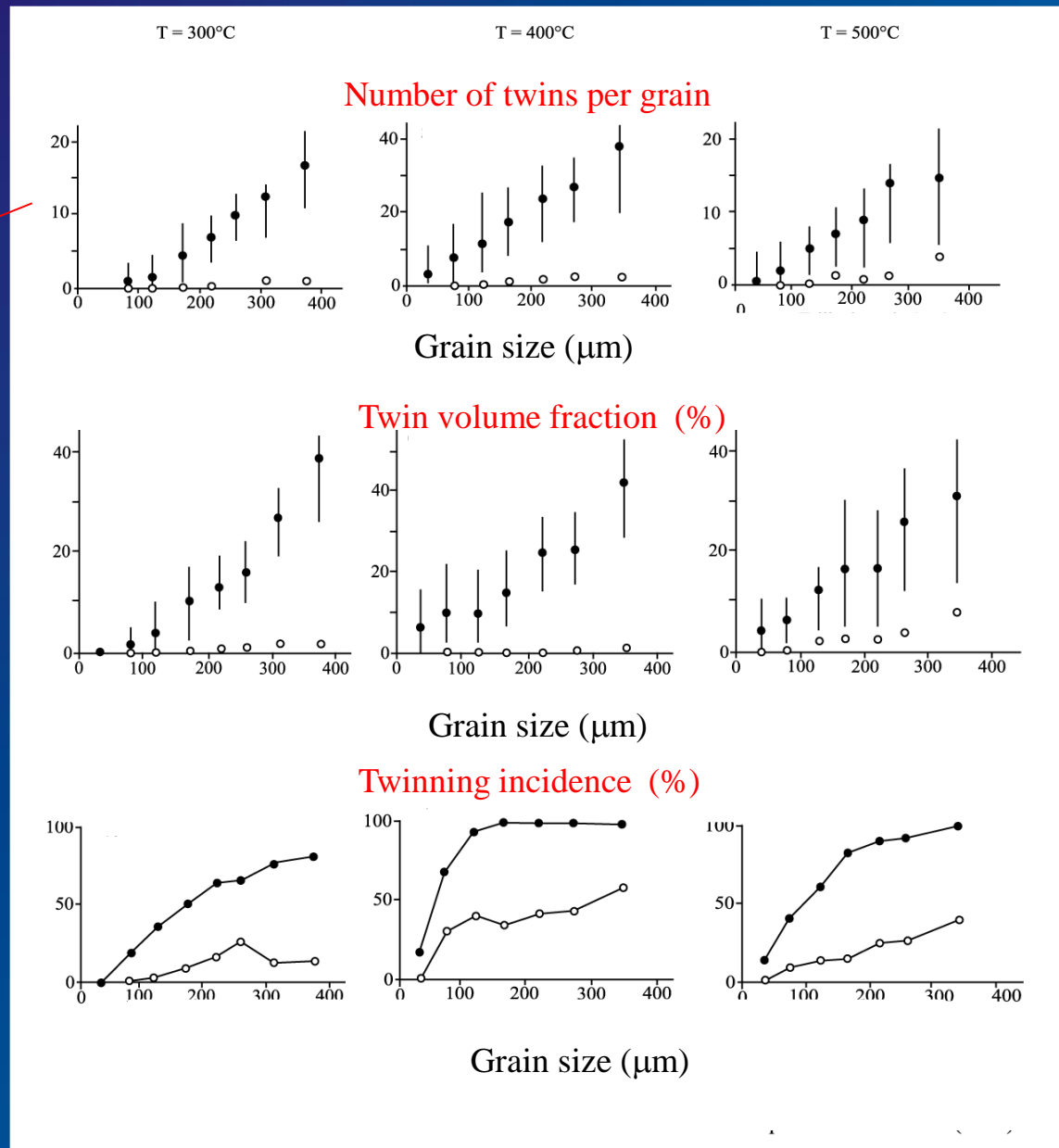
Rowe and Rutter (1990) : determination of differential stress magnitudes



$$\sigma = 523 + 2,13 It - 204 \cdot \log d$$

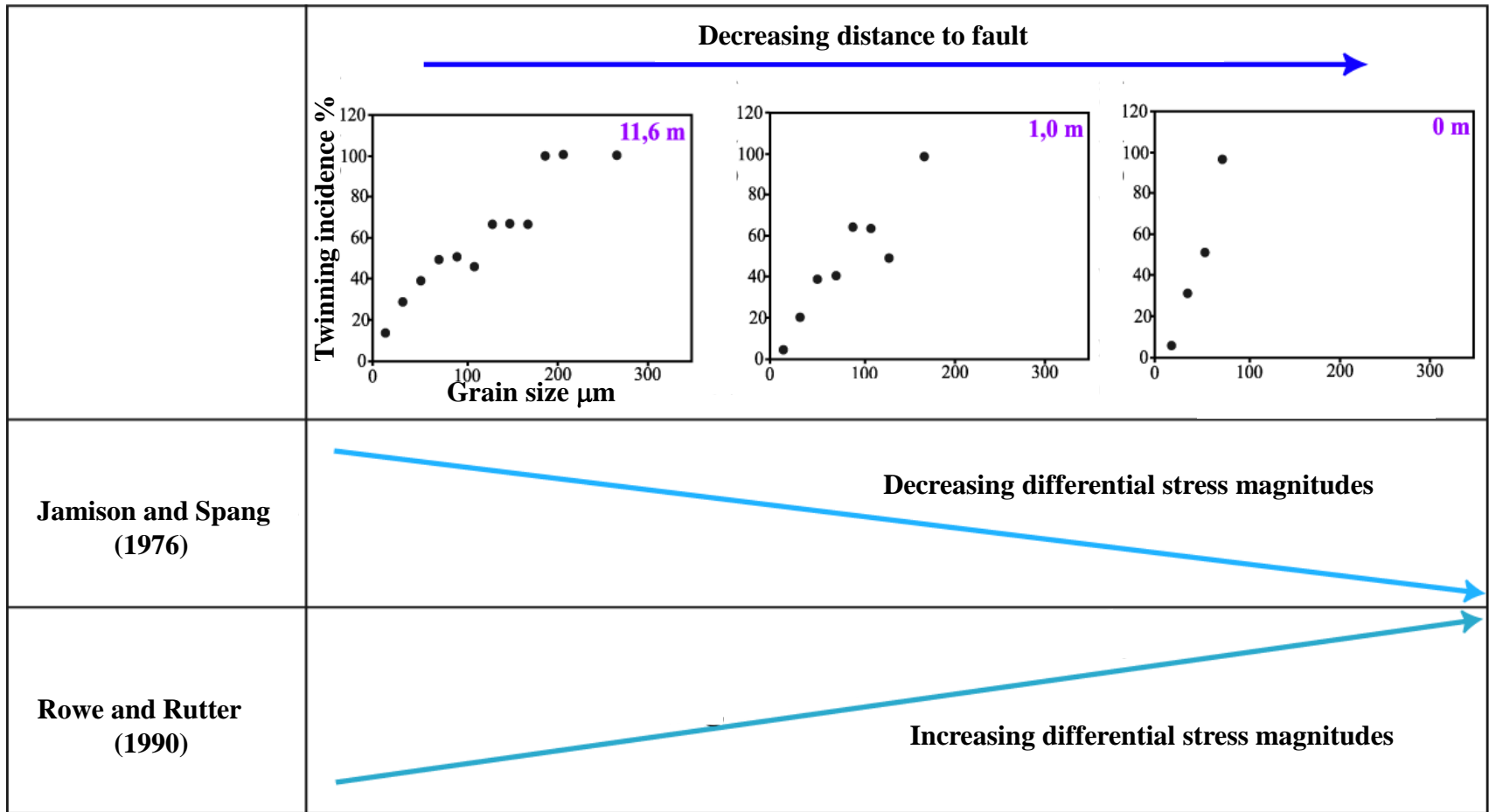
Influence of grain size

(Rowe and Rutter, 1990)



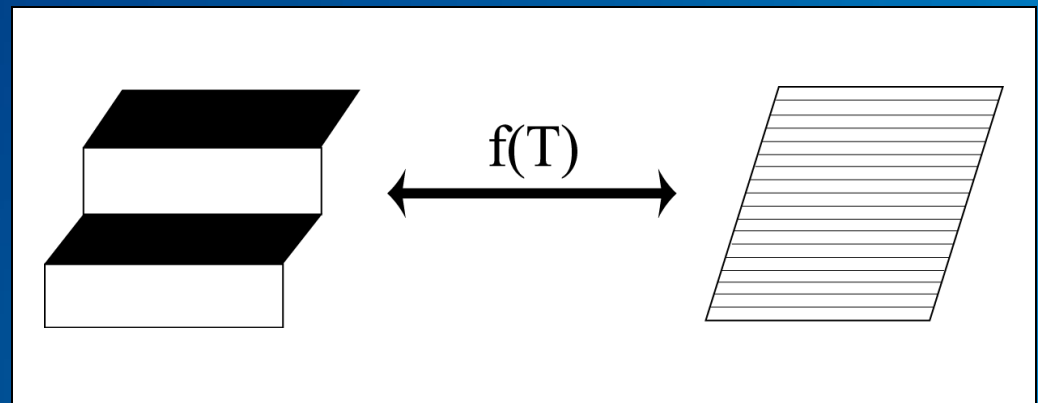
Slope = twin density,
does not depend on grain size

Influence of grain size distribution on estimates of differential stress magnitudes (after Newman, 1994)

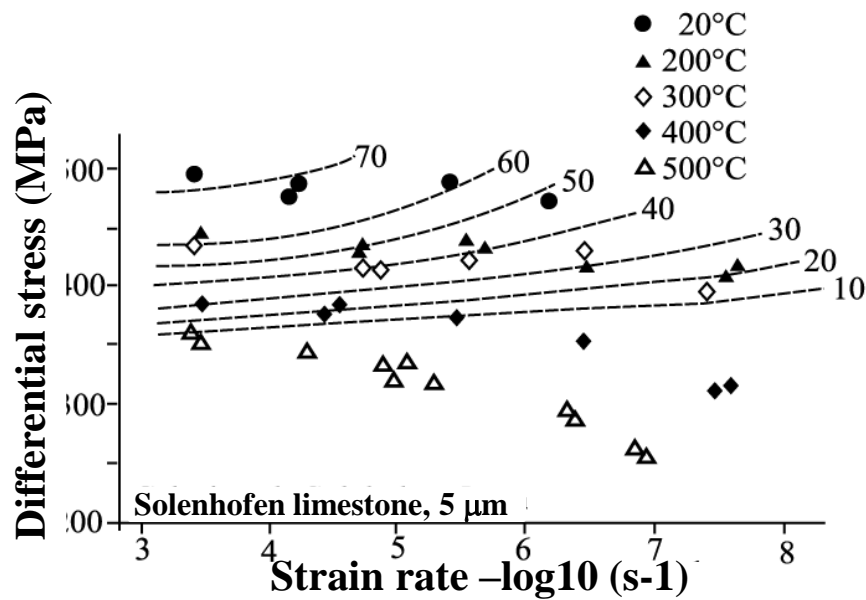
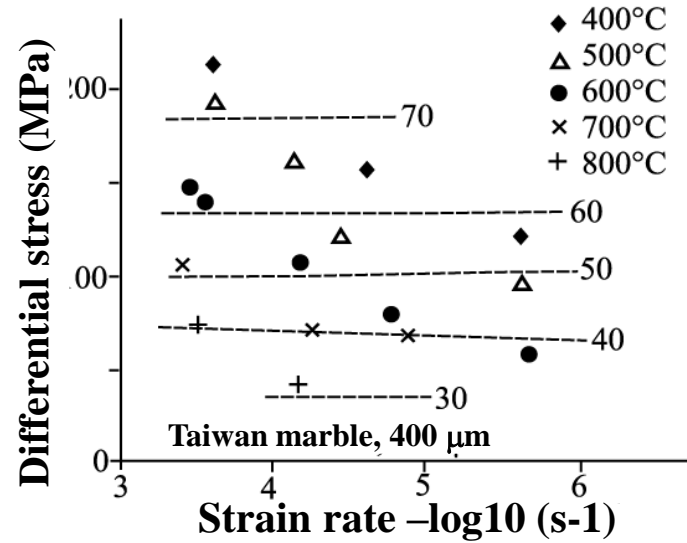
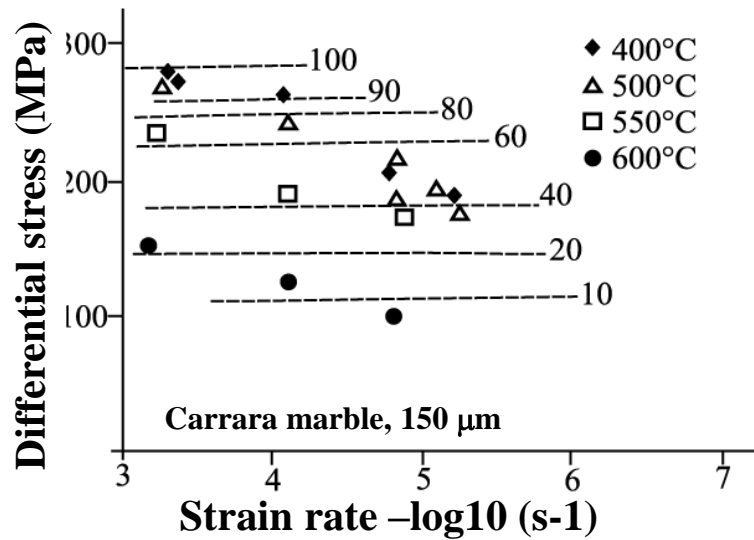


Influence of temperature on estimates of differential stress magnitudes (Ferrill, 1998)

	Référence			
Subalpine belt	Ferrill (1998)	Jamison et Spang (1976)	44 MPa	75 - 250 °C
		densité de macles de Rowe et Rutter (1990)	235 MPa	
Southern Pyrenees	Holl & Anastasio (1995)	Jamison et Spang (1976)	65 MPa	190 - 235 °C
		densité de macles de Rowe et Rutter (1990)	249 MPa	



⇒ Rowe and Rutter technique : well calibrated for temperature $> 400^{\circ}\text{C}$, BUT cannot be used at low $T^{\circ}\text{C}$



(Rowe and Rutter, 1990)

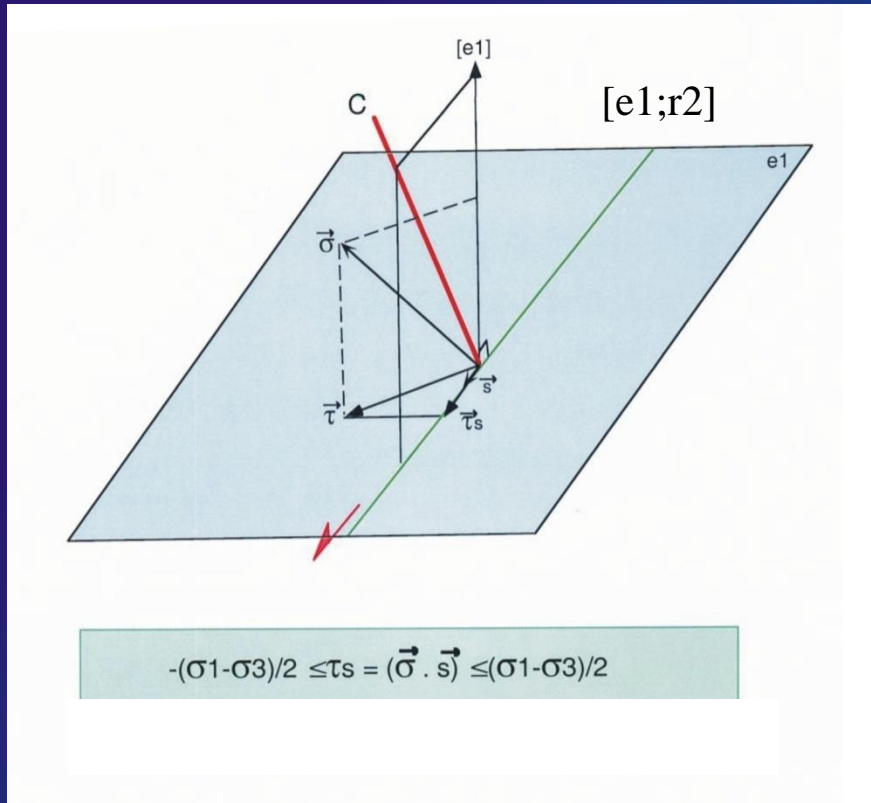
To sum up :

- Turner's (1953) dynamic analysis : yields only σ_1 and σ_3 orientations
- Groshong's (1984) strain gauge technique : yields a twin strain tensor
- Jamison and Spang (1976) and Rowe and Rutter (1990) techniques :
yield only 'bulk' maximum differential stress ($\sigma_1 - \sigma_3$)

None of these techniques allows to relate differential stresses to principal stress orientations and stress regimes;
moreover,
they are commonly used separately
without care of their specific limitations

The Calcite Stress Inversion Technique
(Etchecopar, 1984)

« Etchecopar » (1984) technique : determination of the reduced stress tensor



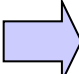
The inversion process is very similar to that used for fault-slip data :
 twin gliding along the twinning direction within the twin plane is geometrically comparable to slip along a slickenside lineation within a fault plane.

But the inversion process takes into account both twinned planes (resolved shear stress > CRSS)

AND

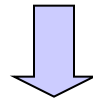
untwinned planes (resolved shear stress < CRSS),
a major difference with inversion of fault-slip data

$$\begin{bmatrix} \sigma_1 \\ \sigma_2 \\ \sigma_3 \\ \Phi \end{bmatrix} \quad \Phi = \frac{(\sigma_2 - \sigma_3)}{(\sigma_1 - \sigma_3)}$$

Inversion of calcite twin data  **Reduced stress tensor
(4 parameters)**

Orientation of principal stresses and stress ellipsoid shape ratio

$$\Phi = \frac{(\sigma_2 - \sigma_3)}{(\sigma_1 - \sigma_3)}$$



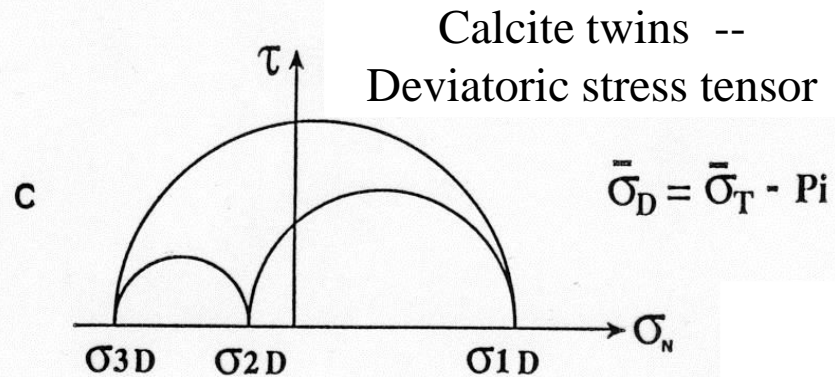
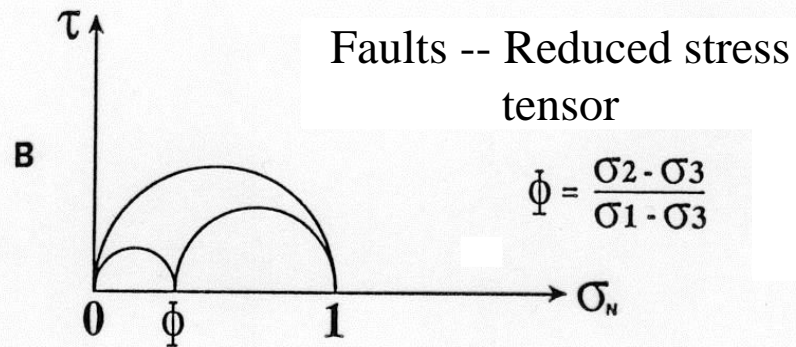
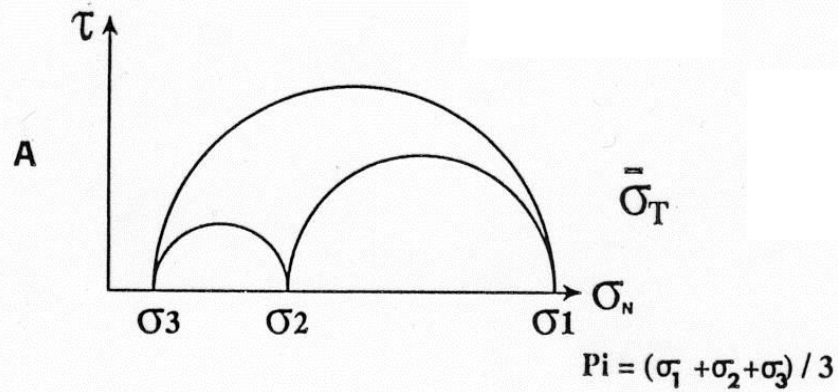
‘constant’ CRSS
for a set of calcite grains
of homogeneous size

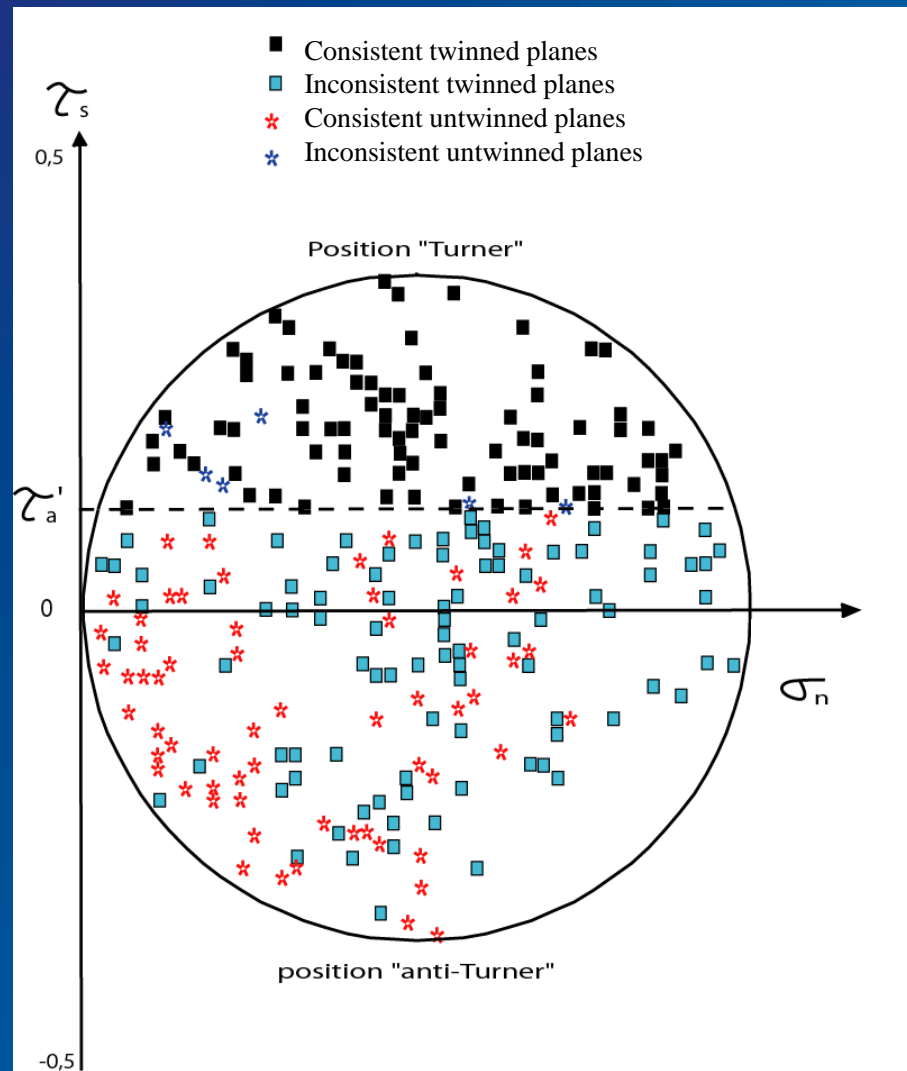
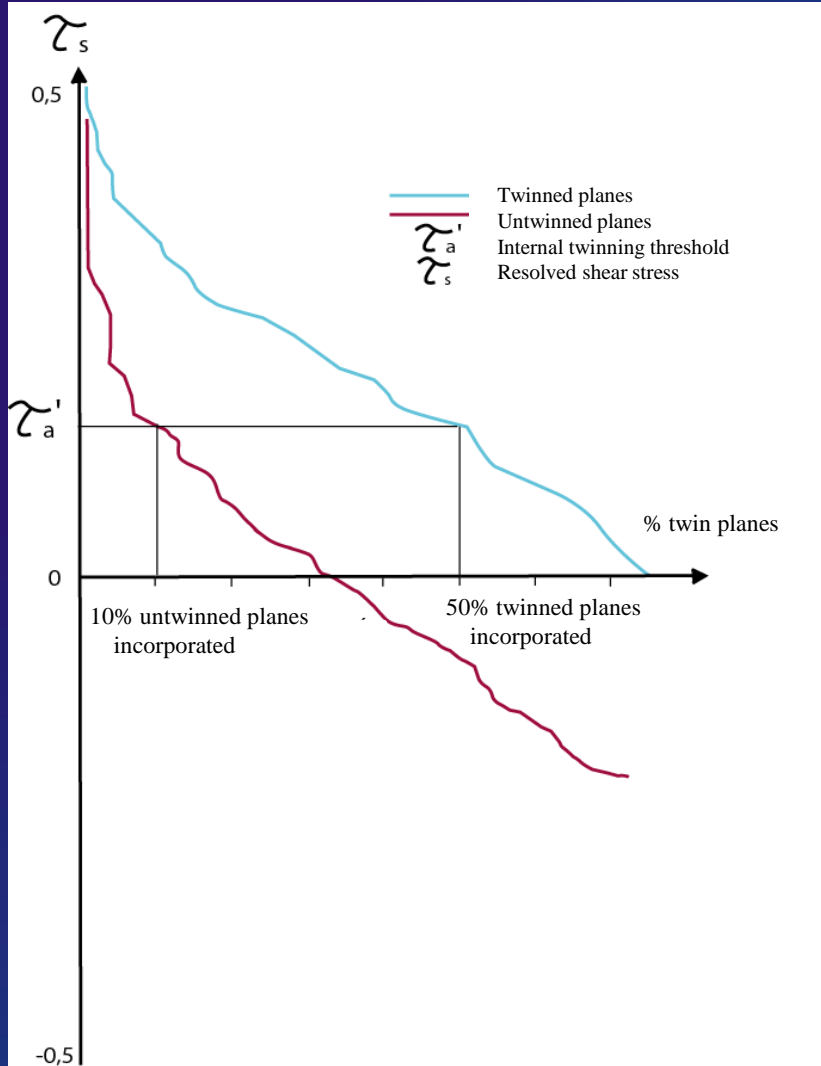
Deviatoric stress tensor (5 parameters)

$$T_D = T - \left(\frac{\sigma_1 + \sigma_2 + \sigma_3}{3} \right) \cdot I$$

Orientation of principal stresses and differential stress magnitudes

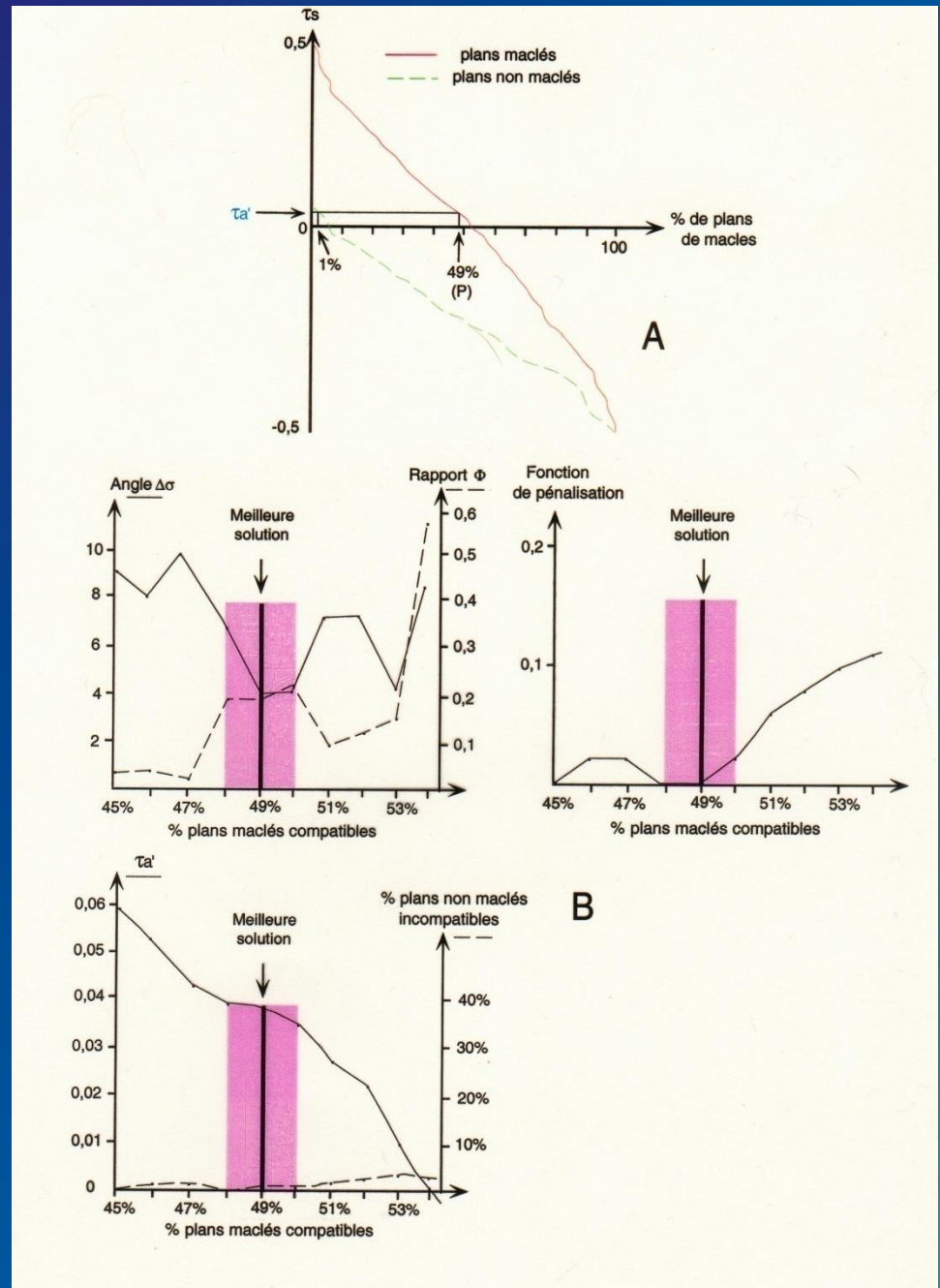
$$(\sigma_1 - \sigma_3) \quad (\sigma_2 - \sigma_3)$$



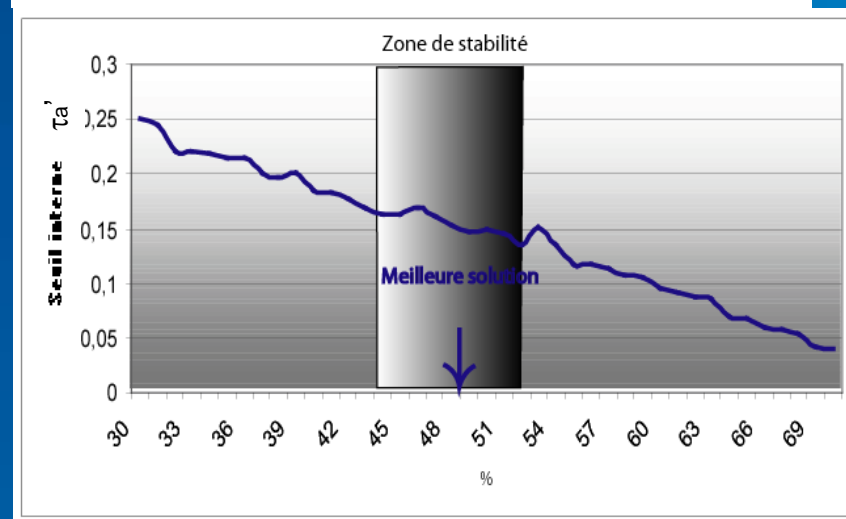
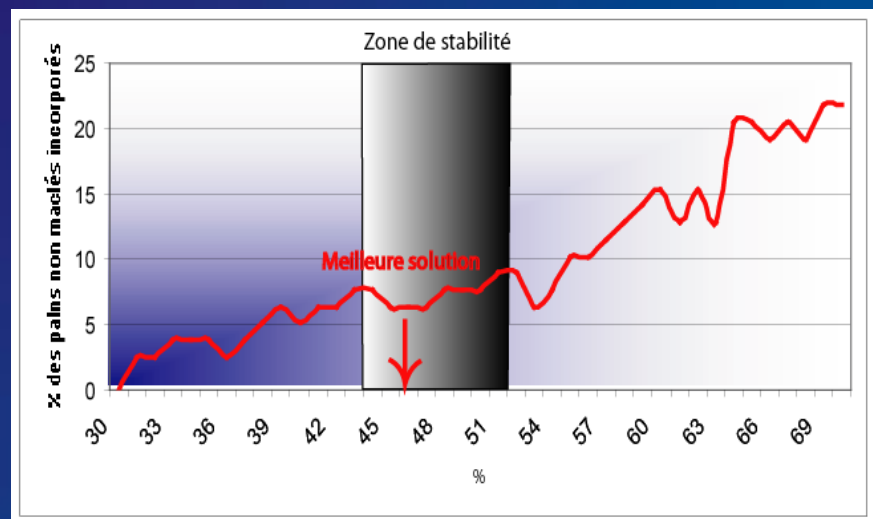
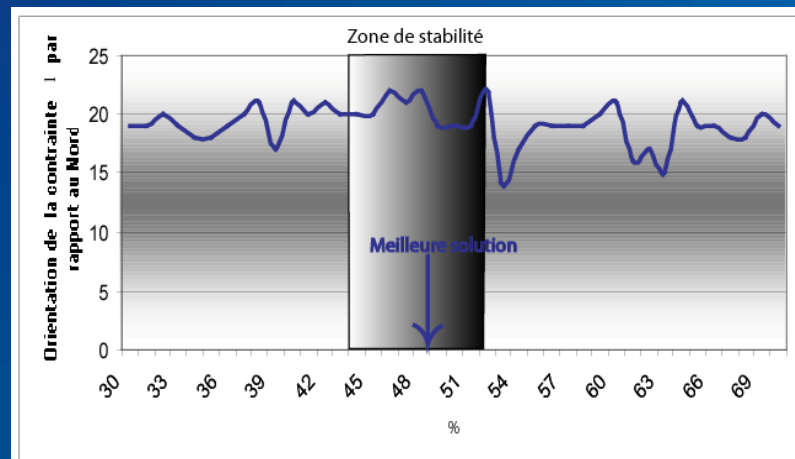
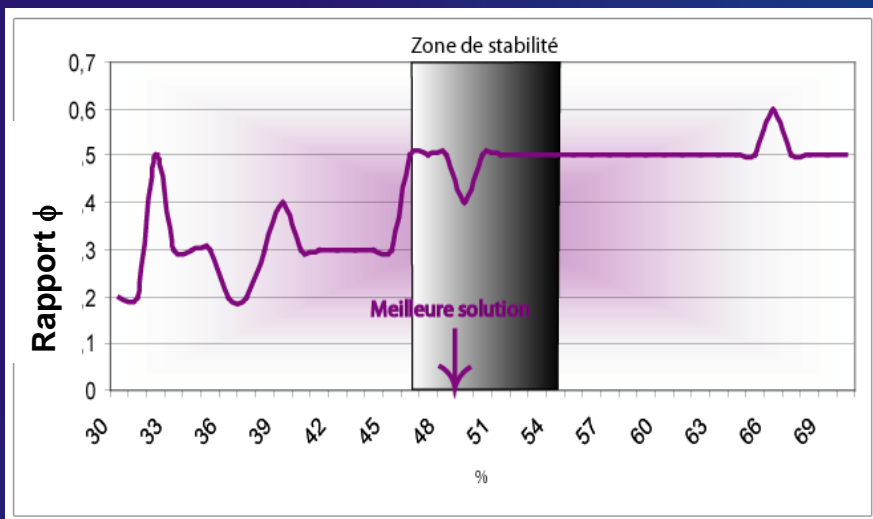


Definition of optimal stress tensor solution

(Laurent et al., 2000;
Lacombe, 2000)



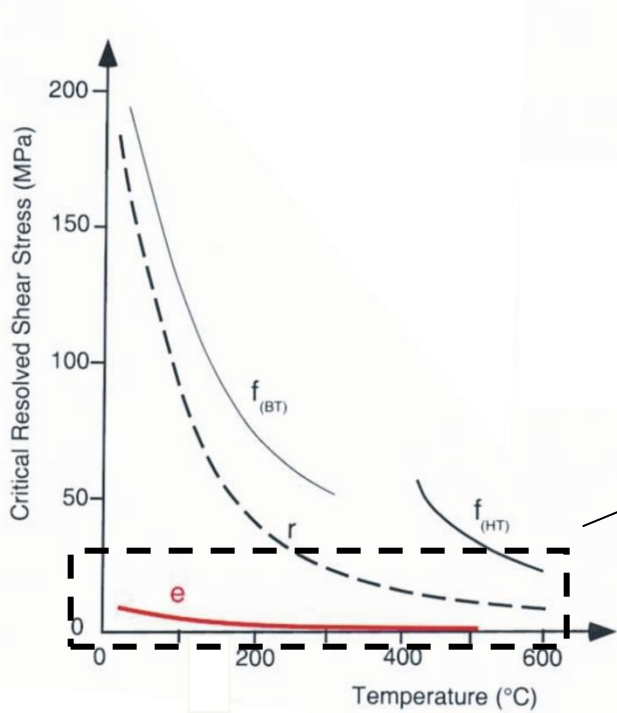
Searching for the best solution ...



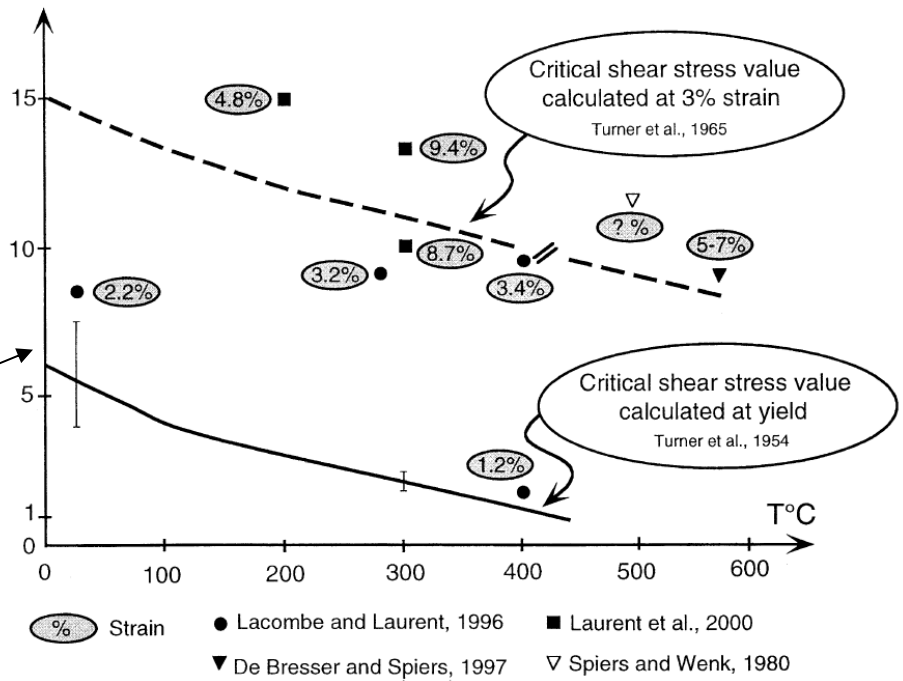
The strength of a sliding system (twinning or sliding ss) is conventionally expressed by a Critical Resolved Shear Stress (CRSS). It corresponds to the resolved shear stress along the sliding plane along the sliding direction that must be reached to induce a significant plastic (permanent) deformation, i.e., to induce motion of a number of dislocations, so that sliding becomes macroscopically observable independently of the orientation of the deformed grain. Such a behavior is commonly associated with a critical point on the stress-strain curve for a monocrystal.

The value of the CRSS is given by : $\tau_C = s \times S$. s corresponds to the applied stress at the critical point; S is the Schmid's factor, such as $S = \cos \alpha \times \cos \beta$, with α the angle between compression and the normal to the twin plane and β the angle between compression and the twin vector. The RSS along the twin vector is maximum when α et β are equal to 45° , S varying between 0 and 0,5 depending on crystal orientation.

The sources of stress concentrations like grain-scale heterogeneities being very numerous in natural crystals (dislocations, fractures, indenters, preexisting twins), the twinning threshold (= the CRSS) likely reflects the stress required to propagate rather than to nucleate twins.

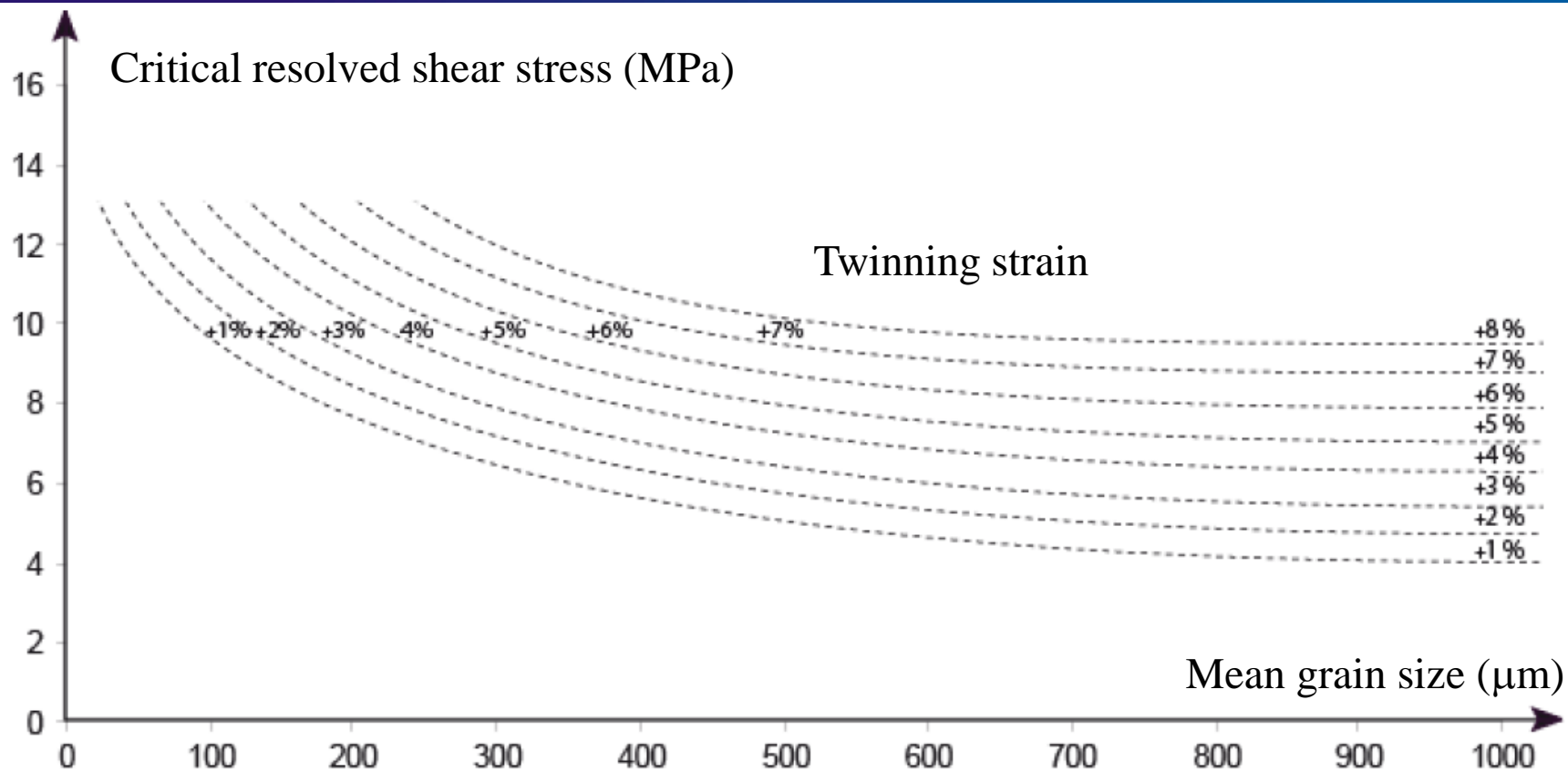


Critical shear stress value for twinning (MPa)

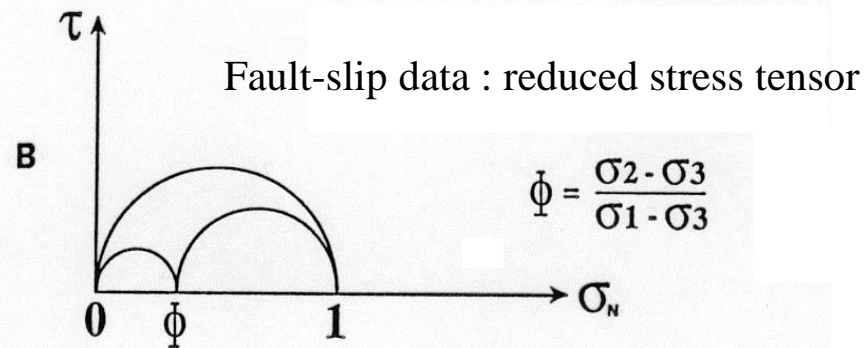
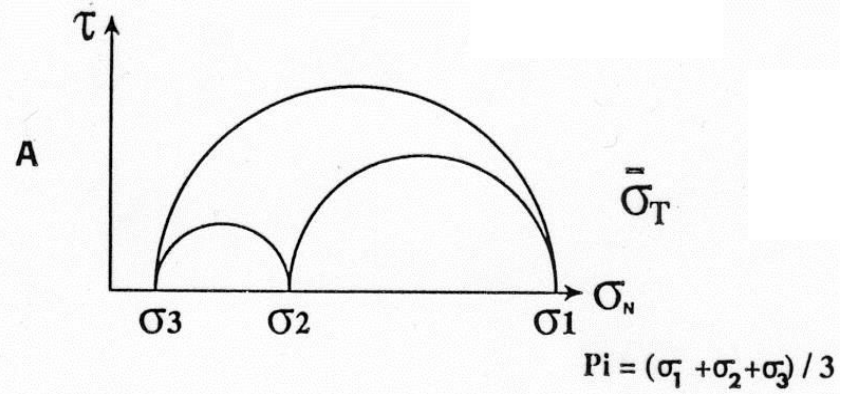


The Critical Resolved Shear Stress for twinning is ~ independent on $T^{\circ}\text{C}$ but depends on grain size and internal strain (hardening)

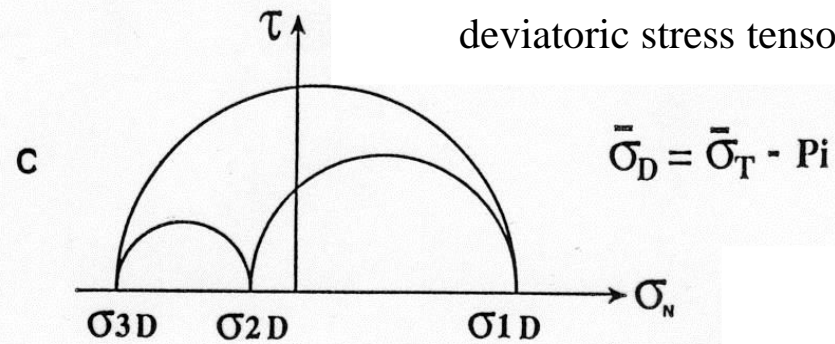
(Lacombe, 2001, 2010)



(Amrouch, 2010)

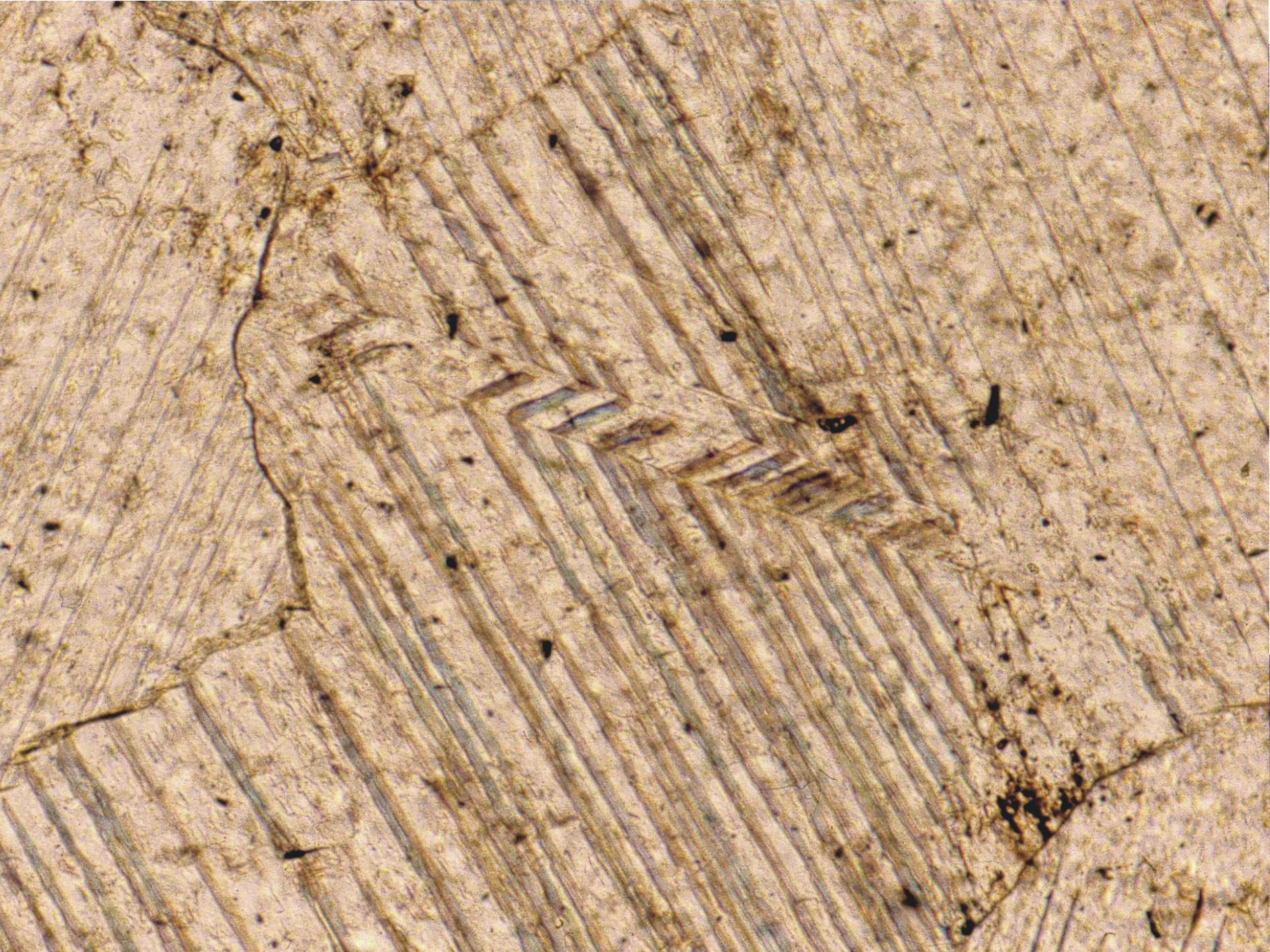


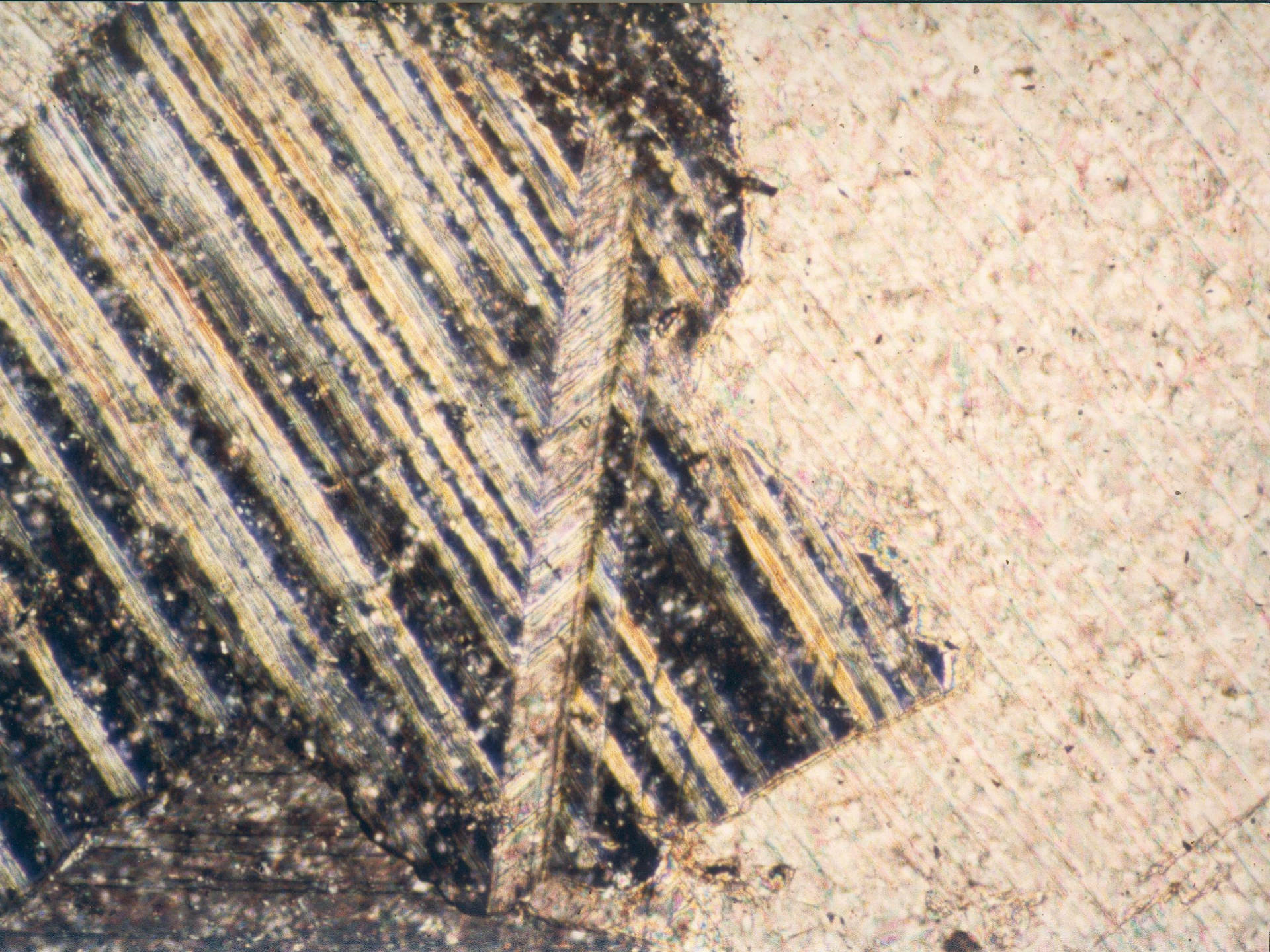
Calcite twin data :
deviatoric stress tensor

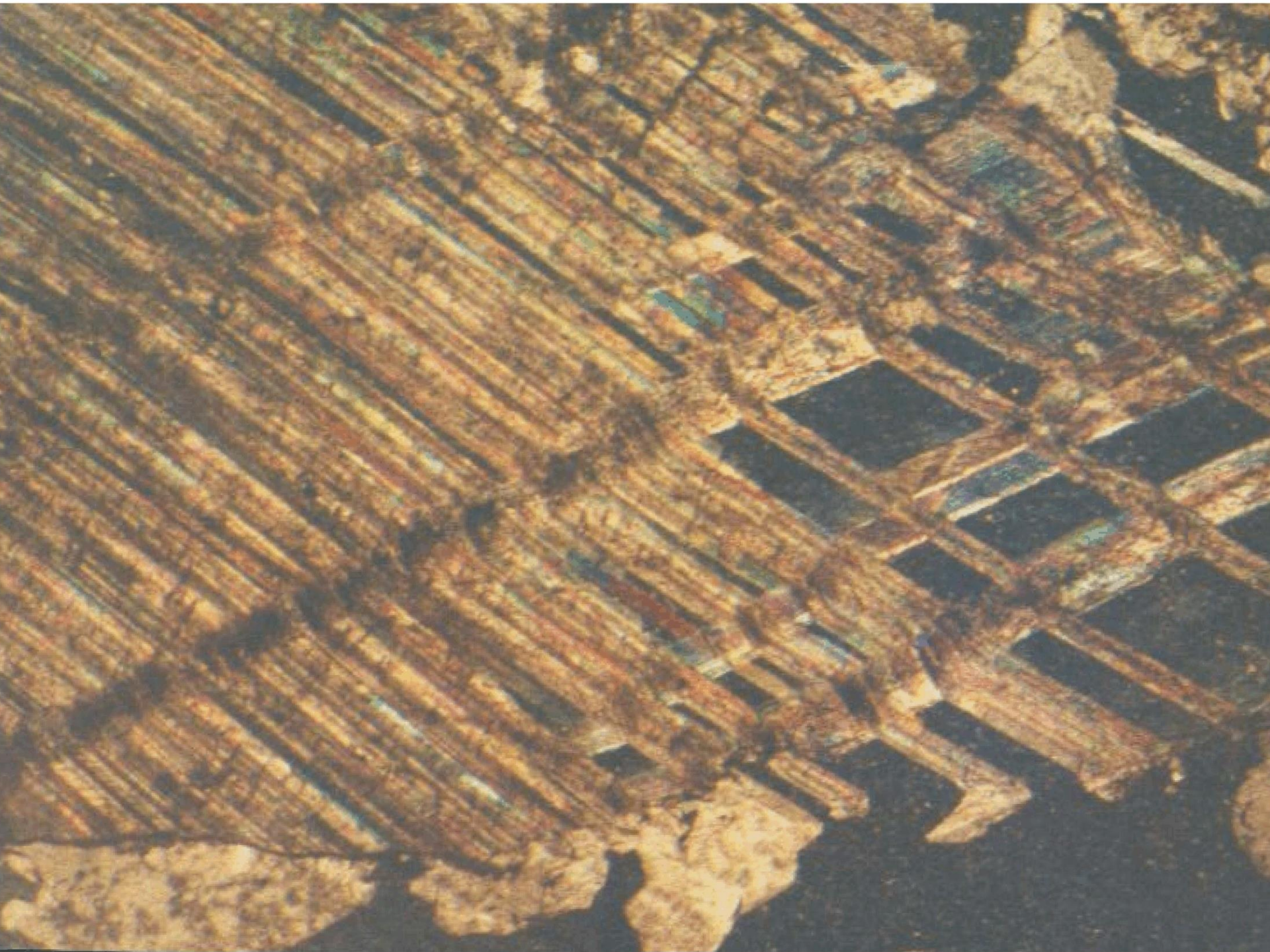


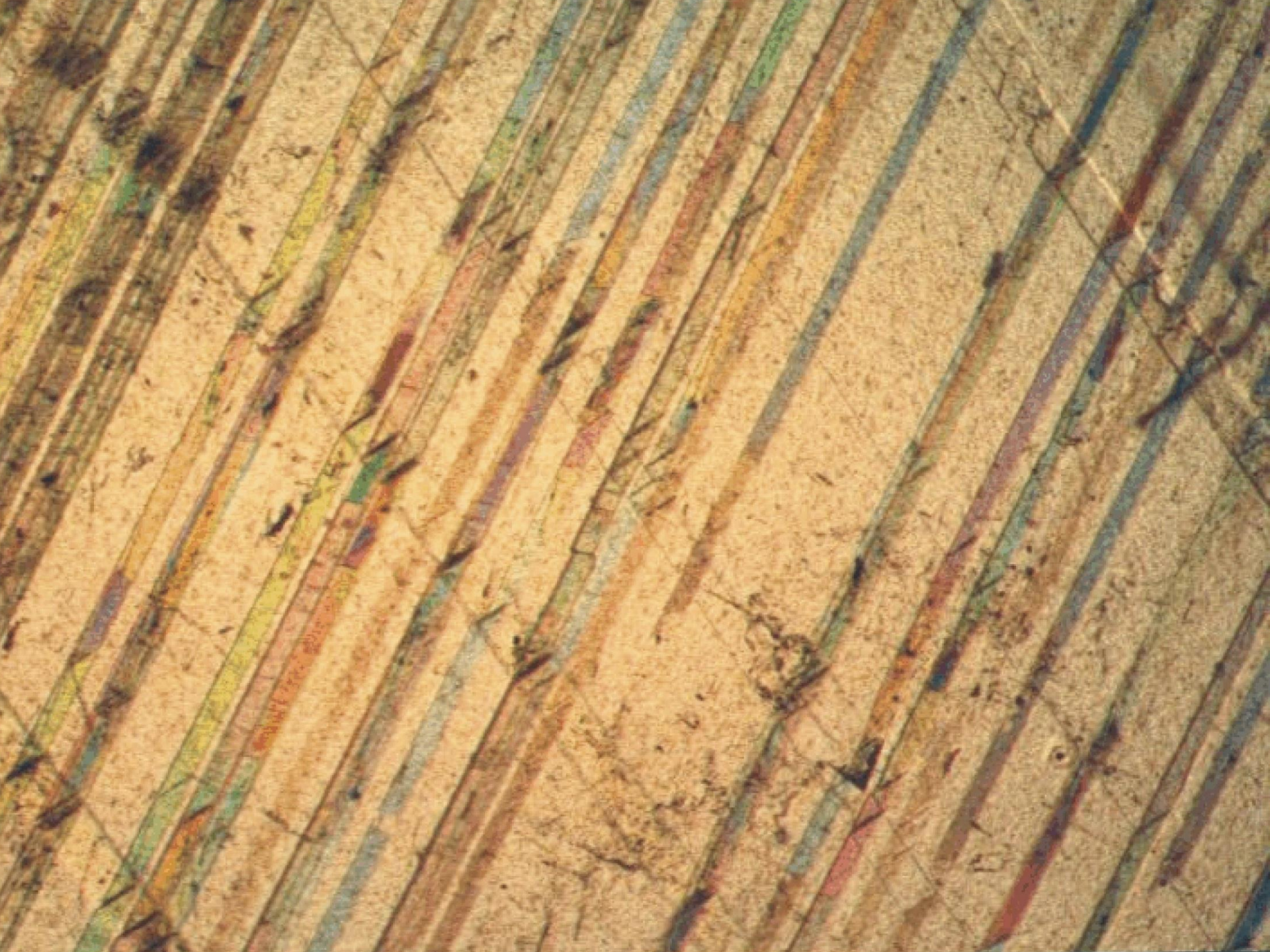
Linking paleostresses
with tectonic evolution and crustal mechanics

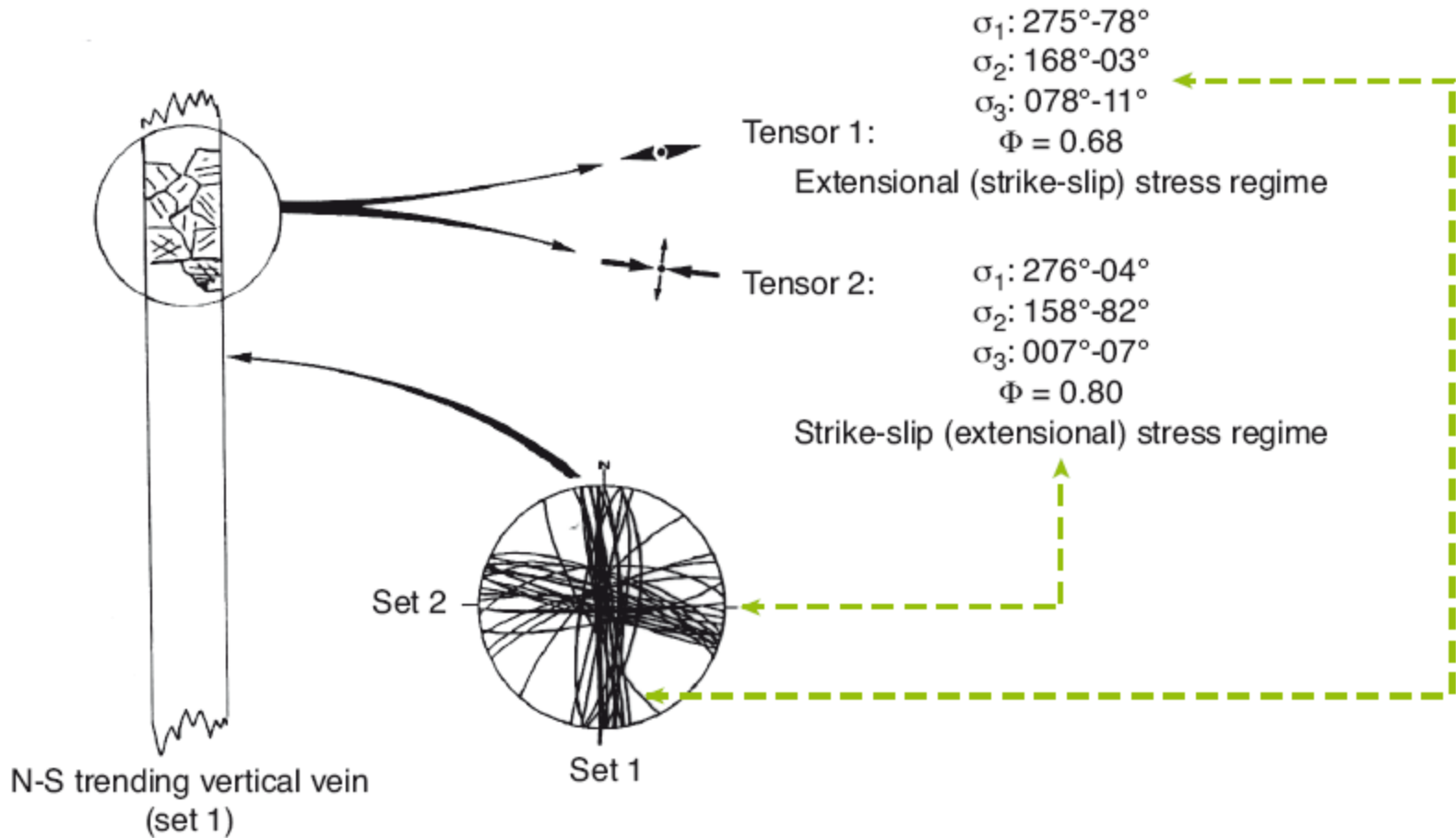
How to establish relative chronology ?









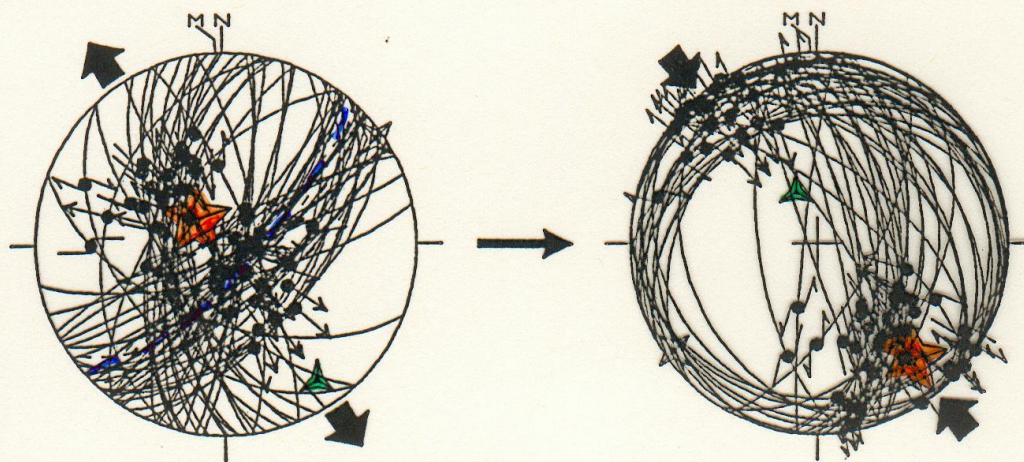


Ardèche (*Lacombe, 1992*)

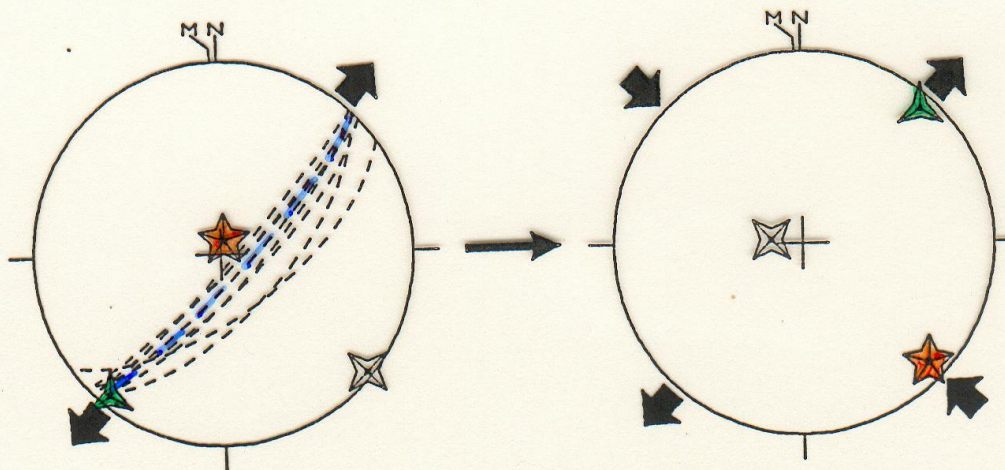
This reasoning can be reasonably extended to a first approximation to stress tensors recorded by calcite filling veins by considering that the tensor consistent with vein opening was likely recorded during (or at the latest stage) of vein opening while other (unconsistent) tensors reflect later, post-opening stress regimes

With respect
to folding...

FAILLES

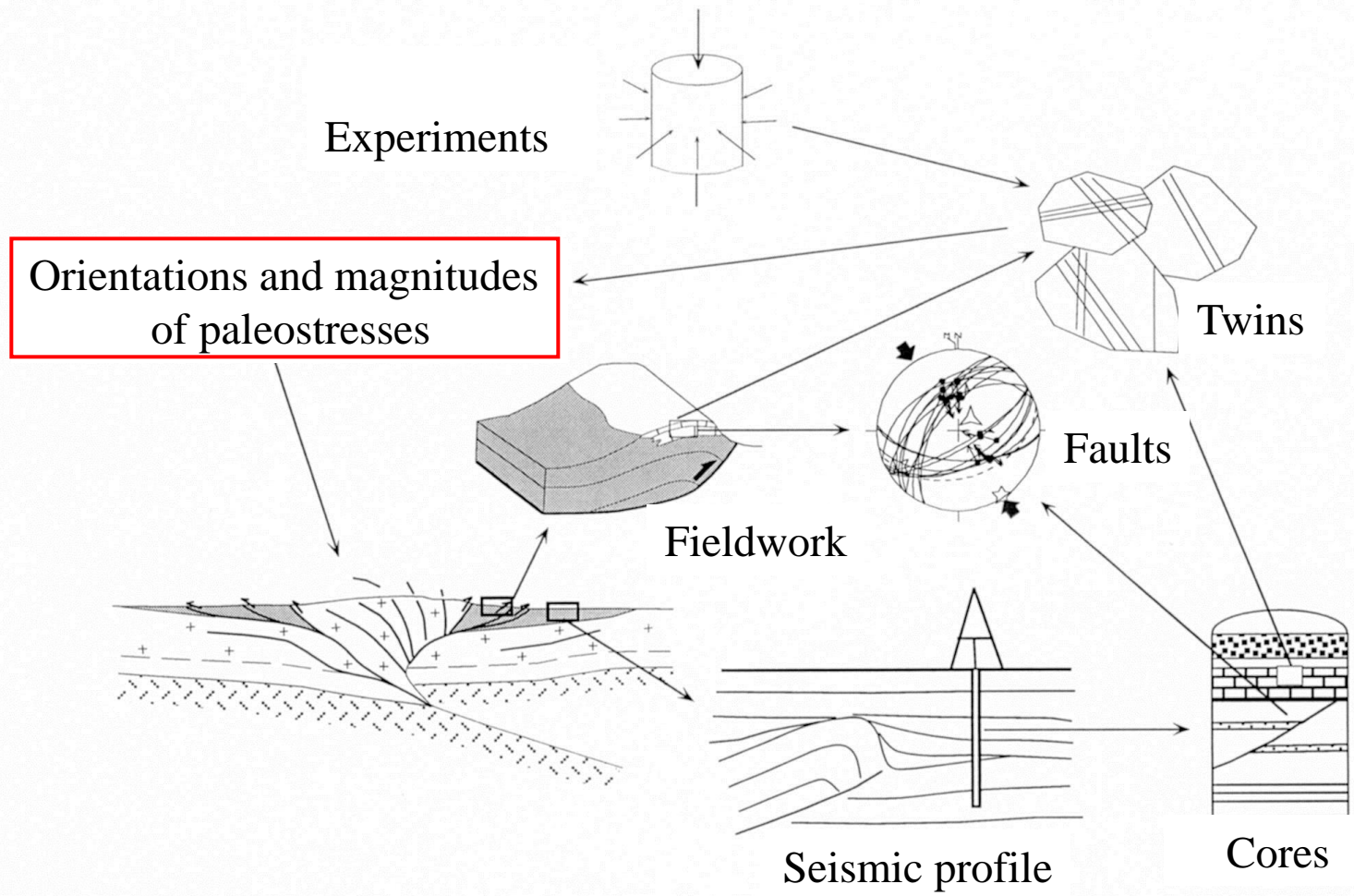


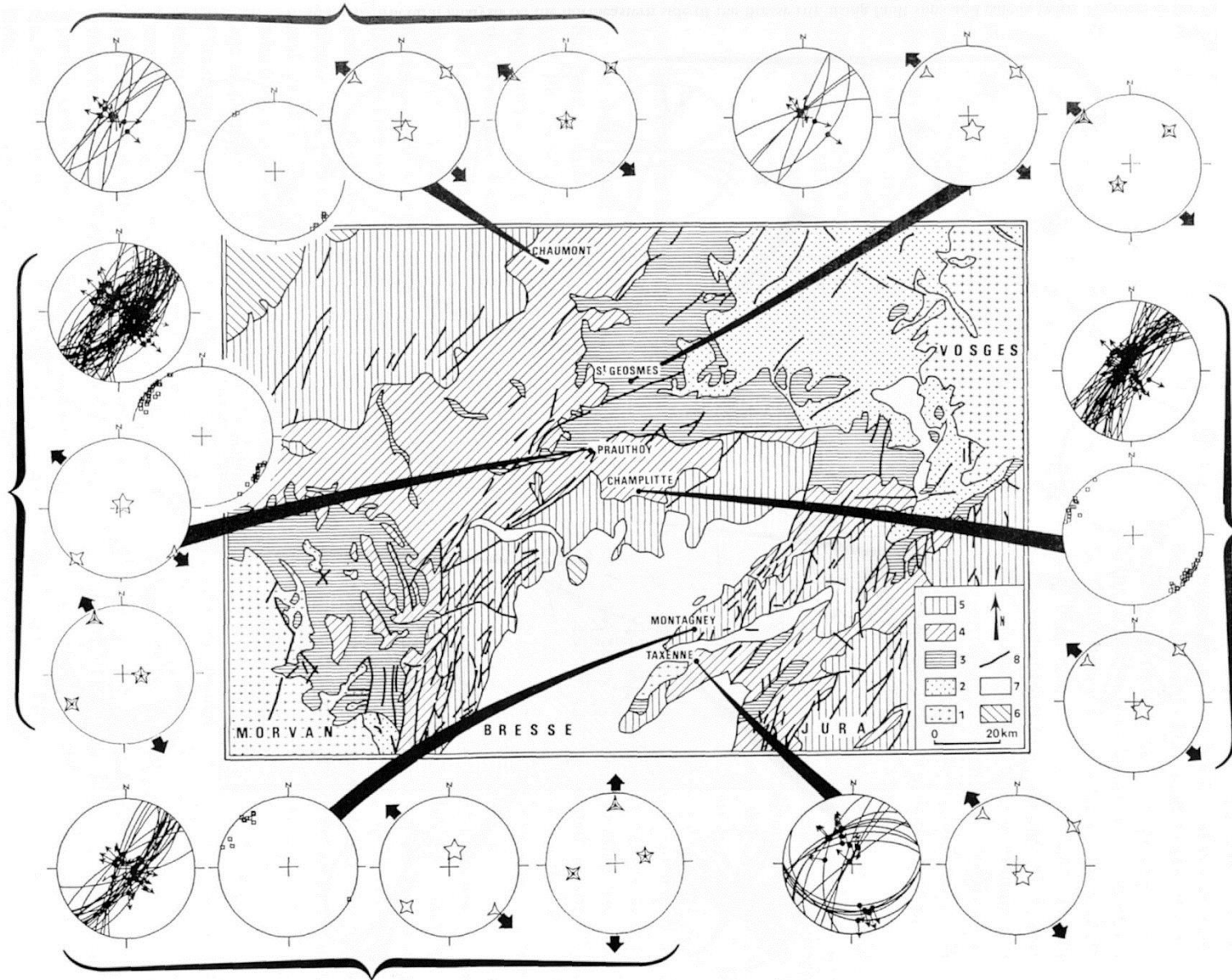
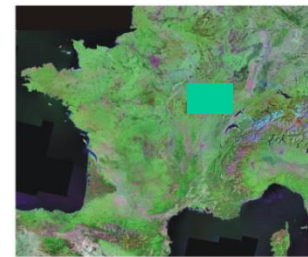
MACLES



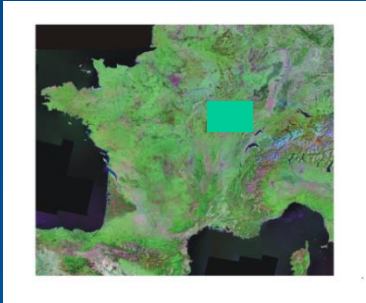
Taiwan (*Lacombe et al., 1996*)

**Some applications of calcite twin analysis
for reconstructing regional tectonic evolution**



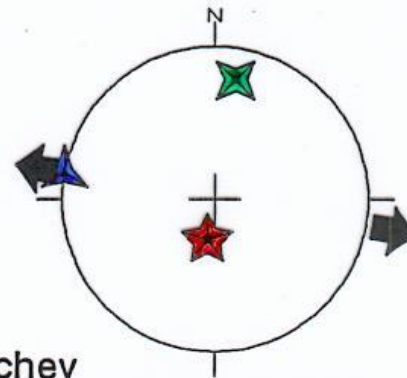
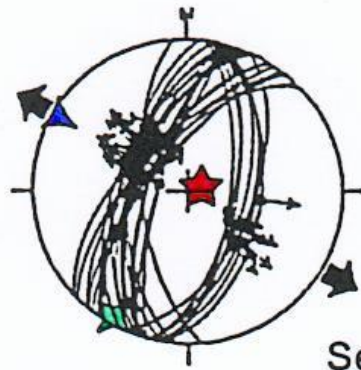


Burgundy (*Lacombe et al., 1990*)



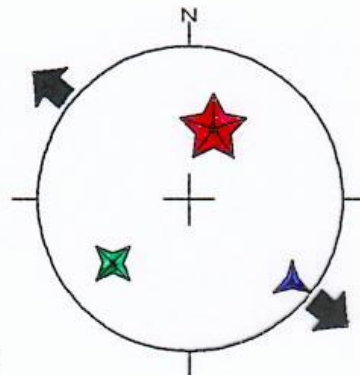
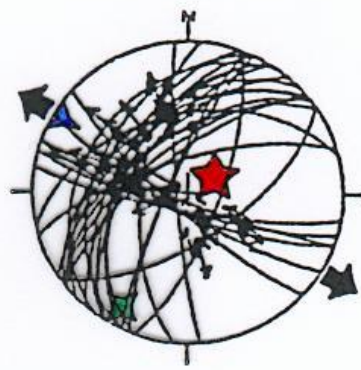
Faults

Calcite twins

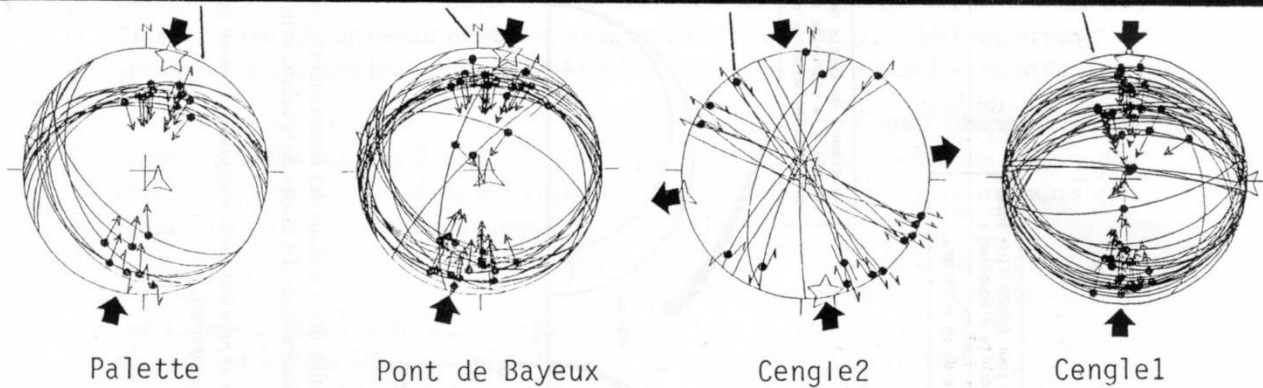
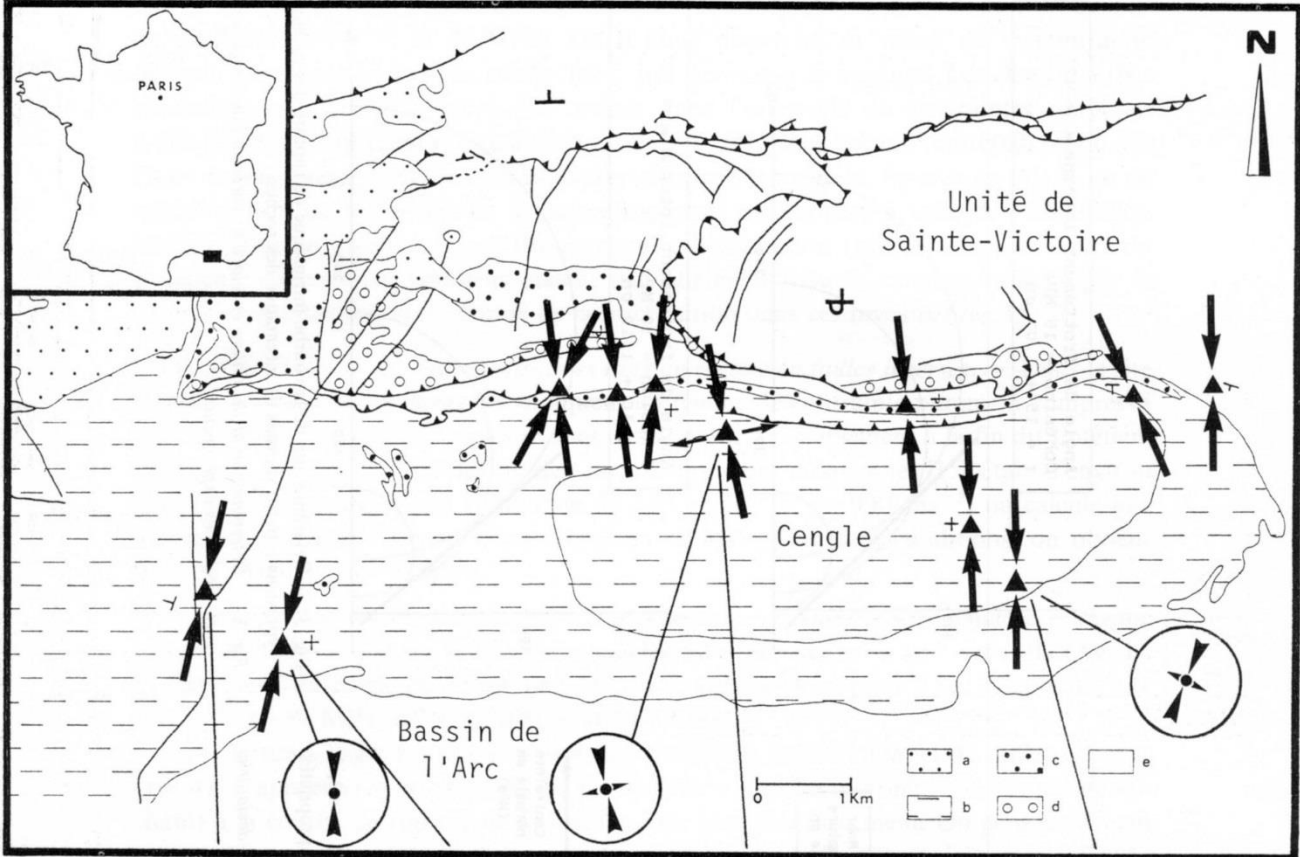


Seuchey

OLIGOCENE EXTENSION

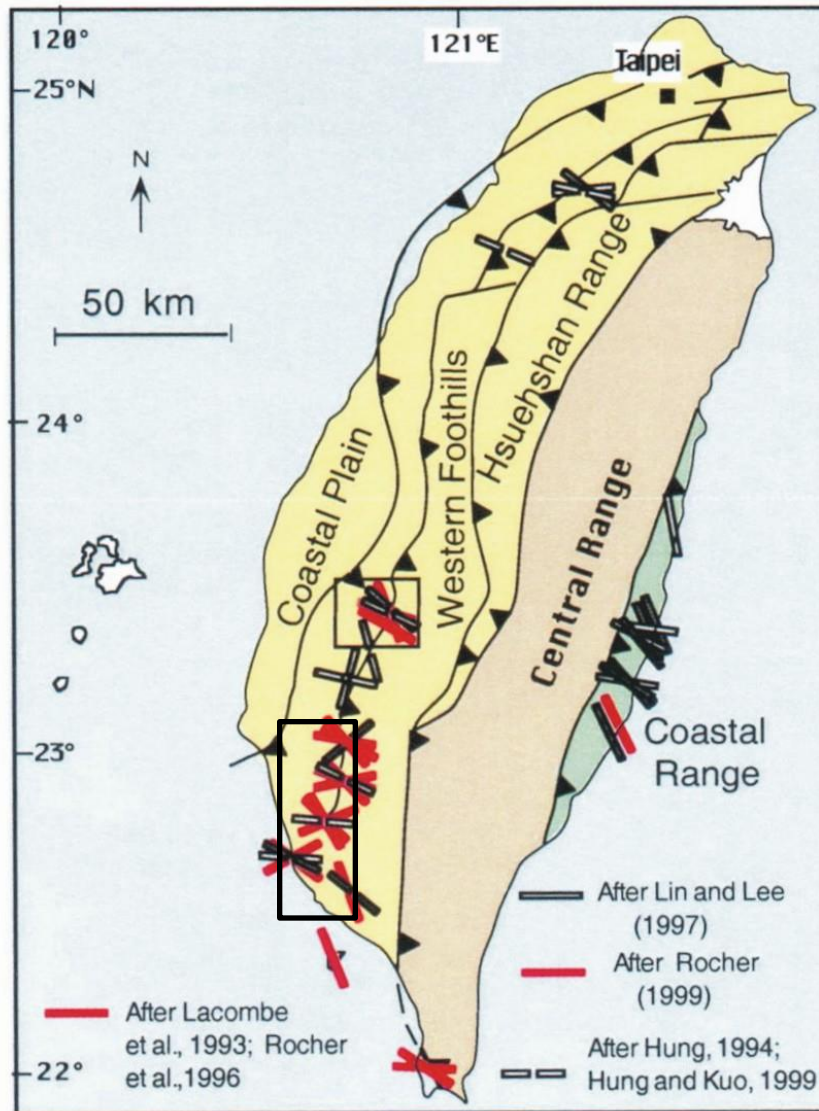


Gy



*Lacombe et al.,
1991*

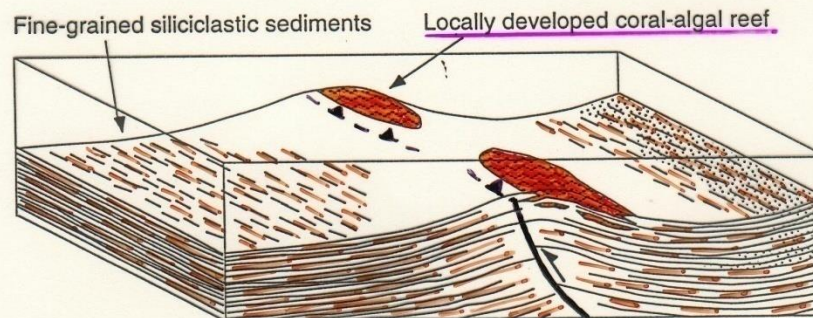
(Lacombe, 2001)

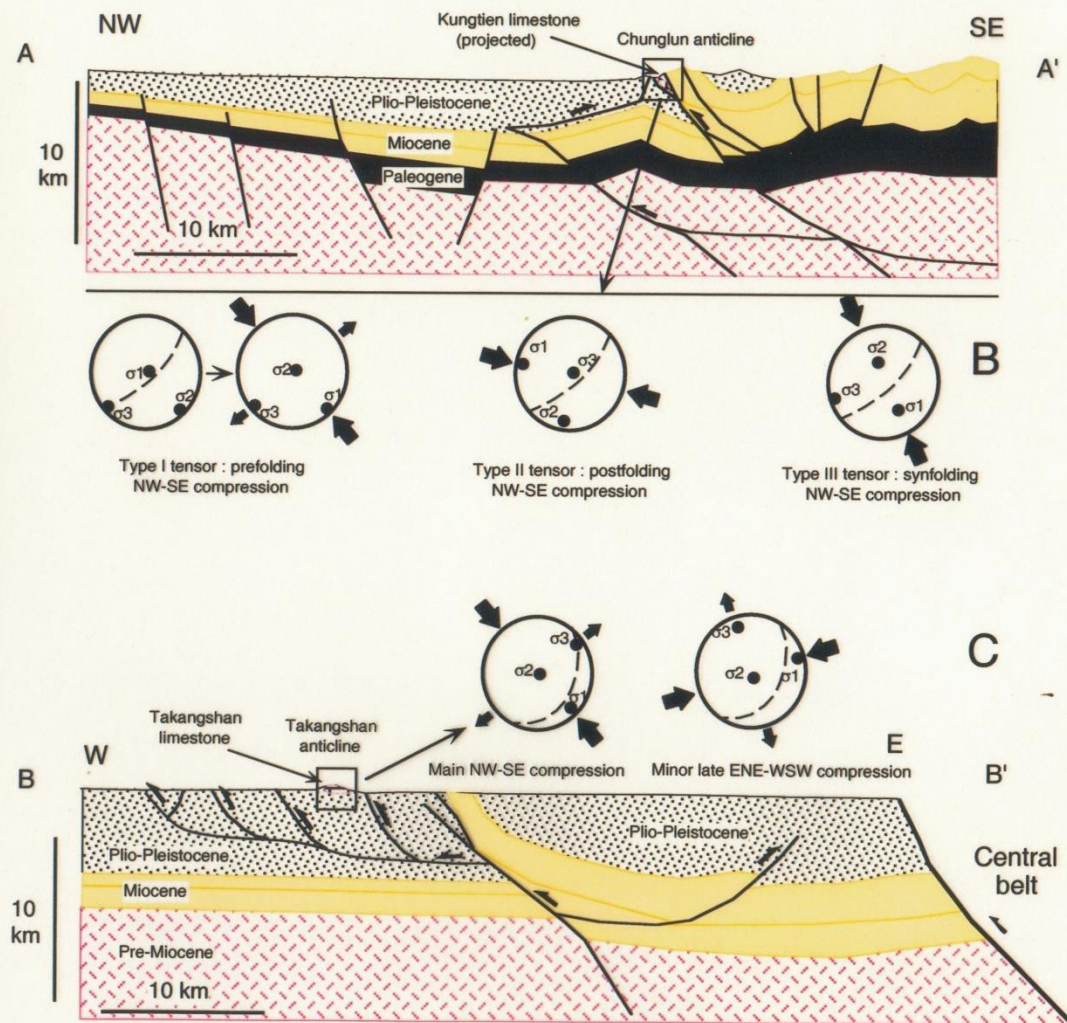
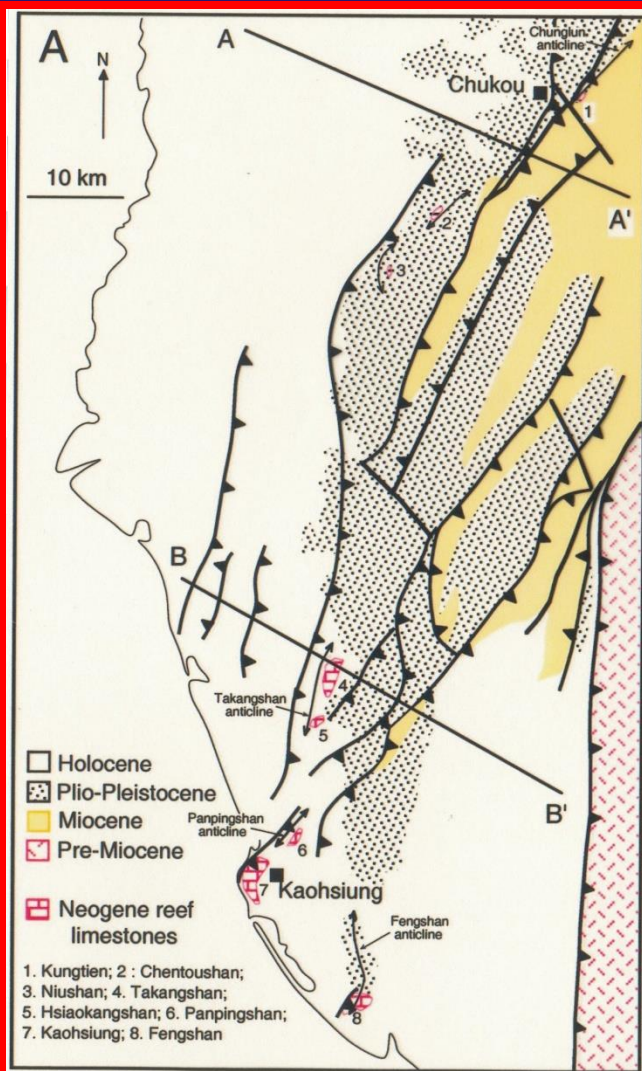


Age		Martini's zones	Chiayi-Hsinying area	Kaohsiung area	
Pleistocene	Late	NN20	Liushuang	Liushuang	Lingkou Congl.
			Erchungchi	Erchungchi U. Gutingkeng	
	Early	NN19	Kanhsialiao	TKS	Nanshihulun
			NS	HKS PPS KH	
			Liuchungchi	L. Gutingkeng F	
Pliocene	L.	NN16-18	Yunshuichi	L. Gutingkeng	
	Early	NN15 NN13	KT CTS		
			Niaotsui		
			Chunglun		Mucha
Mio-cene	Late	NN12		Wushan	
		NN11			

Stratigraphy of the reef limestones of the southwestern Taiwan.

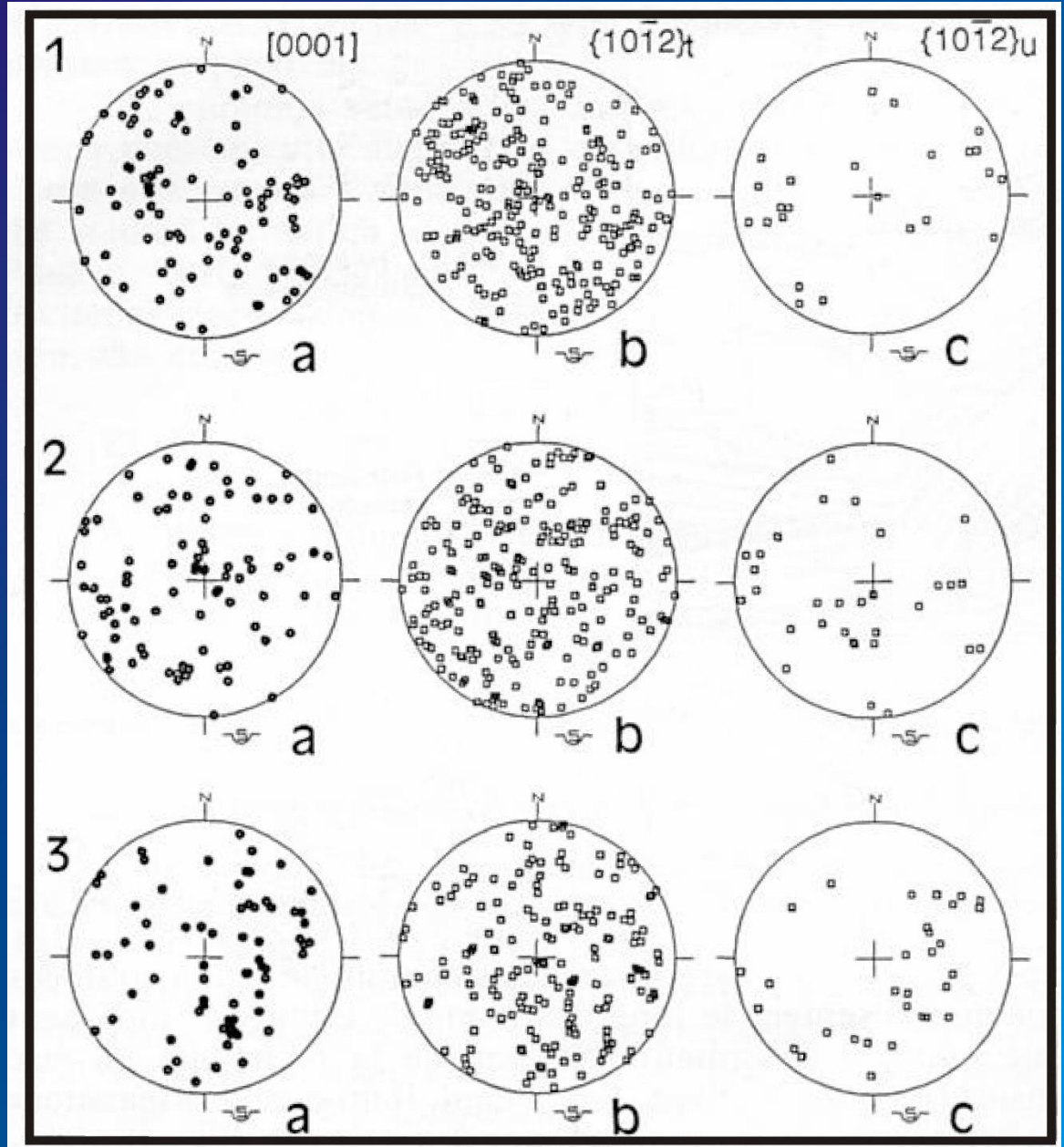
(Gong et al., 1995)

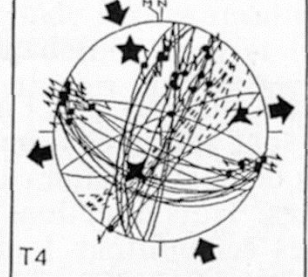
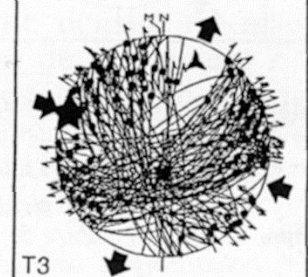
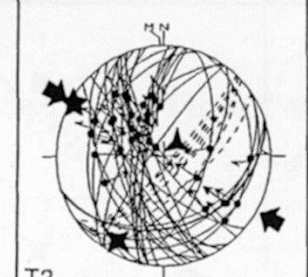
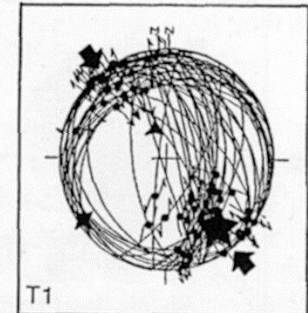
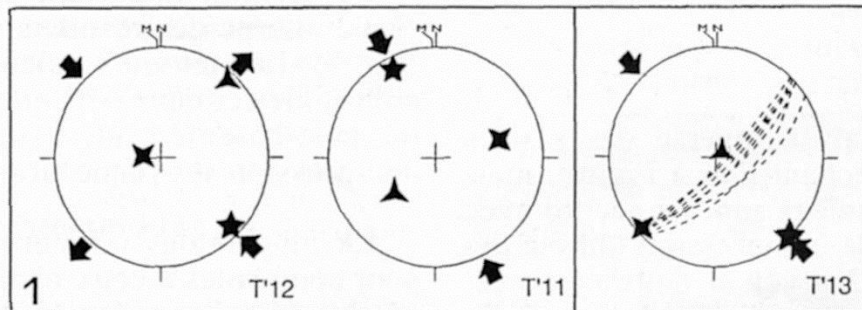
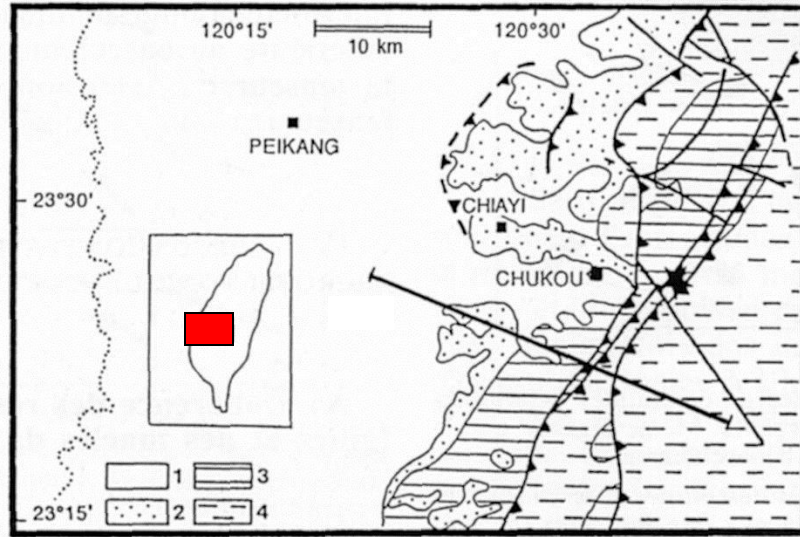
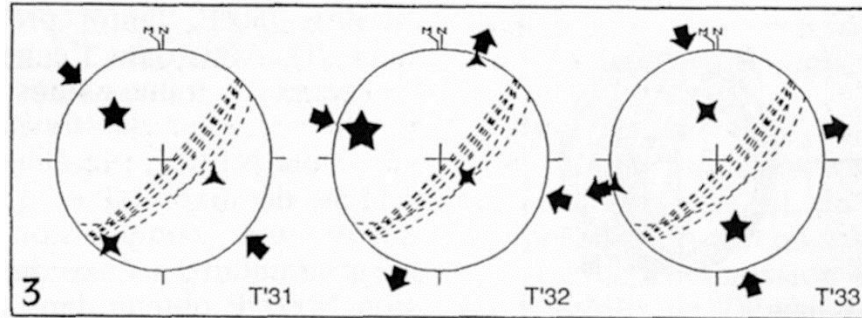
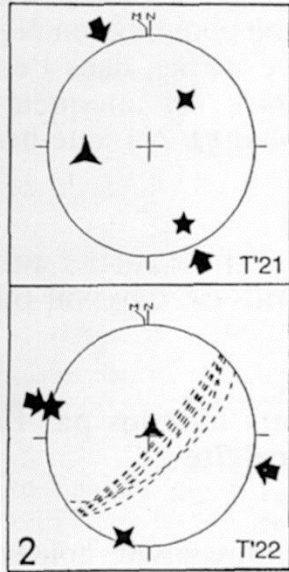




(Lacombe, 2001)

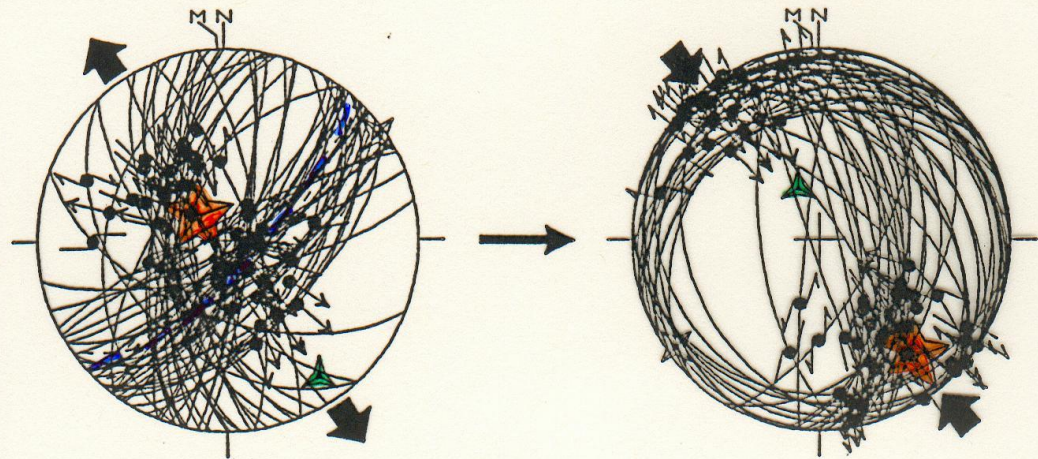
(Lacombe et al., 1996)



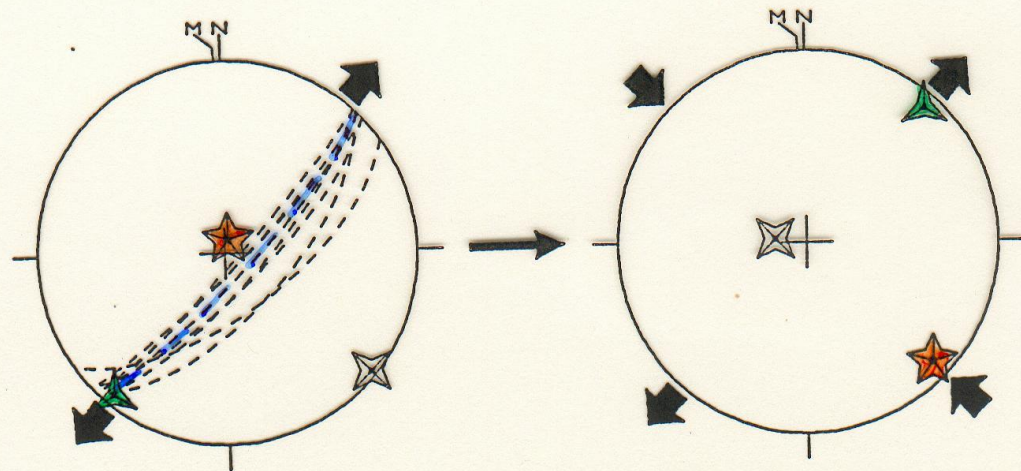


(Lacombe et al.,
1996)

FAILLES



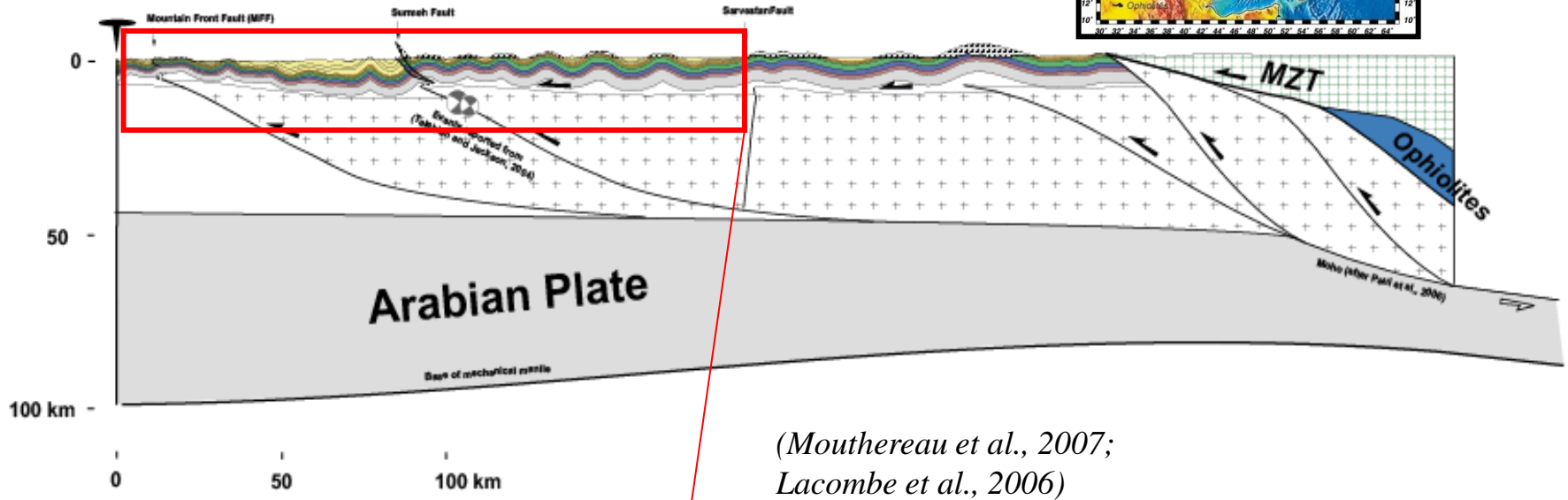
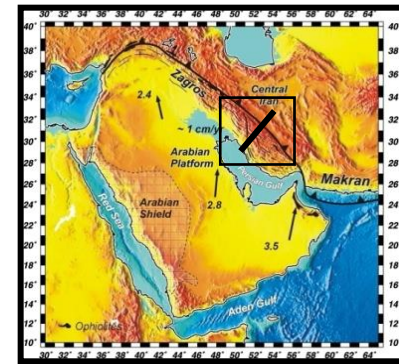
MACLES



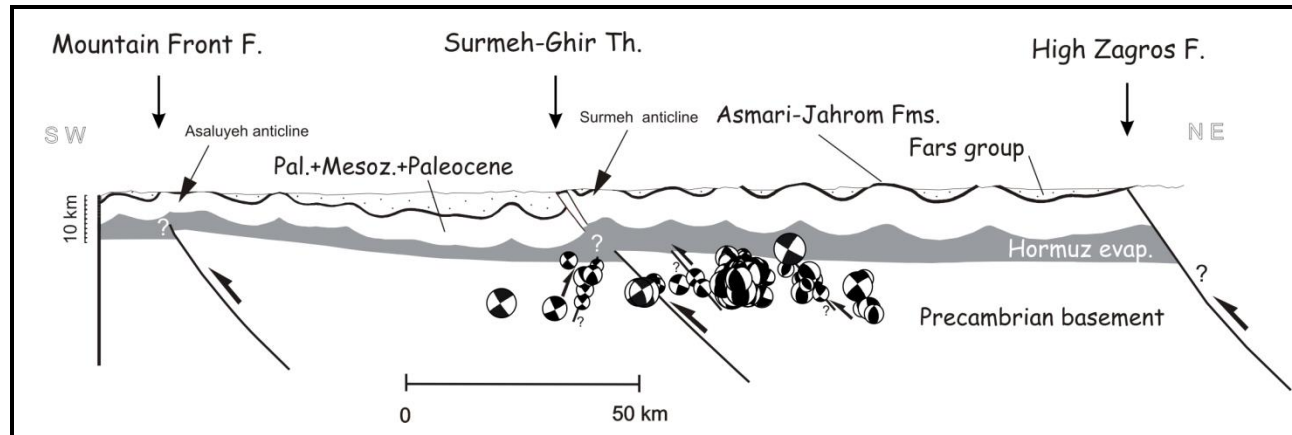
Taiwan (*Lacombe et al., 1996*)

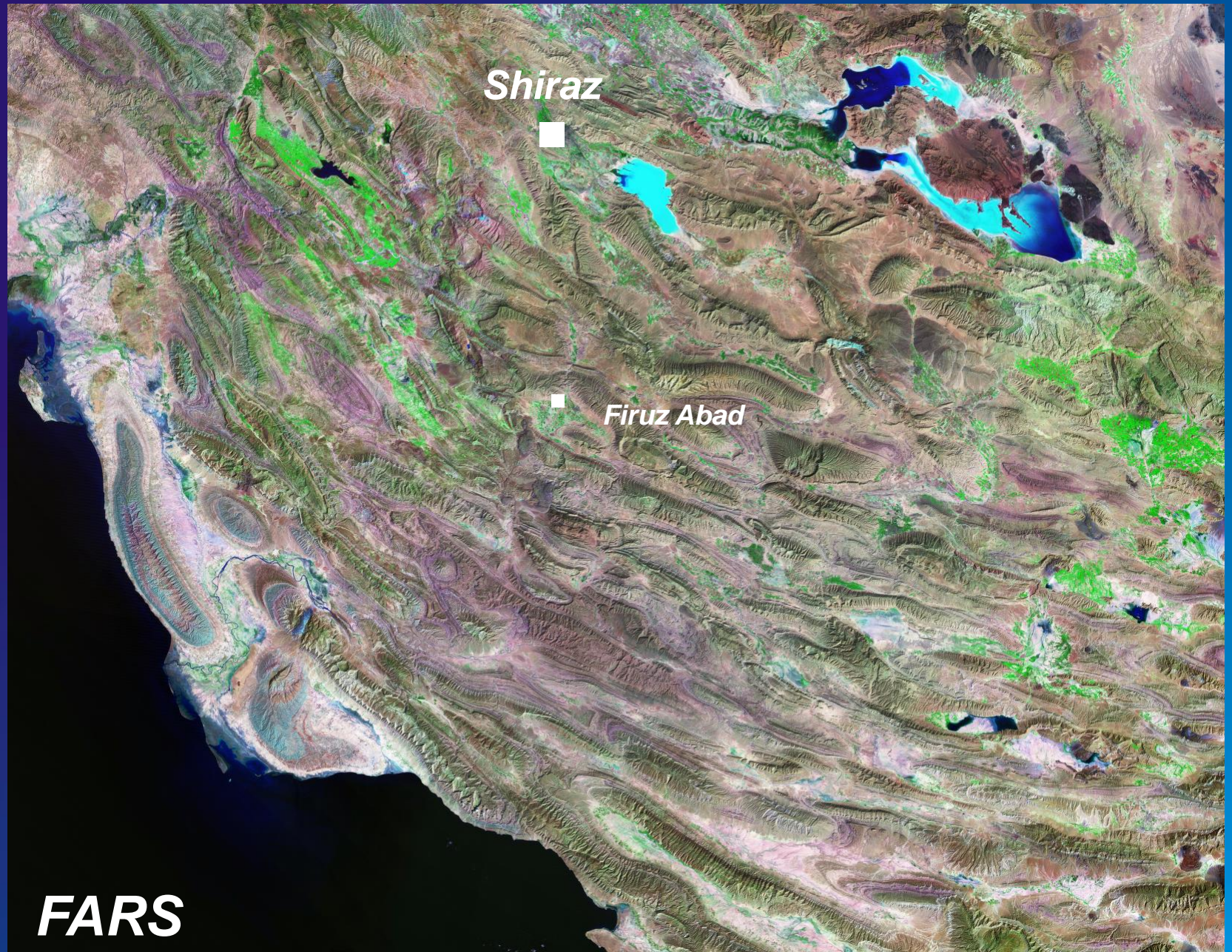
The Zagros belt results from the collision between Arabia and Central Iran, beginning in (Oligo ?)-Miocene times and continuing today.

About one third of the 22-25 mm/yr Arabia-Eurasia convergence is currently accommodated in the Zagros.



(Mouthereau et al., 2007;
Lacombe et al., 2006)





Shiraz

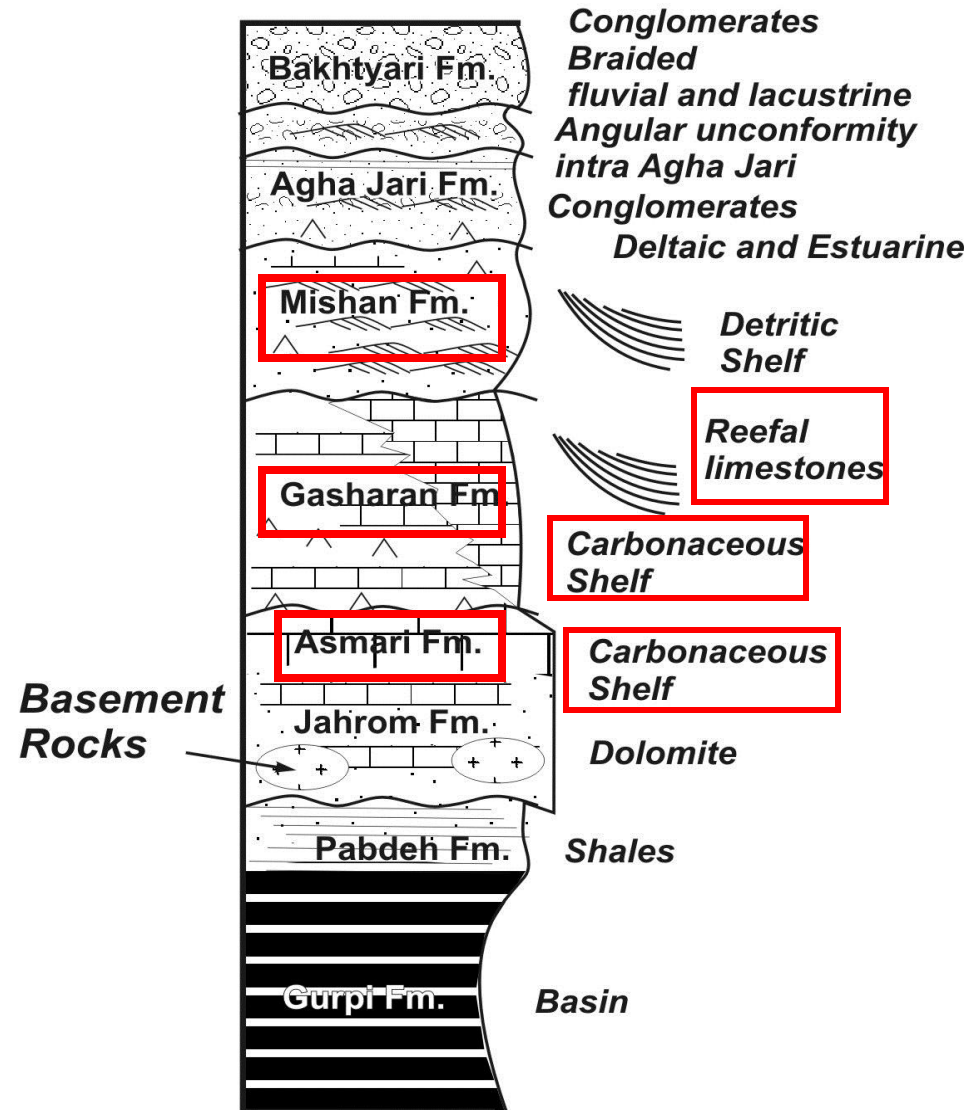


Firuz Abad

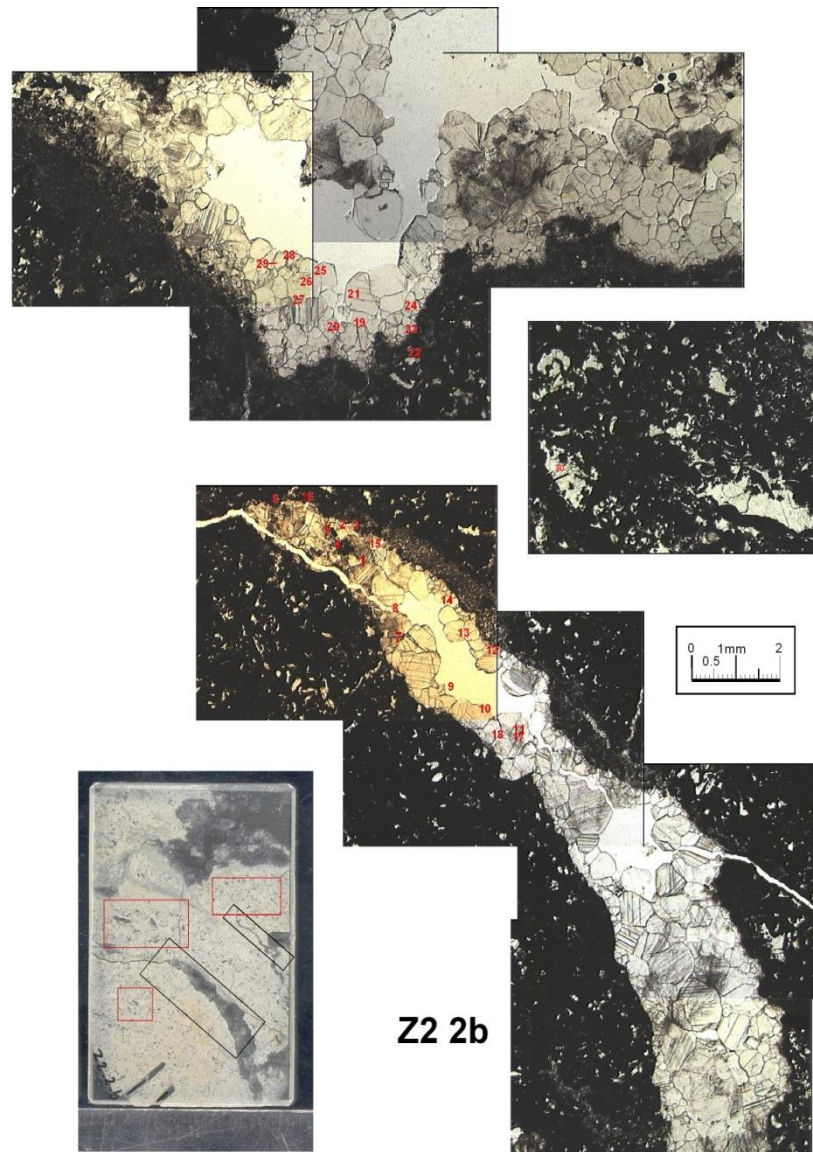
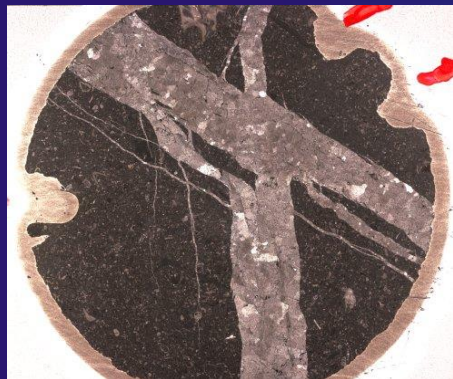
FARS

Oligocene Asmari Fm
and
Miocene Gasharan and
Mishan Fms
provide suitable
calcareous material
for calcite twin
analysis

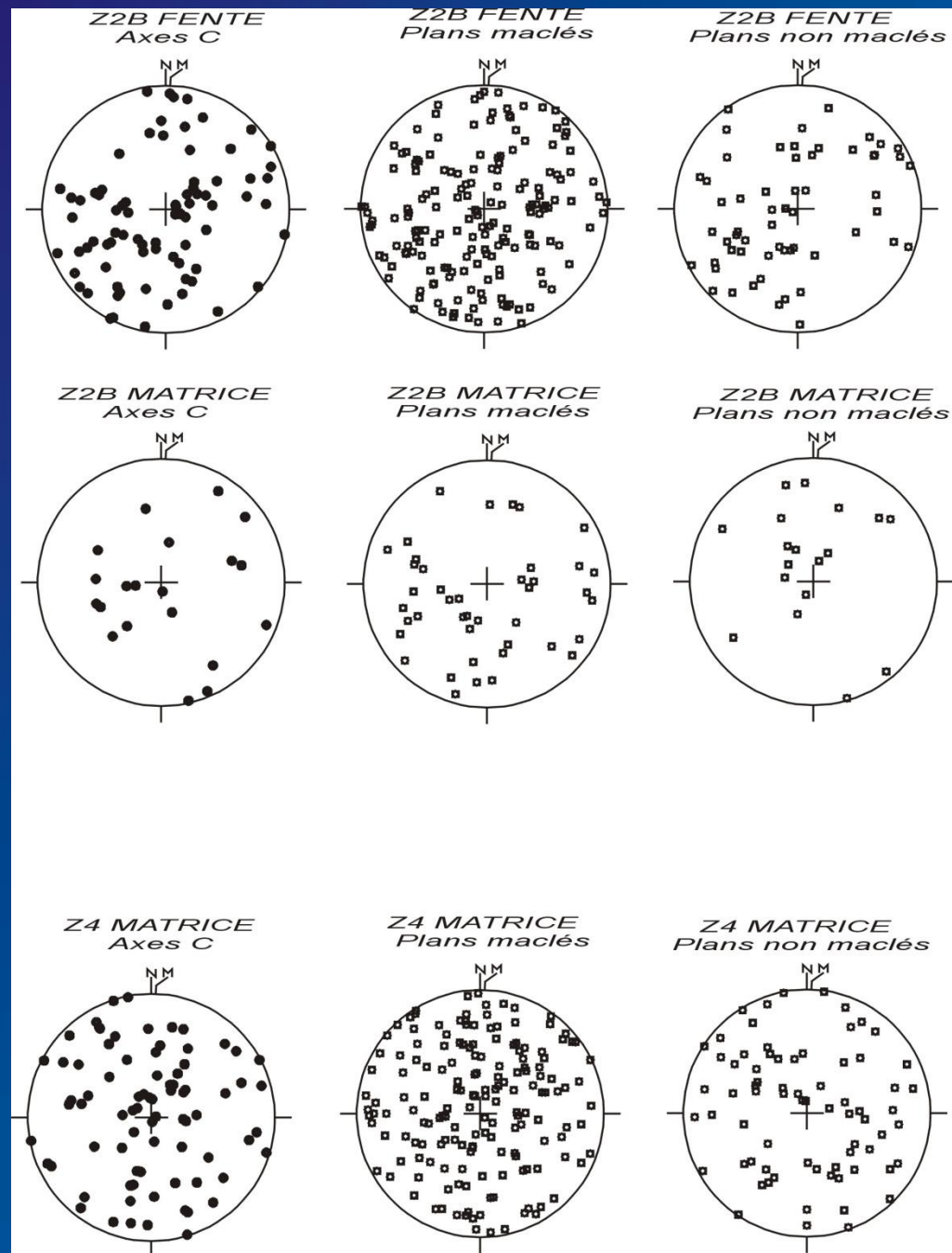
FARS



Twins are analysed within host rock matrix and veins from field samples and/or drill cores

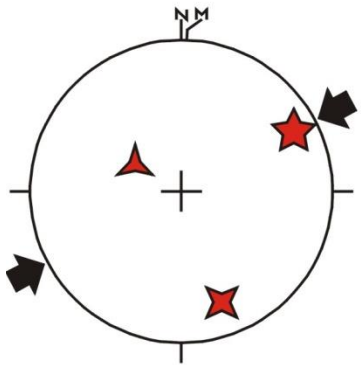


Spatial distribution of
C axes, and poles to
twinned and
untwinned planes
for 2 studied samples

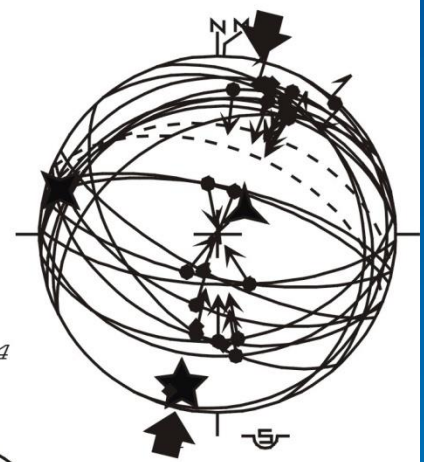
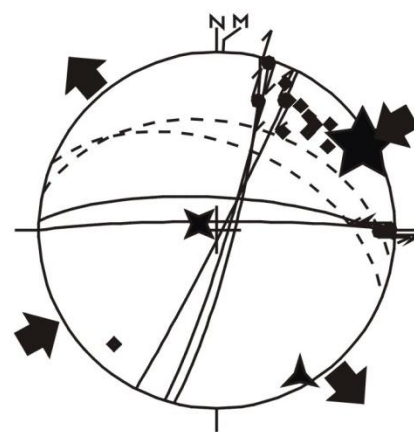


LM 044

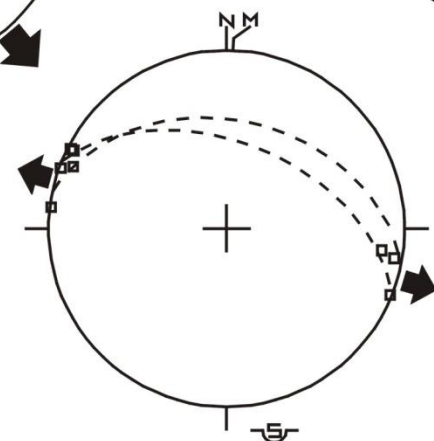
IRANO43



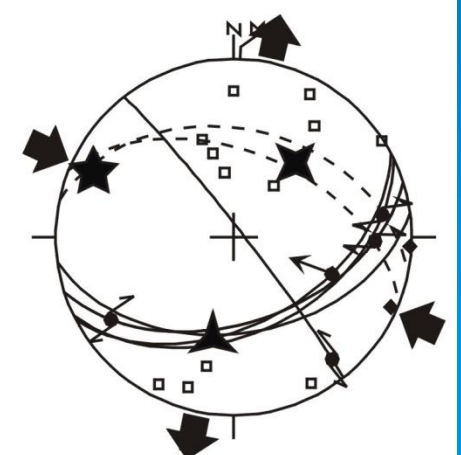
LM 044



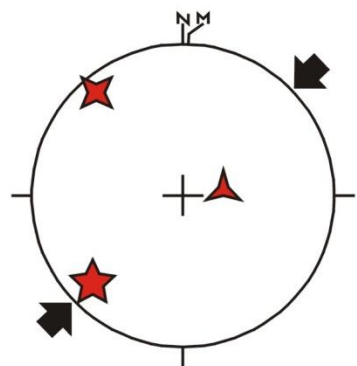
LM 044



LM 044

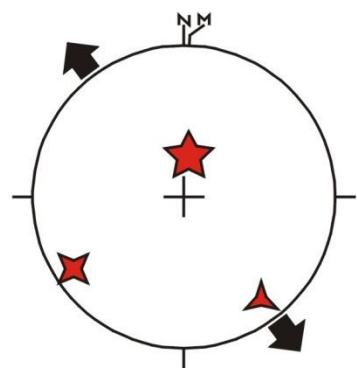


IRANO43

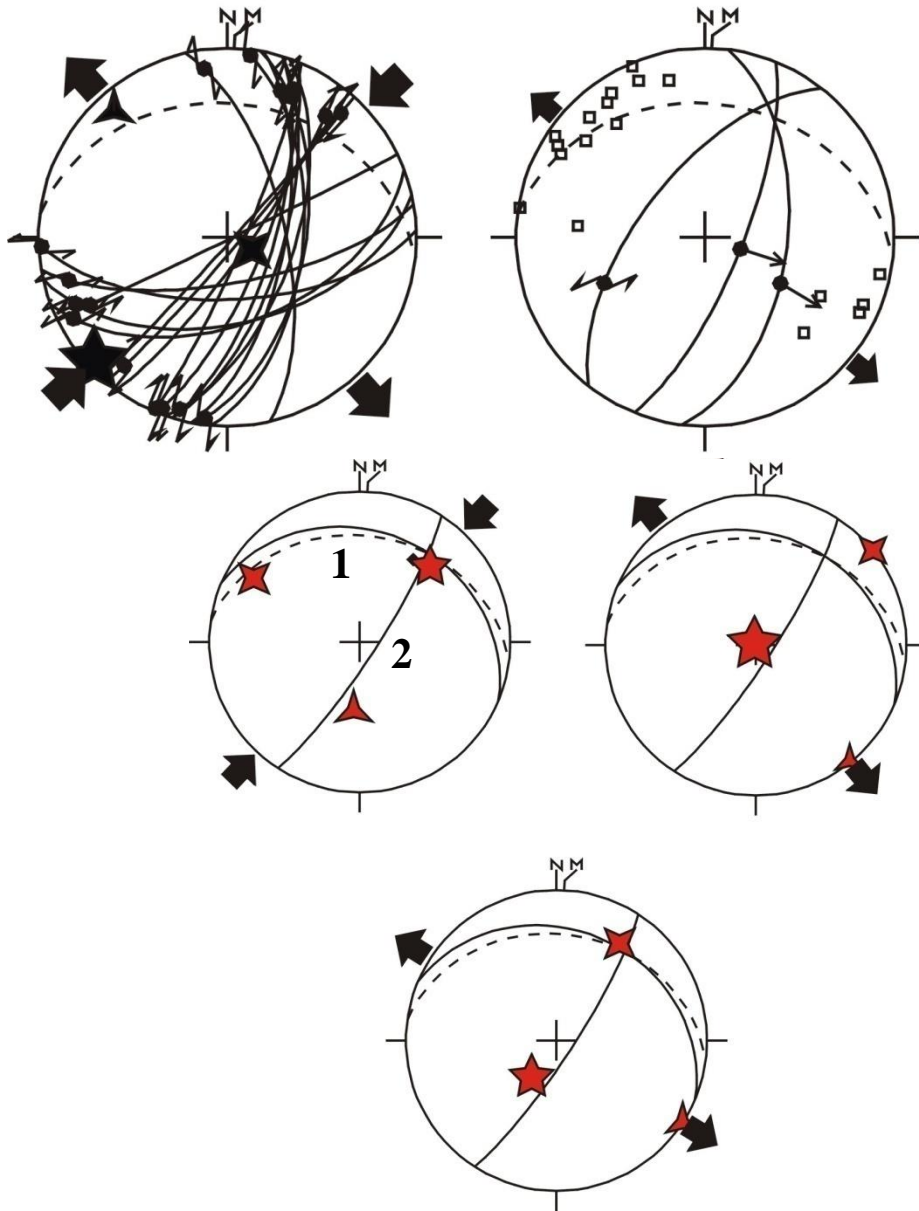


Stress tensors computed from calcite twin data

IRANO43



Stress tensors computed from fault slip data



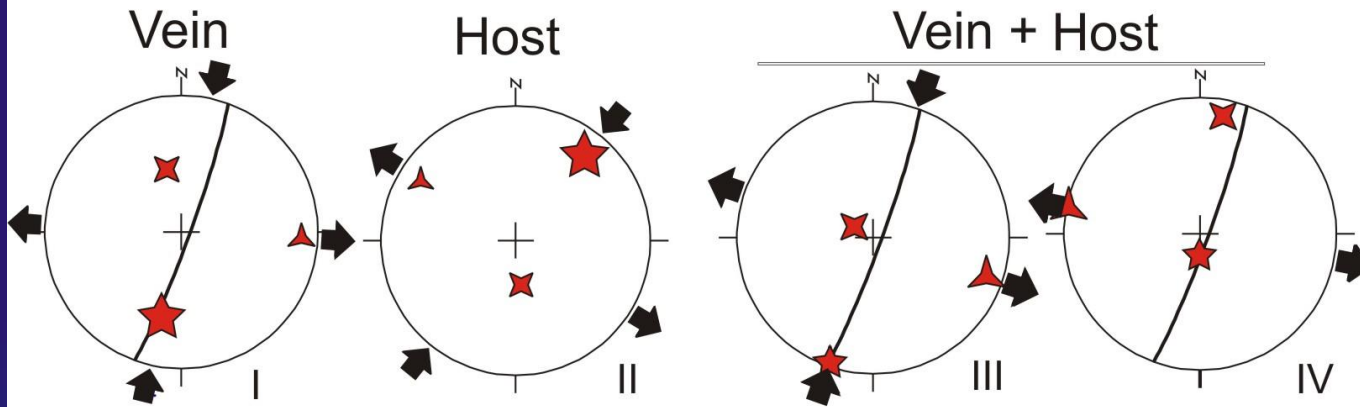
Data coming from host rocks and/or syn-folding veins are treated separately or together to check for internal consistency. Consistency with fracture and fault-slip data is also checked

Tensors determined from vein 1

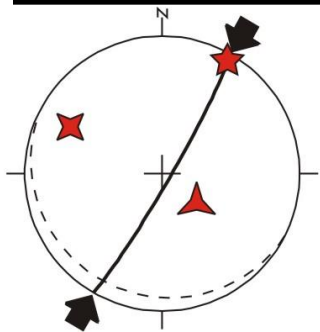
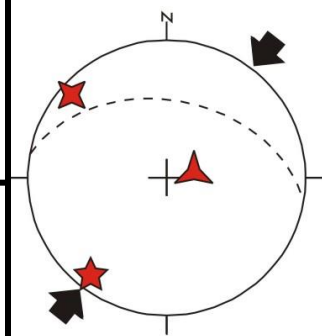
Tensor determined from vein 2

Data coming from host rocks and/or syn-folding veins are treated separately or together to check for consistency

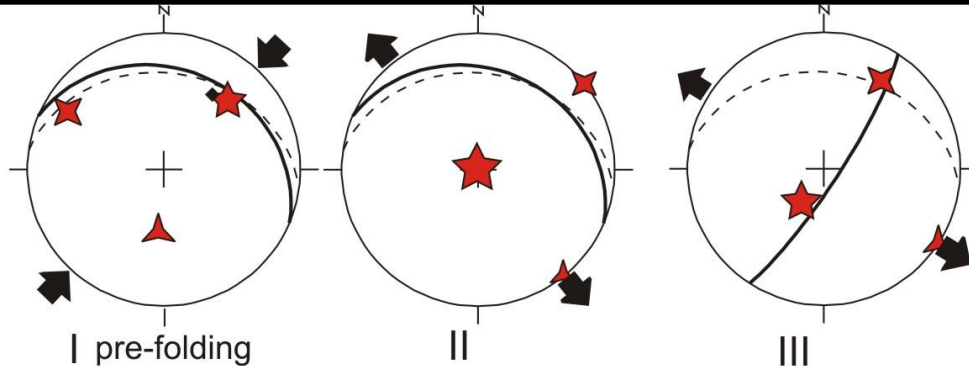
Sample 13



Sample 11



Sample 2 Vein



Vein

Vein

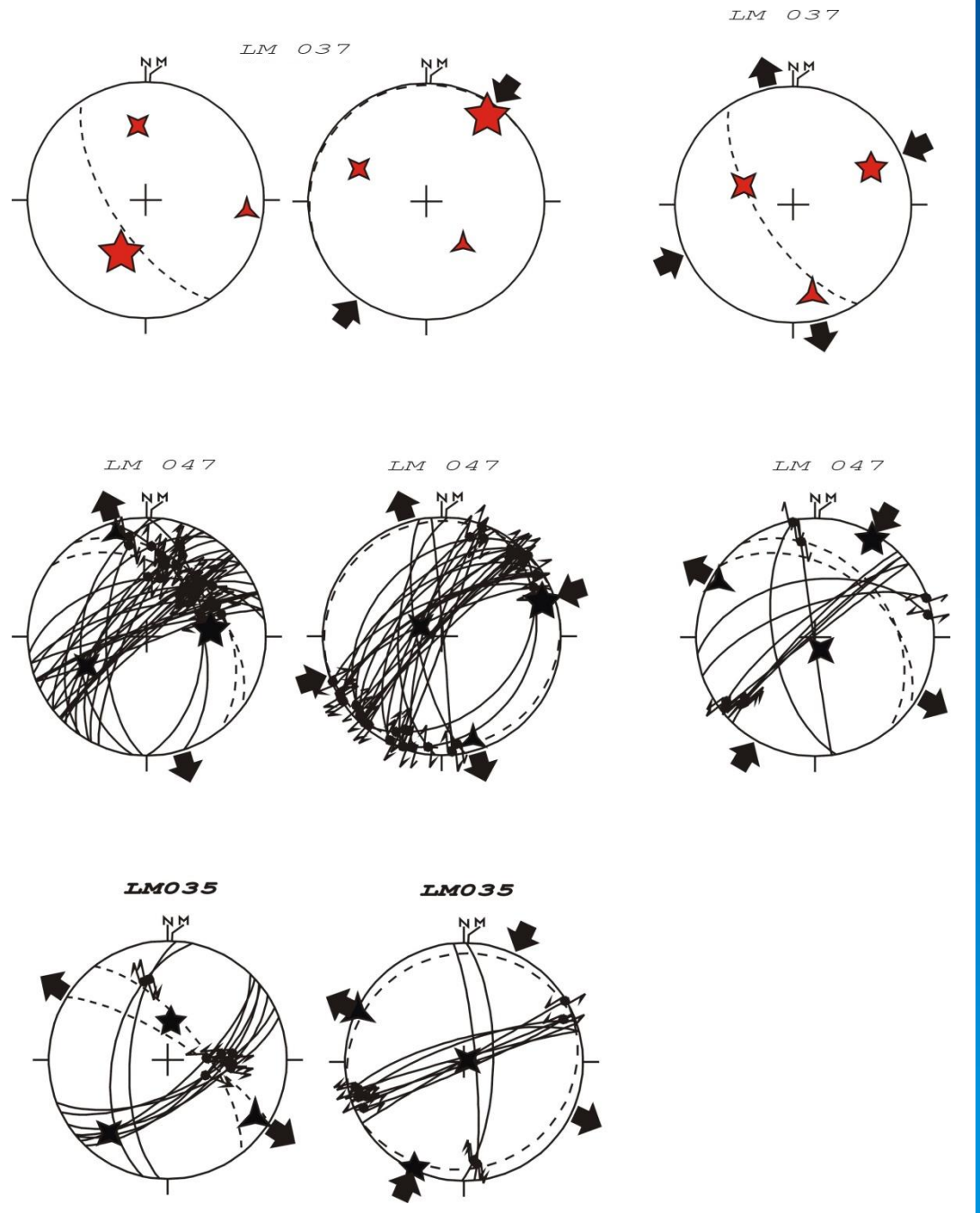
Sample 1

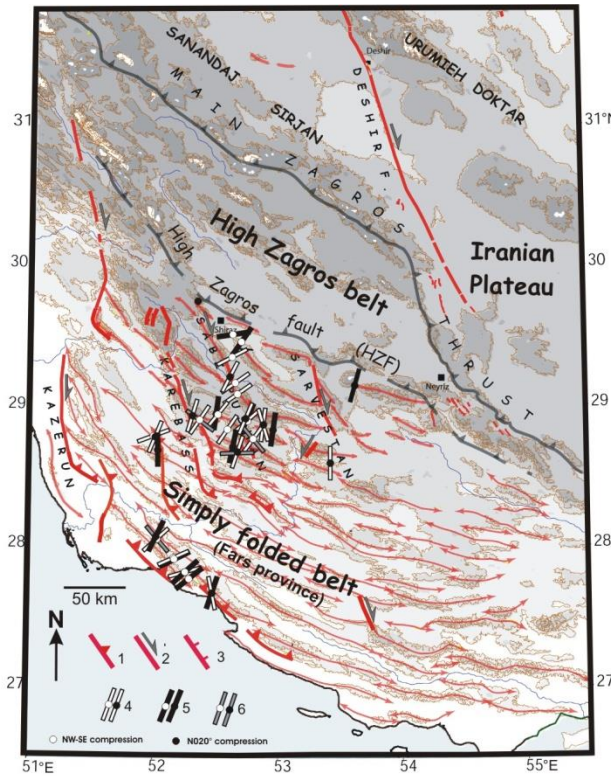
Sampling in fold limbs allows establishing a relative chronology between twinning strain and folding



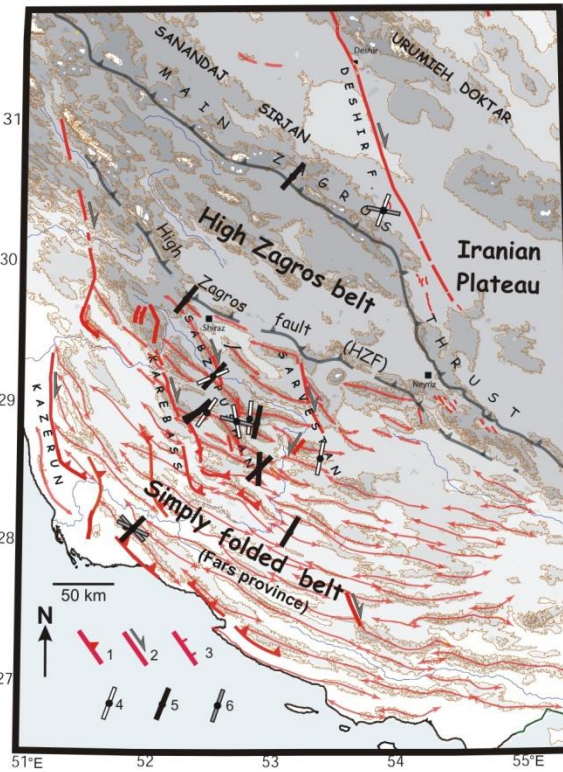
Sampling in fold limbs
allows establishing a relative
chronology
between twinning strain
and folding

Fault slip data and
calcite twin data
indicate that the NE-SW
compression prevailed
before and after folding,
and therefore is
responsible for folding

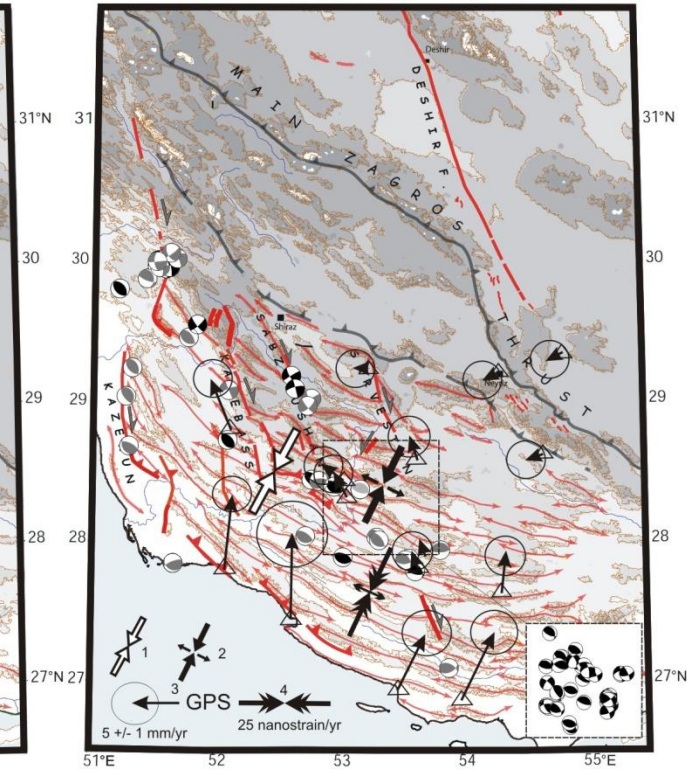




Neogene compressional trends from fault slip data in the cover (Lacombe et al., 2006)

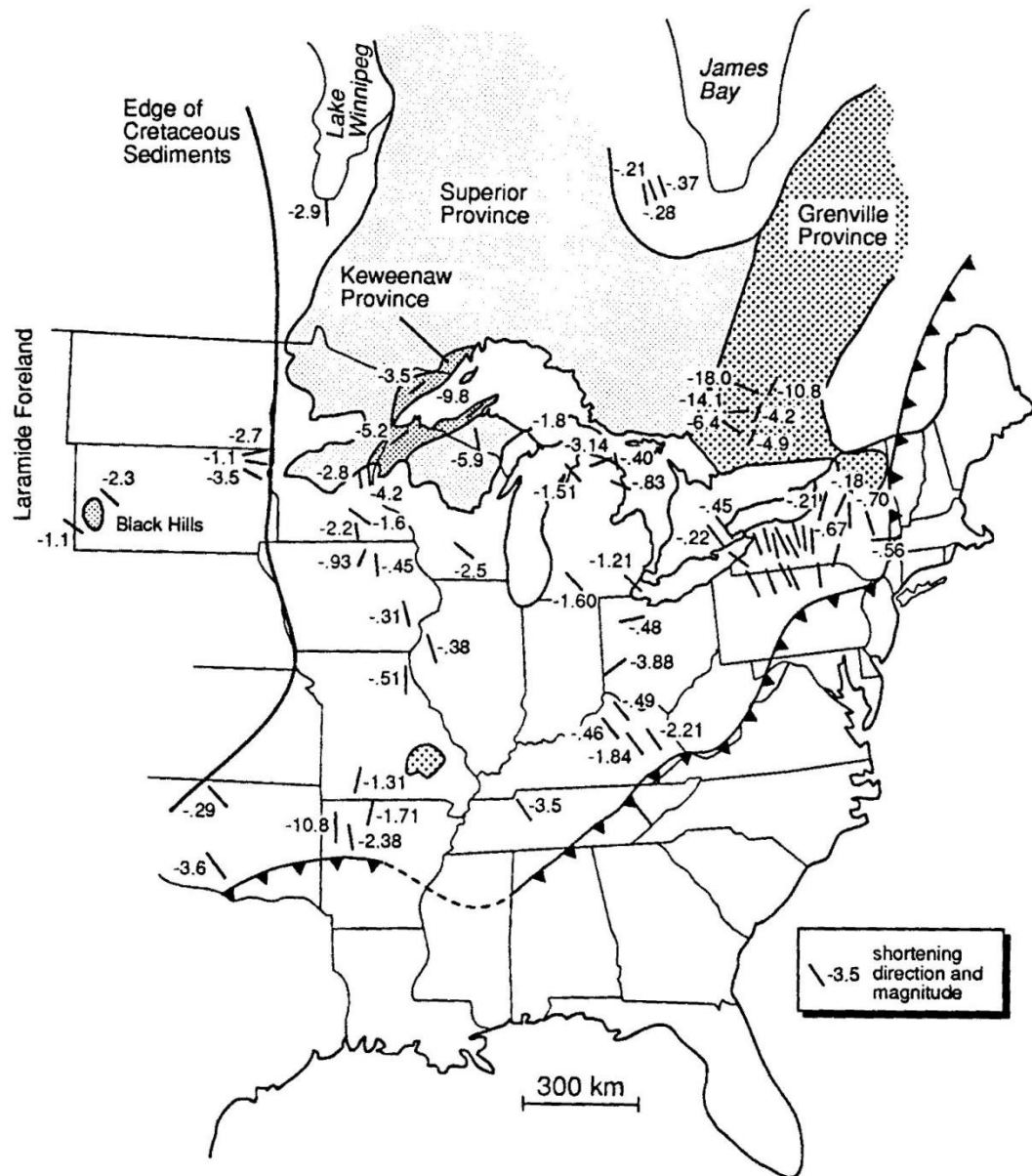


Neogene compressional trends from calcite twin data in the cover (Lacombe et al., 2007)



Current compressional trends from earthquake focal mechanisms in the basement (Lacombe et al., 2006) and GPS shortening rates (Walpersdorf et al., 2006)

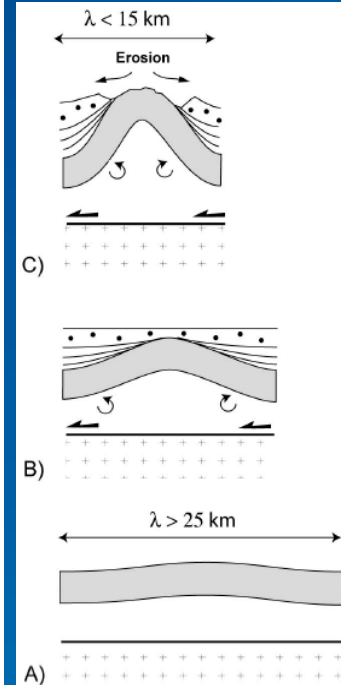
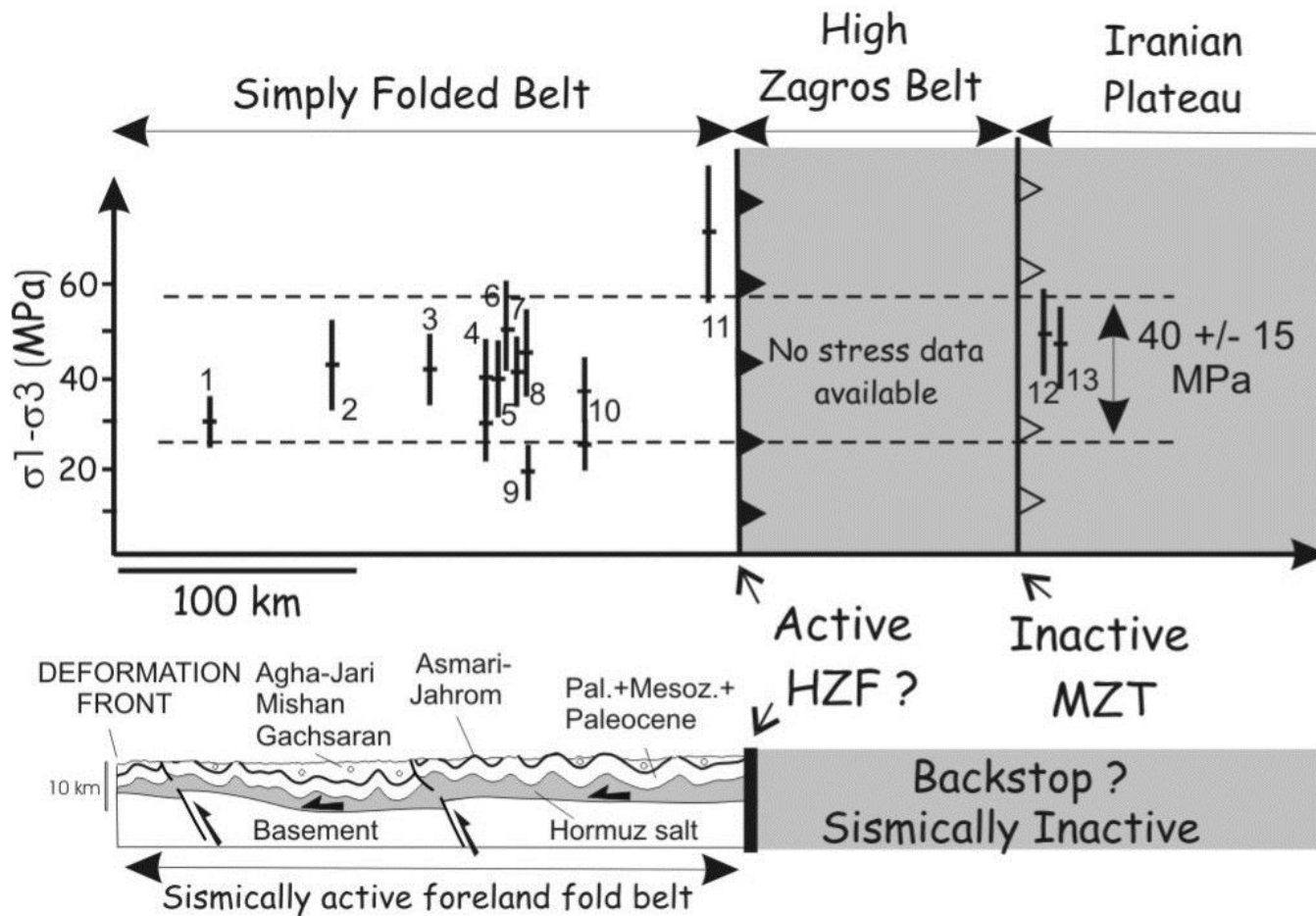
→ Neogene collisional stresses consistently recorded at all scales



(Craddock et al.,
1993)

**Differential stress magnitudes
in fold-and-thrust belts and orogenic forelands
Some examples**

(Lacombe et al.,
Geology,
2007)

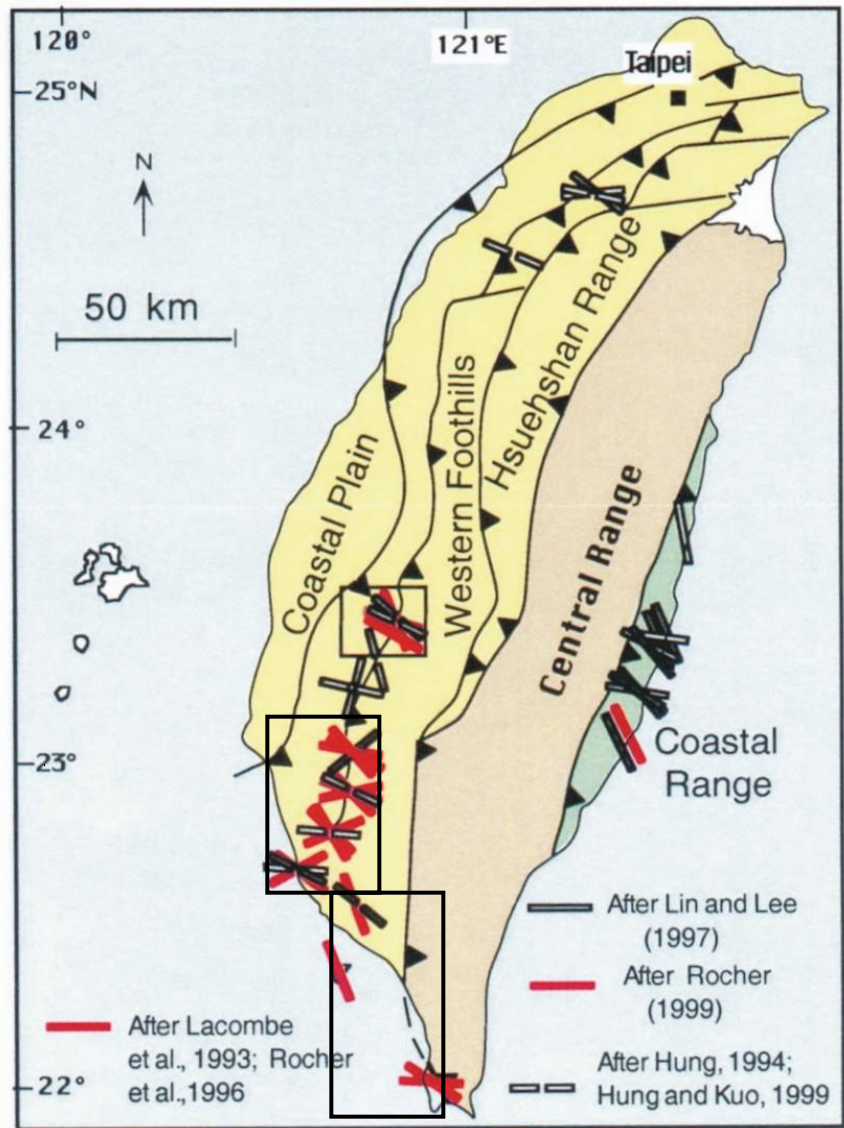


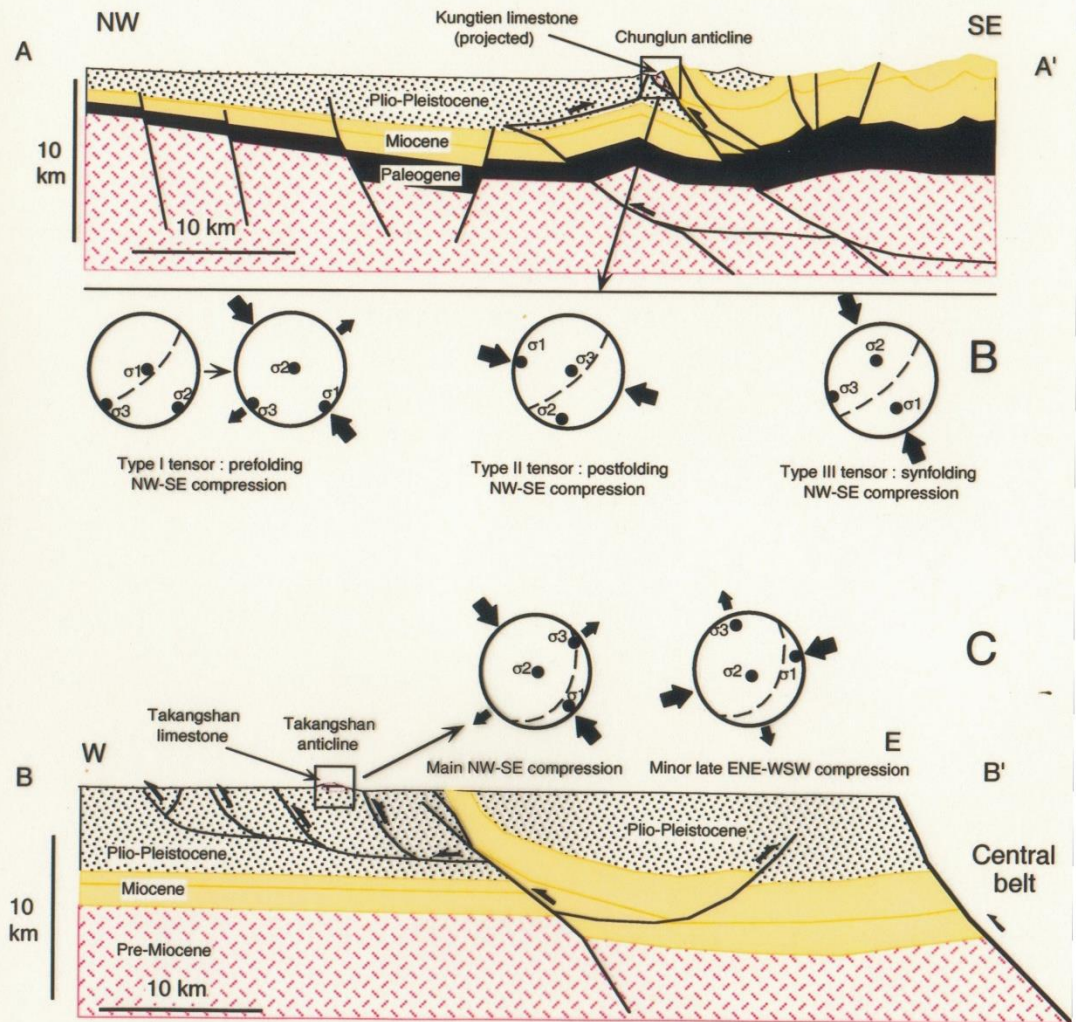
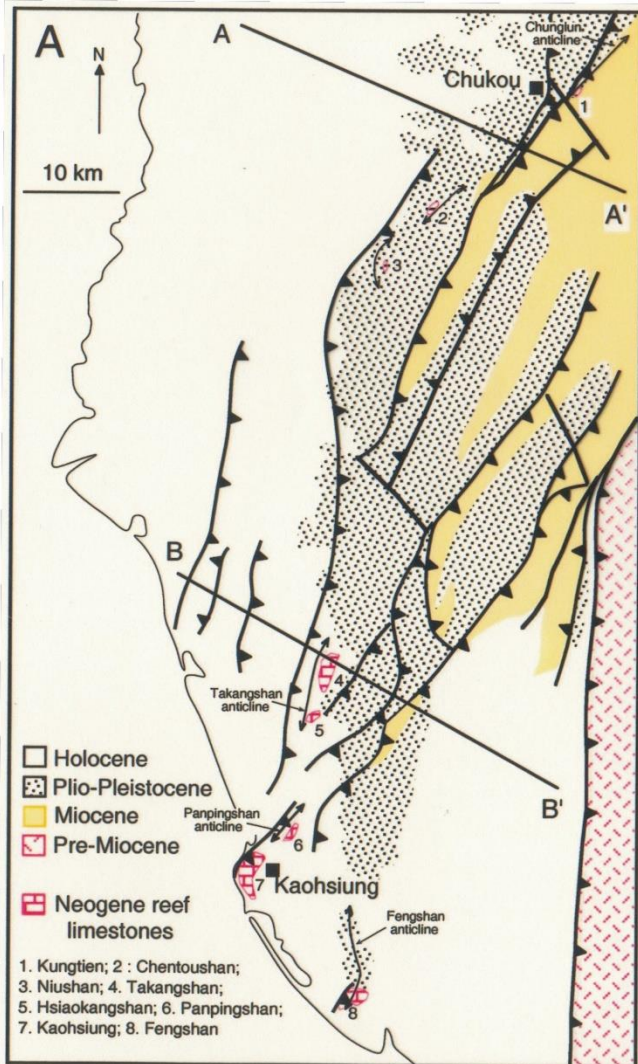
The relative homogeneity of differential stresses agrees with the homogeneously distributed shortening across the SFB, where no deformation gradient toward the backstop is observed in contrast to classical fold-thrust wedges

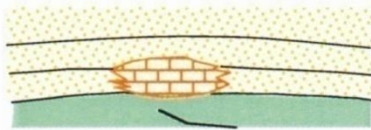
Both pre- and post-folding differential stresses are low --> folding likely occurred at low stresses; this favours pure-shear deformation and buckling of sedimentary rocks rather than brittle tectonic wedging.

Arabia-Eurasia collisional stresses were consistently recorded by calcite twinning in the detached cover of the Zagros (Fars).

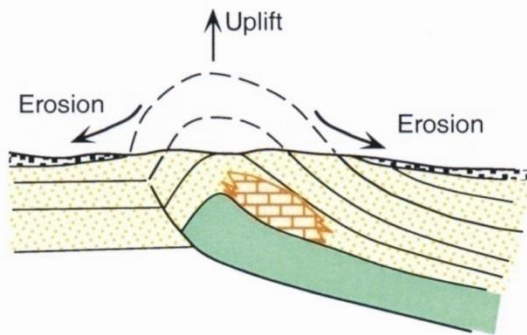
Calcite twinning paleopiezometry reveals an unexpected low level and first-order homogeneity of differential stresses across the SFB, which supports an overall mechanism of buckling of the cover sequence.



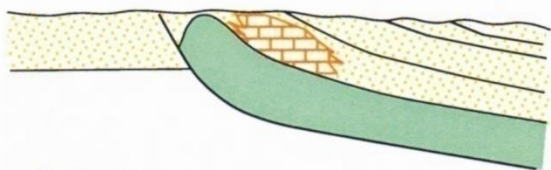




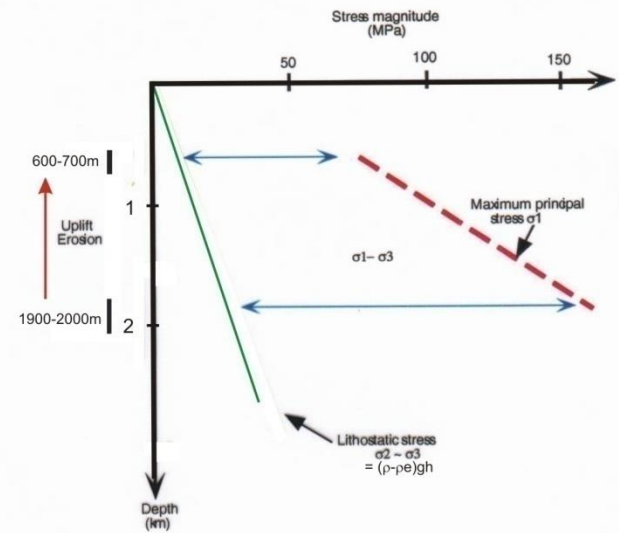
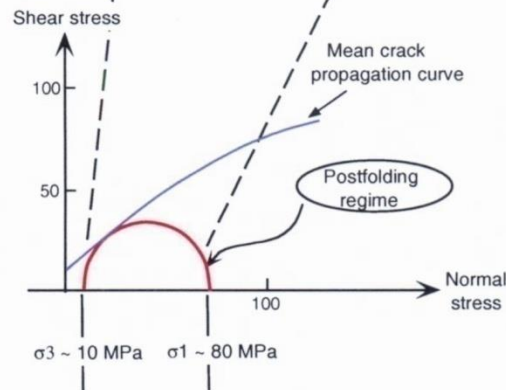
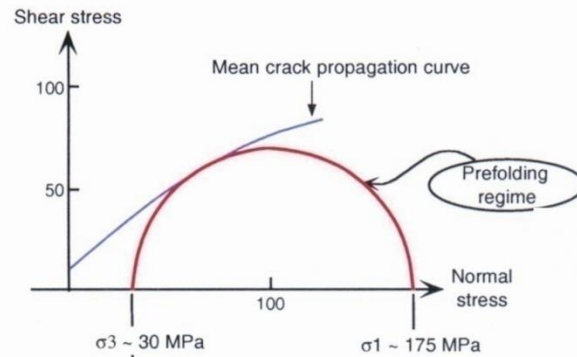
A Prefolding compression (LPS)
Main twinning event

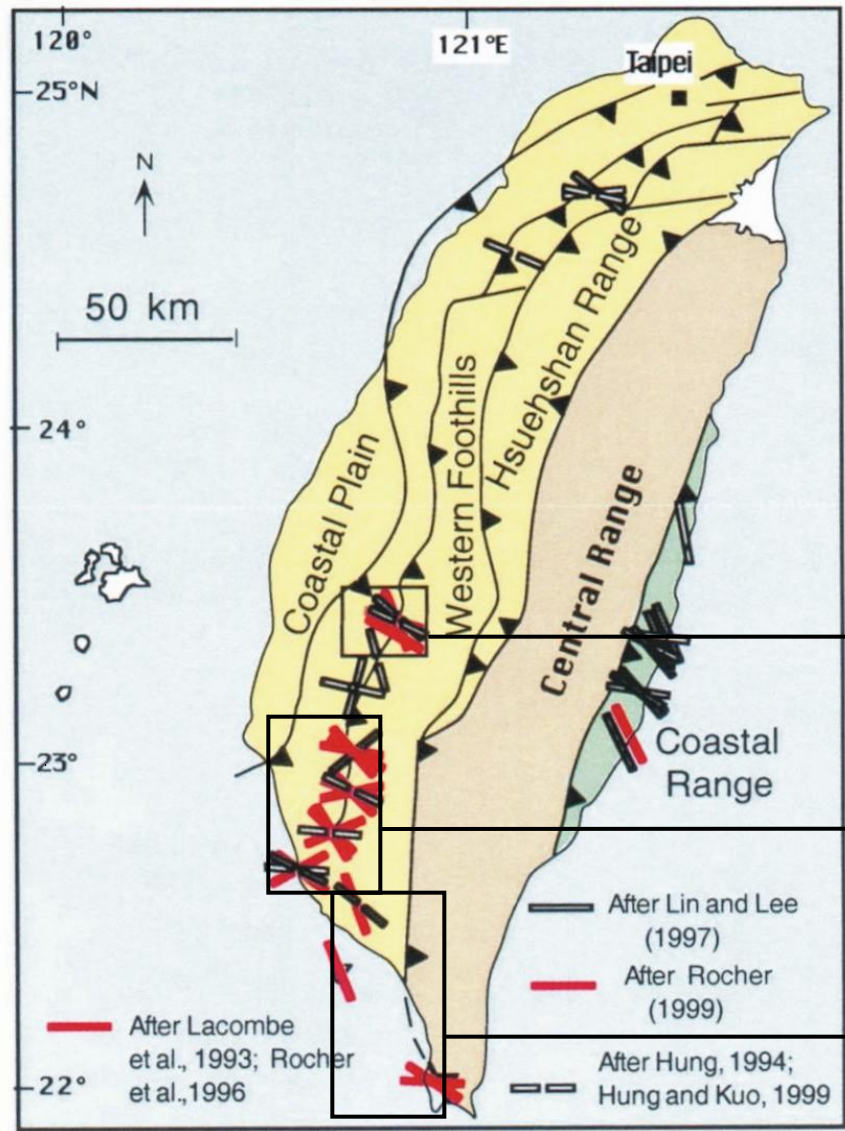


B Synfolding compression and erosion



C Postfolding compression
Main twinning event





After removing the effect of lateral variations of burial...

~ 140 MPa
~ 70 MPa

~ 60 MPa

~ 25-35 MPa

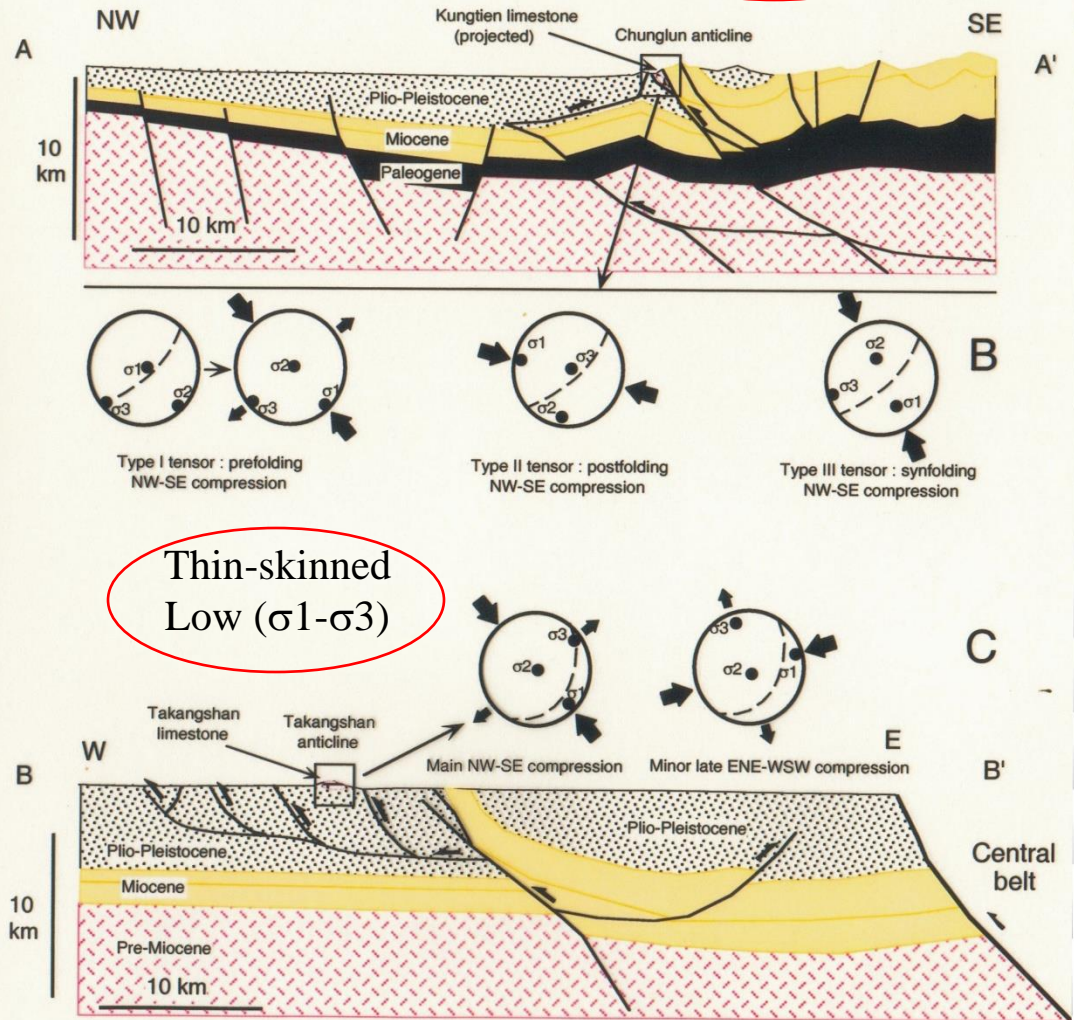
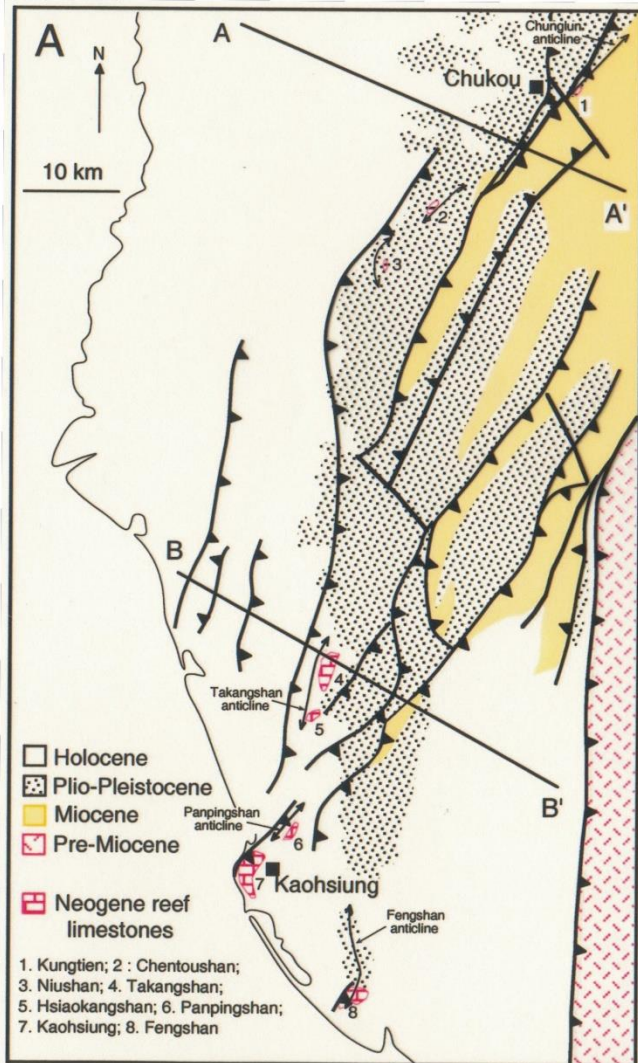
Differential stress decrease

« Collision » stage
Thick-skinned tectonics

« Accretionary wedge » stage
Thin-skinned tectonics

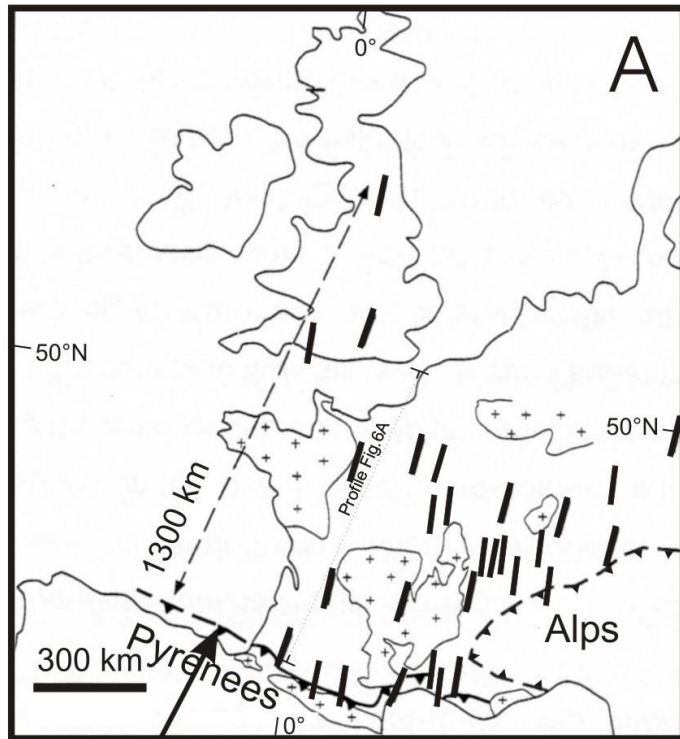
After removing the effect of lateral variations of burial...

Thick-skinned High (σ_1 - σ_3)

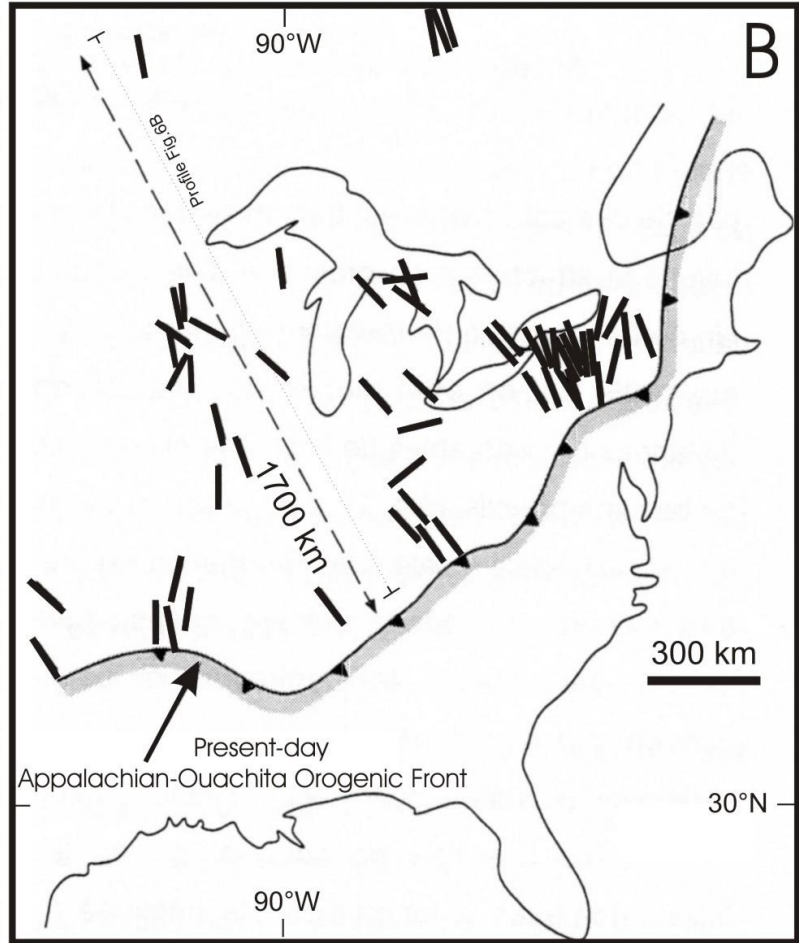


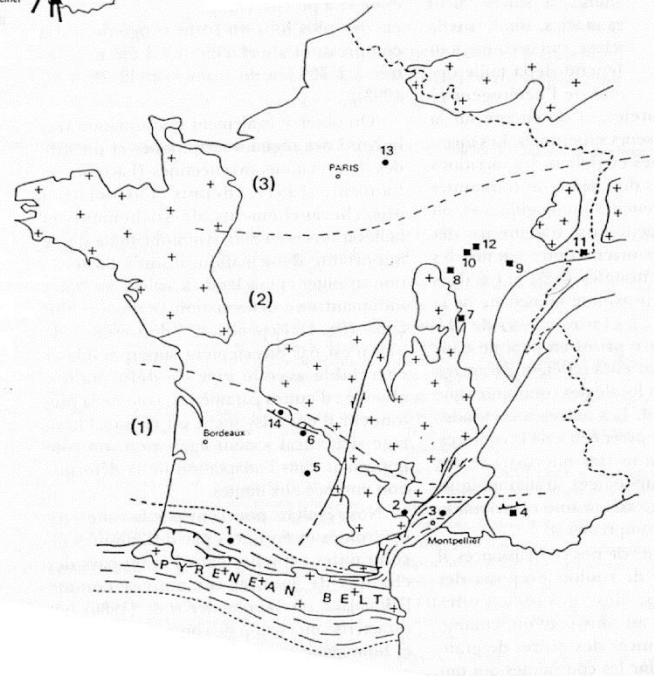
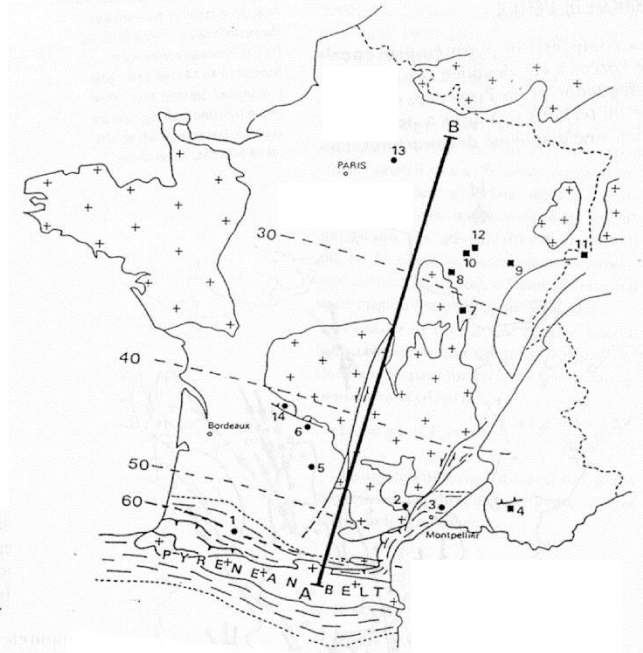
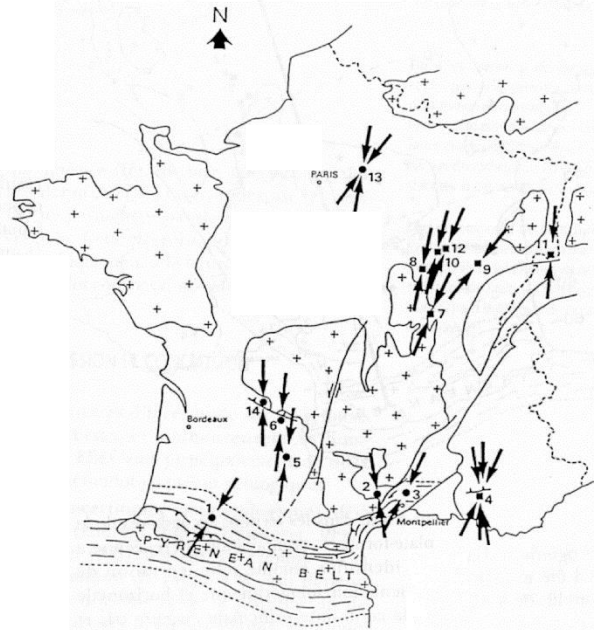
Thin-skinned Low (σ_1 - σ_3)

Calcite twinning analyses in Taiwan Foothills document possible along-strike changes in differential stress magnitudes recorded by cover rocks depending on the tectonic style.

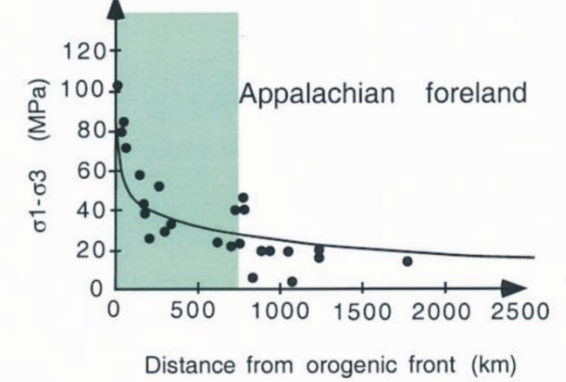
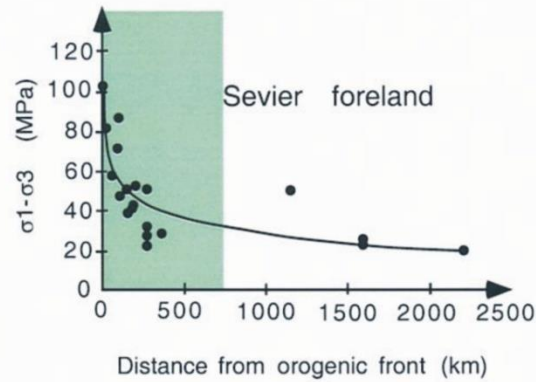
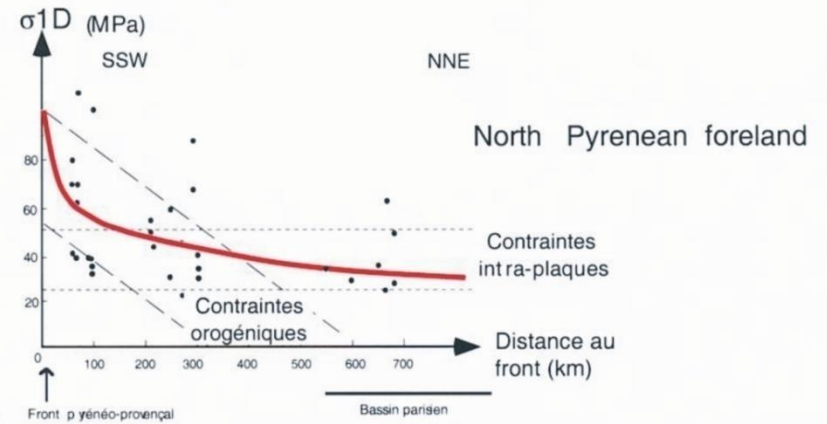
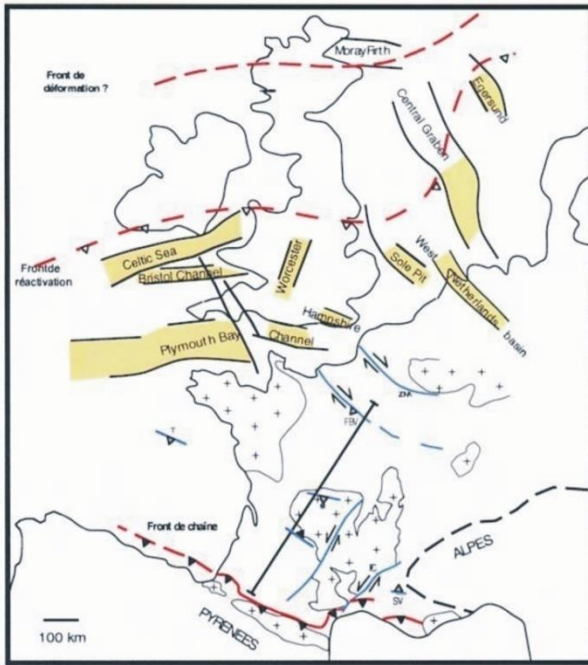


Present-day
Pyrenean-Alpine Orogenic Front

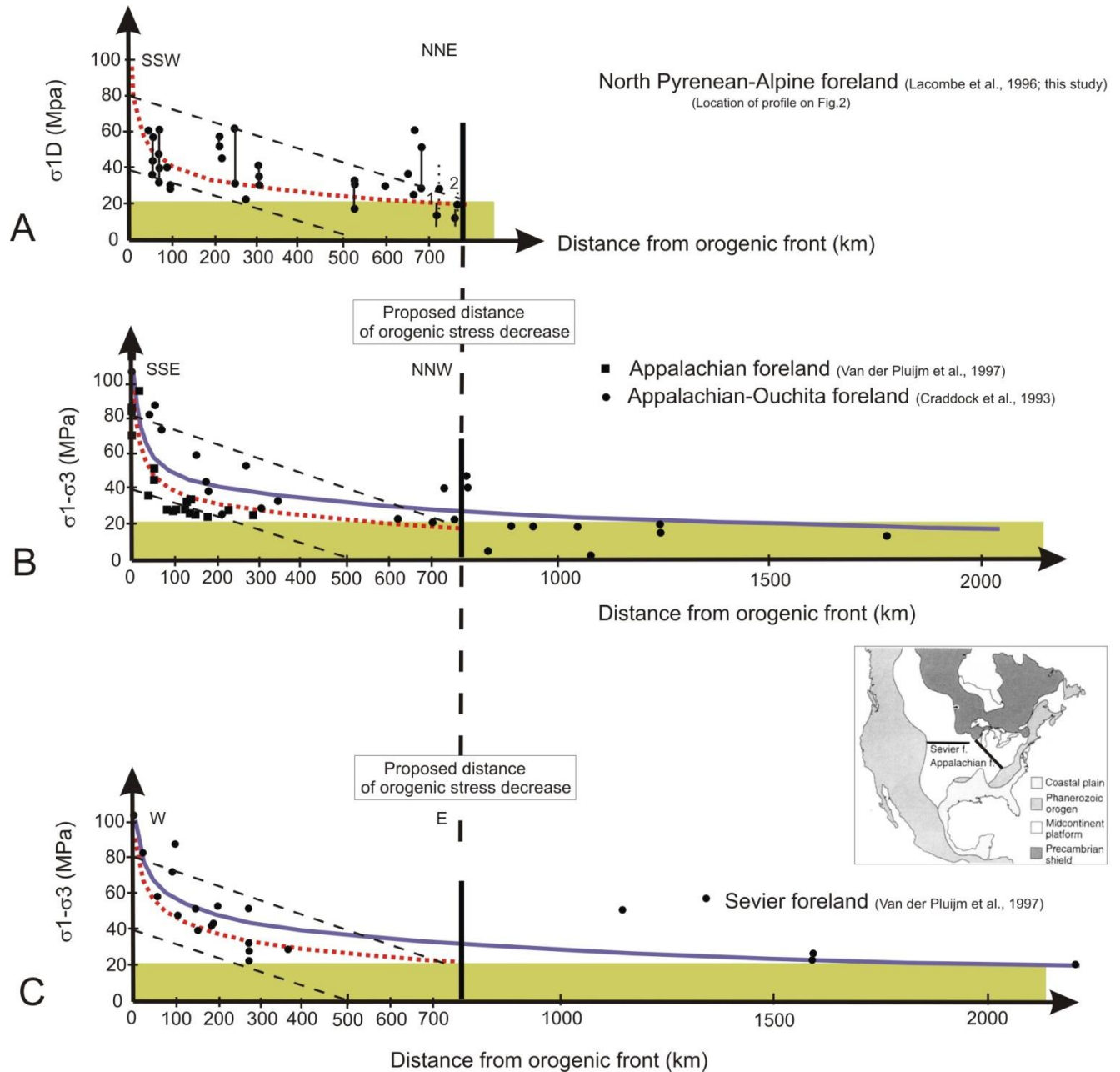




(Lacombe et al., 1996)



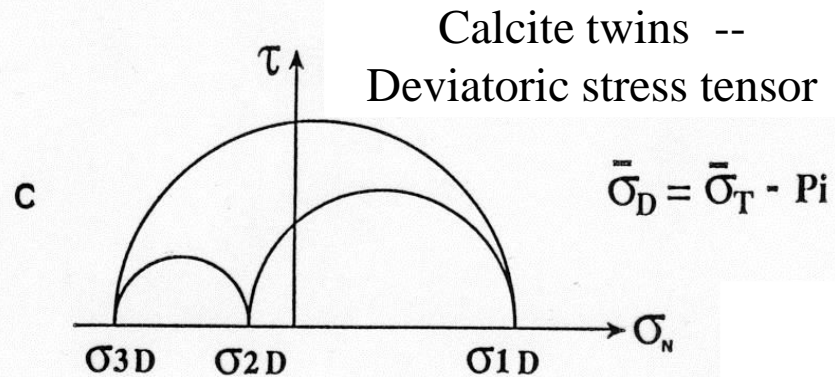
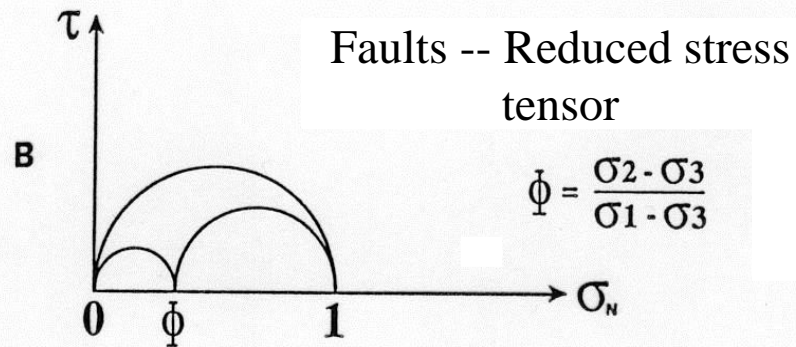
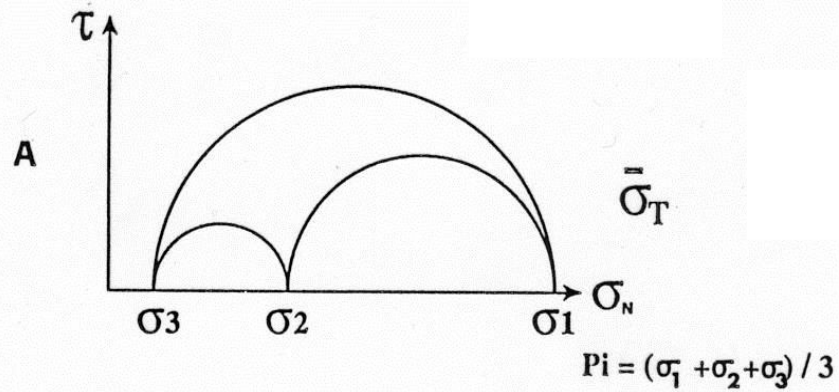
(Lacombe et al., 1996;
Lacombe, 2000)

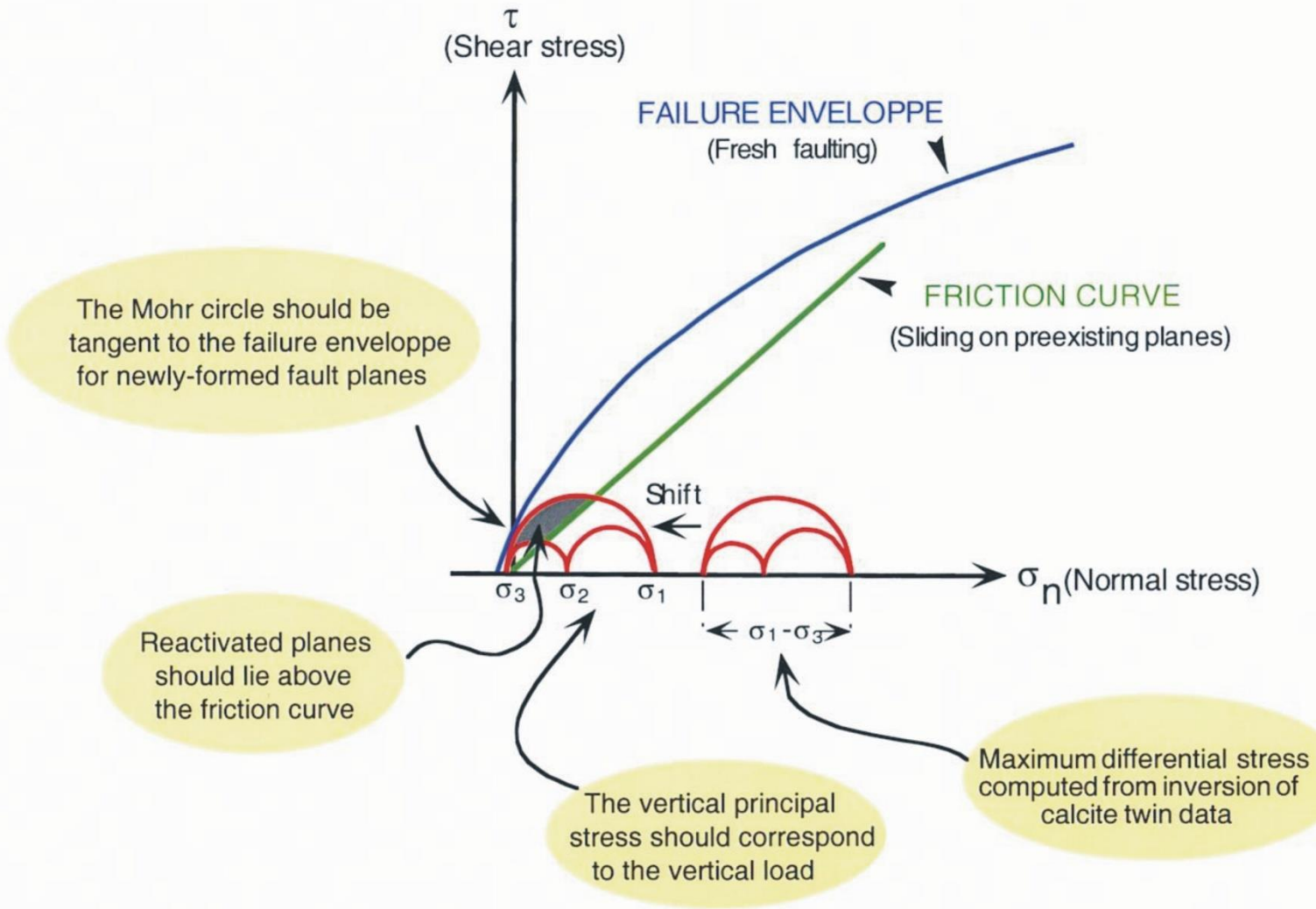


(Lacombe, 2010)

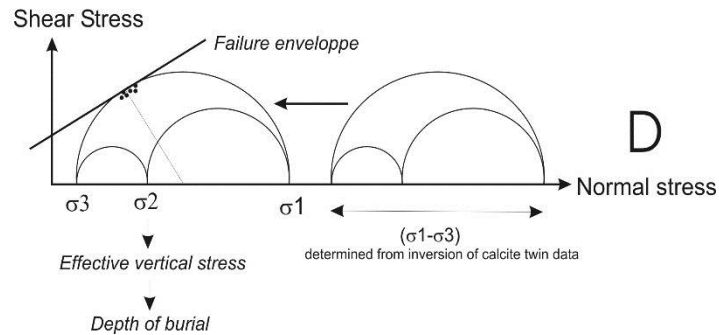
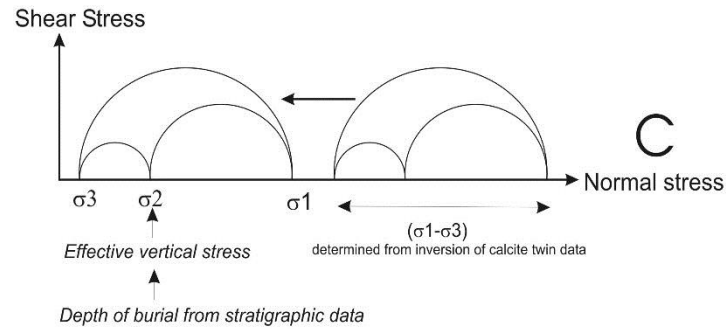
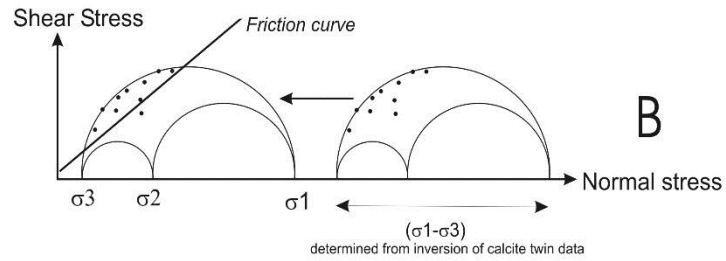
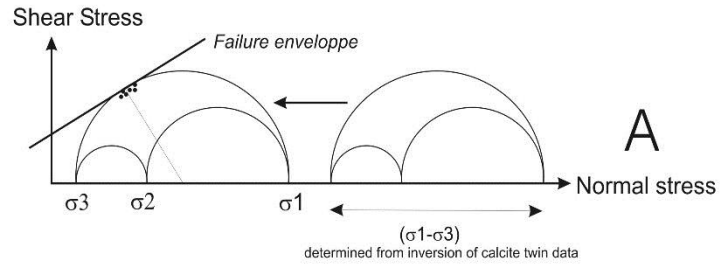
Calcite twinning analyses in orogenic foreland possibly document a decrease of differential stress magnitudes with increasing distance to the belt

**Determination of principal stress magnitudes,
(i.e., the complete stress tensor)**

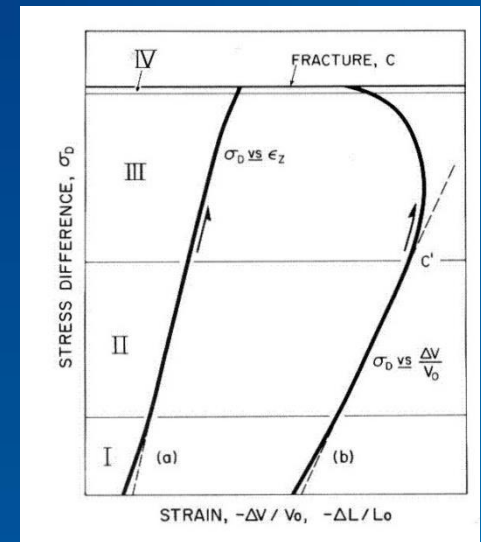
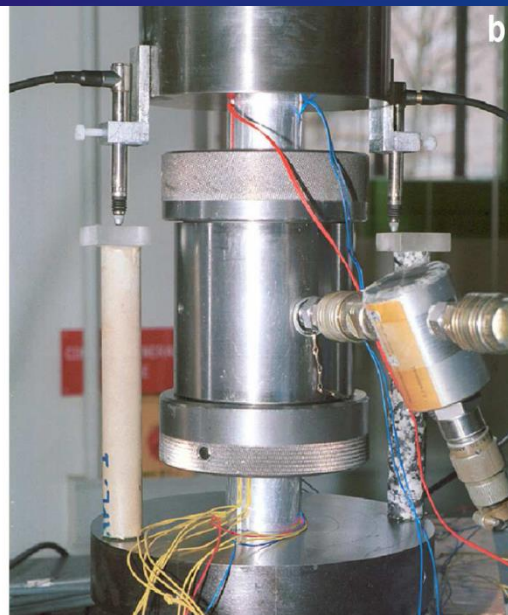
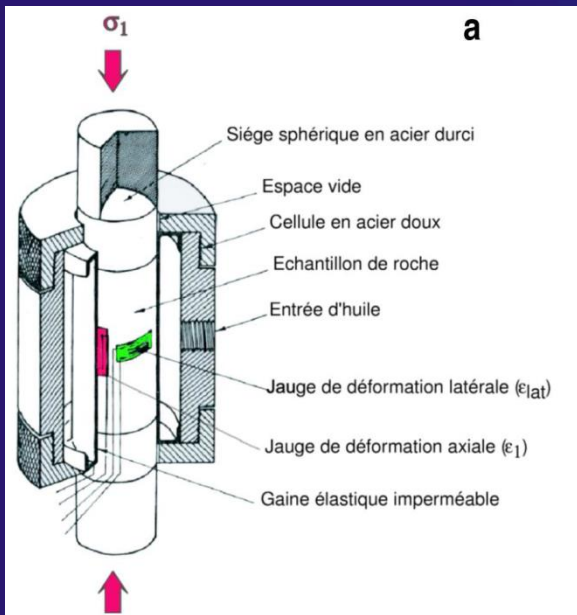




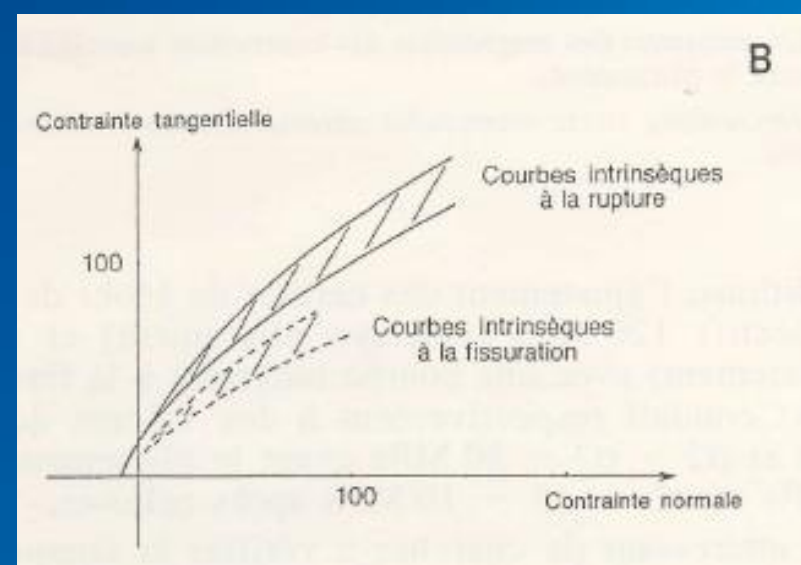
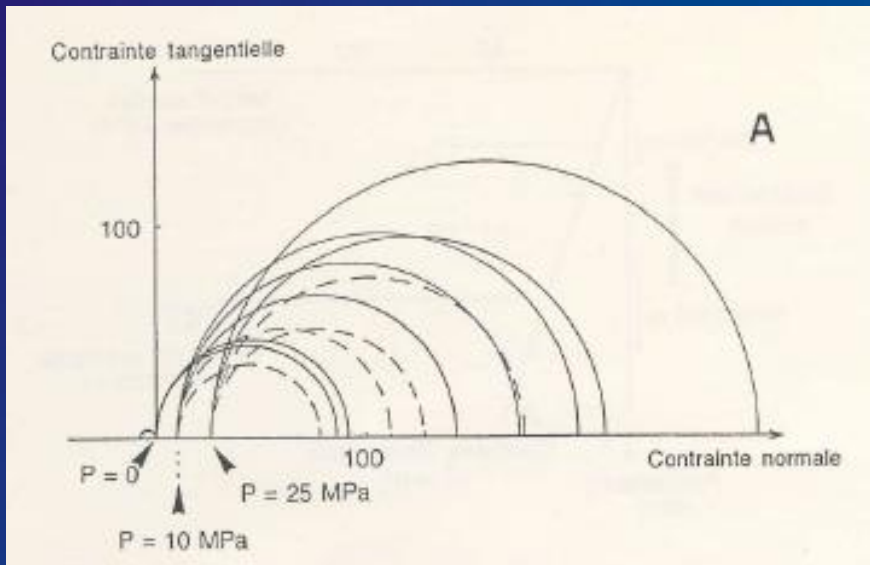
(Lacombe, 2001; modified after Lacombe et Laurent, 1992)

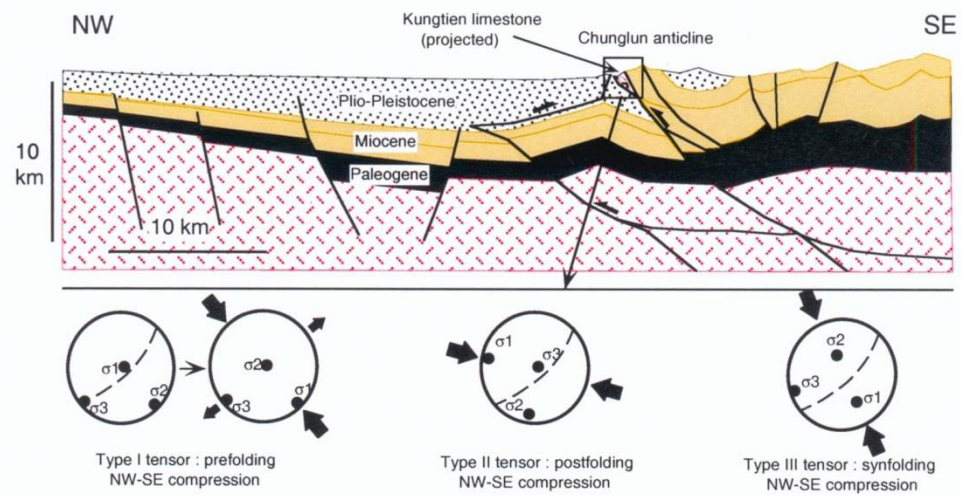
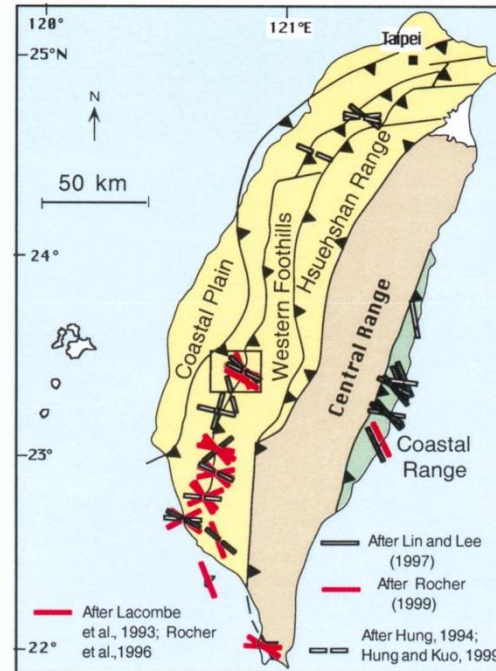


*(Lacombe, 2007;
Modified after
Lacombe et al., 1996)*

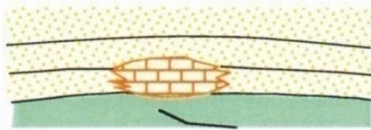


Experimental determination of the intrinsic failure envelopes of the Yutengping limestone

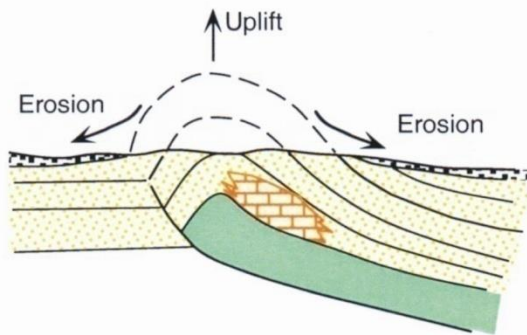




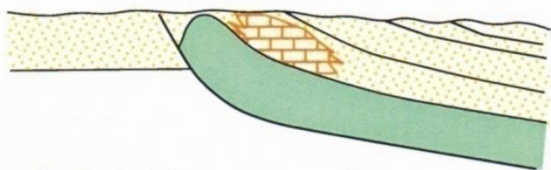
(Lacombe, 2001)



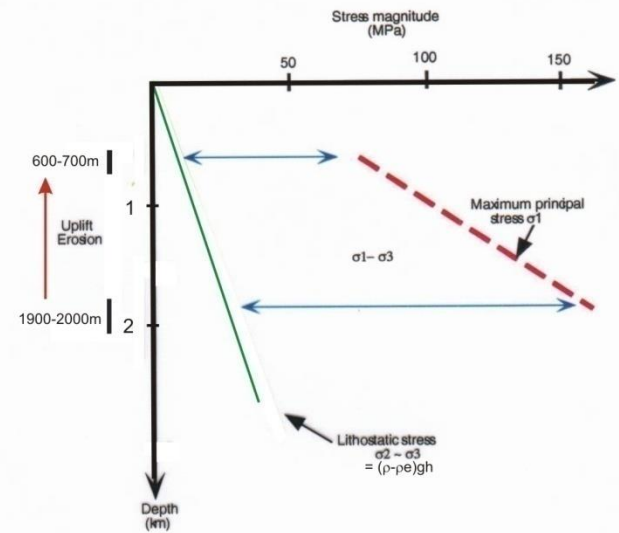
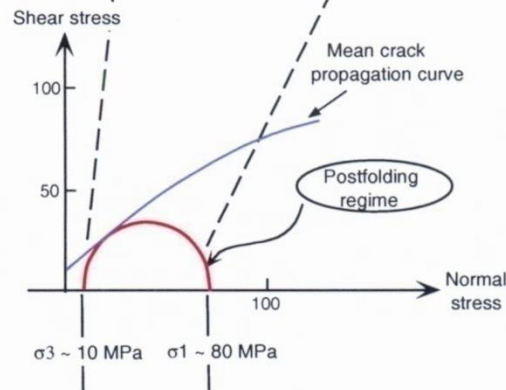
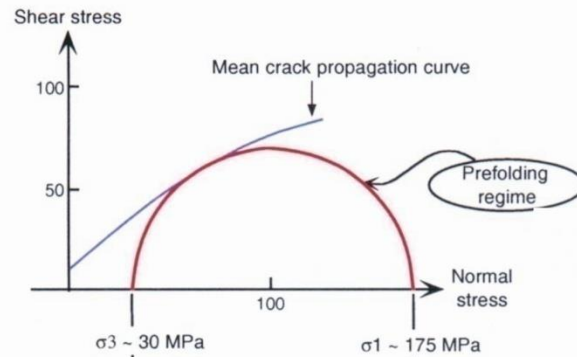
A Prefolding compression (LPS)
Main twinning event



B Synfolding compression and erosion

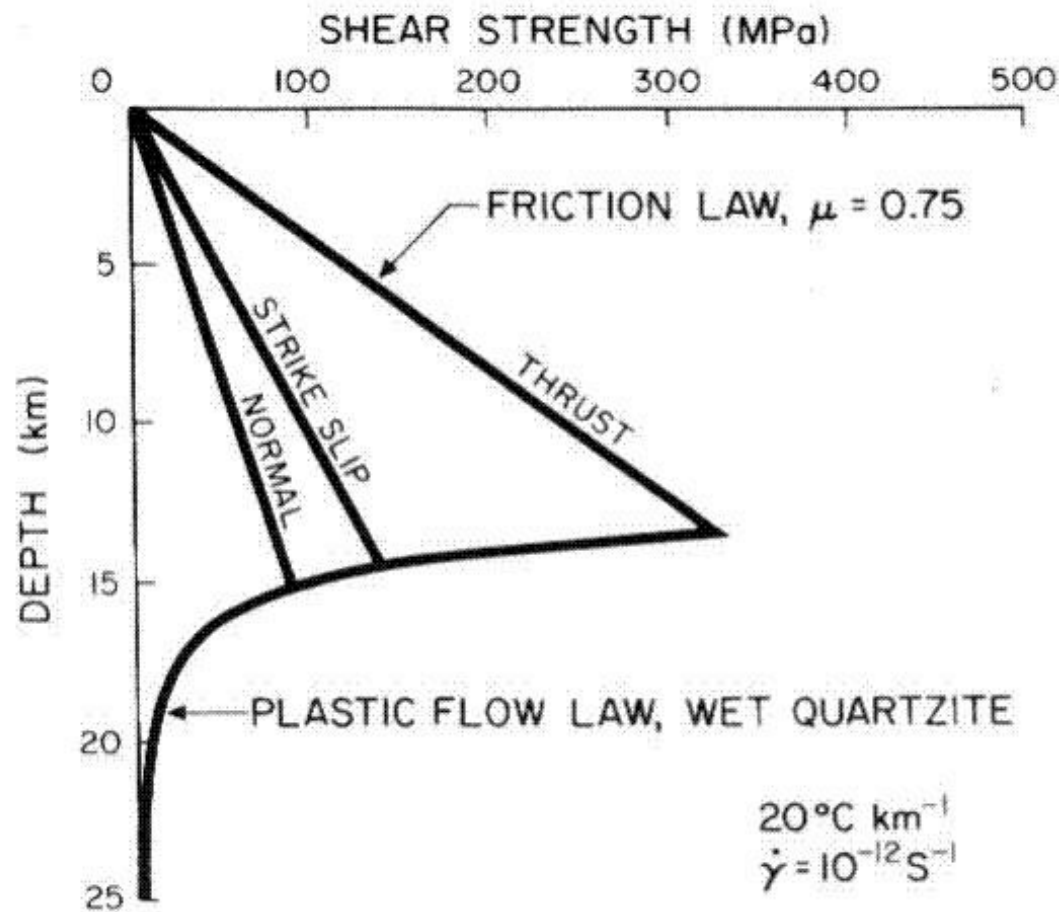


C Postfolding compression
Main twinning event

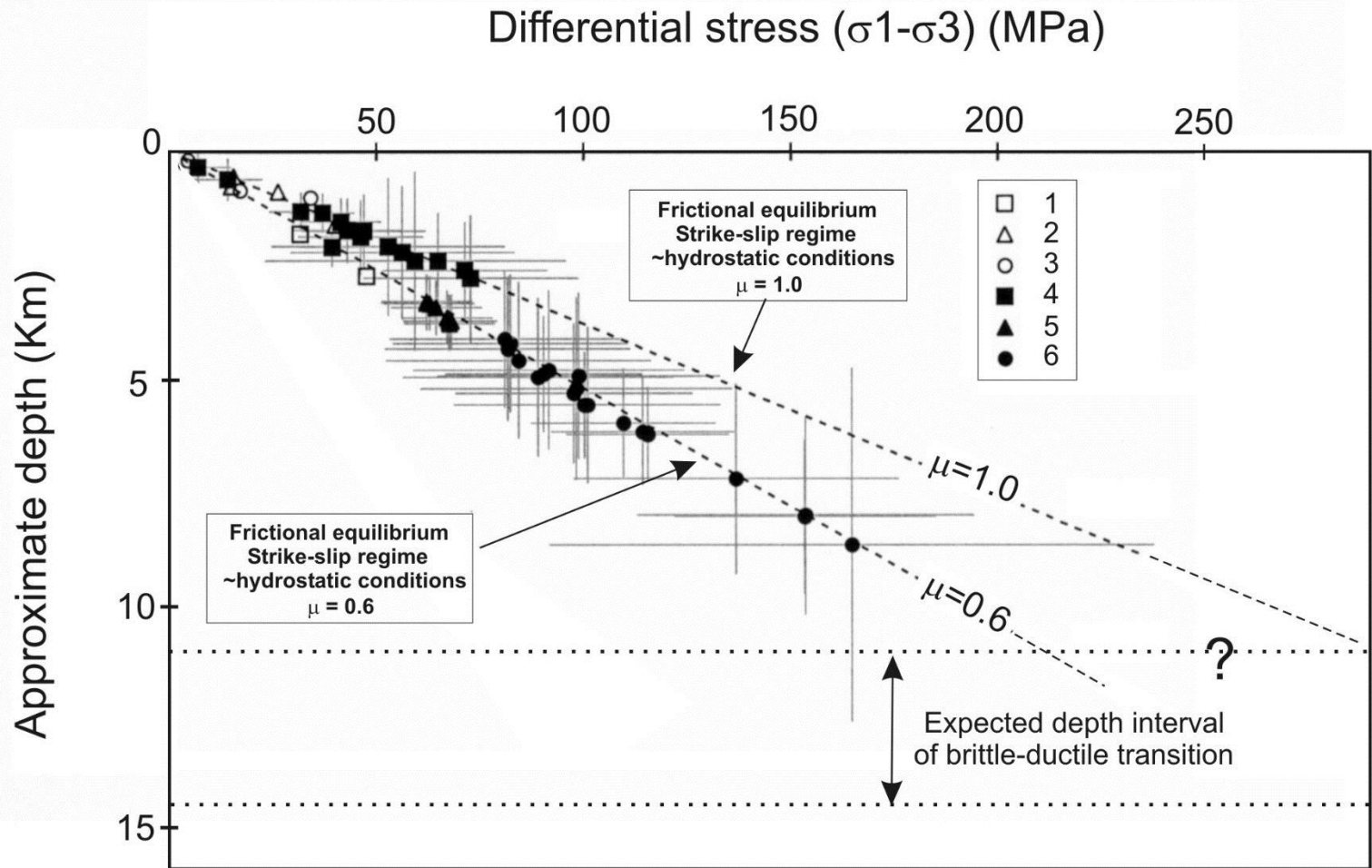


Comparison with modern stresses
in terms of patterns and physical meaning

**Comparison of paleostress magnitudes from
calcite twins with contemporary stress
magnitudes and frictional sliding criteria
in the continental crust: Mechanical implications**



Simple model of the strength of the lithosphere. In the upper part, optimally oriented faults are assumed with Coulomb friction and constant $\mu = 0.75$ and hydrostatic pore pressure. For the lower part, an experimentally determined flow law for wet quartzite (Jaoul, Tullis, and Kronenberg, 1984) has been extrapolated, assuming the strain rate and temperature gradient as indicated.



(Townend and Zoback, 2000)

Application of Coulomb faulting theory with laboratory-derived coefficients of friction (e.g., Byerlee, 1978) allows prediction of critical stress levels in reverse, strike-slip, and normal faulting environments as a function of depth and pore pressure.

The *in situ* stress data compiled by Townend and Zoback (2000) and plotted with the theoretical curves for a critically stressed crust under hydrostatic conditions show consistency with Coulomb frictional-failure theory incorporating laboratory-derived frictional coefficients, μ , of 0.6-1.0 and hydrostatic fluid pressure for a strike-slip stress regime.

The crust's brittle strength is quite high (hundreds of MPa) under conditions of hydrostatic pore pressure.

The stress/depth gradient depends explicitly on the stress configuration, i.e., normal, strike-slip or reverse stress regime.

On the difficulty of establishing a paleostress/ paleodepth relationship

Collecting data on contemporary stress and paleostress magnitudes with depth is fundamentally different.

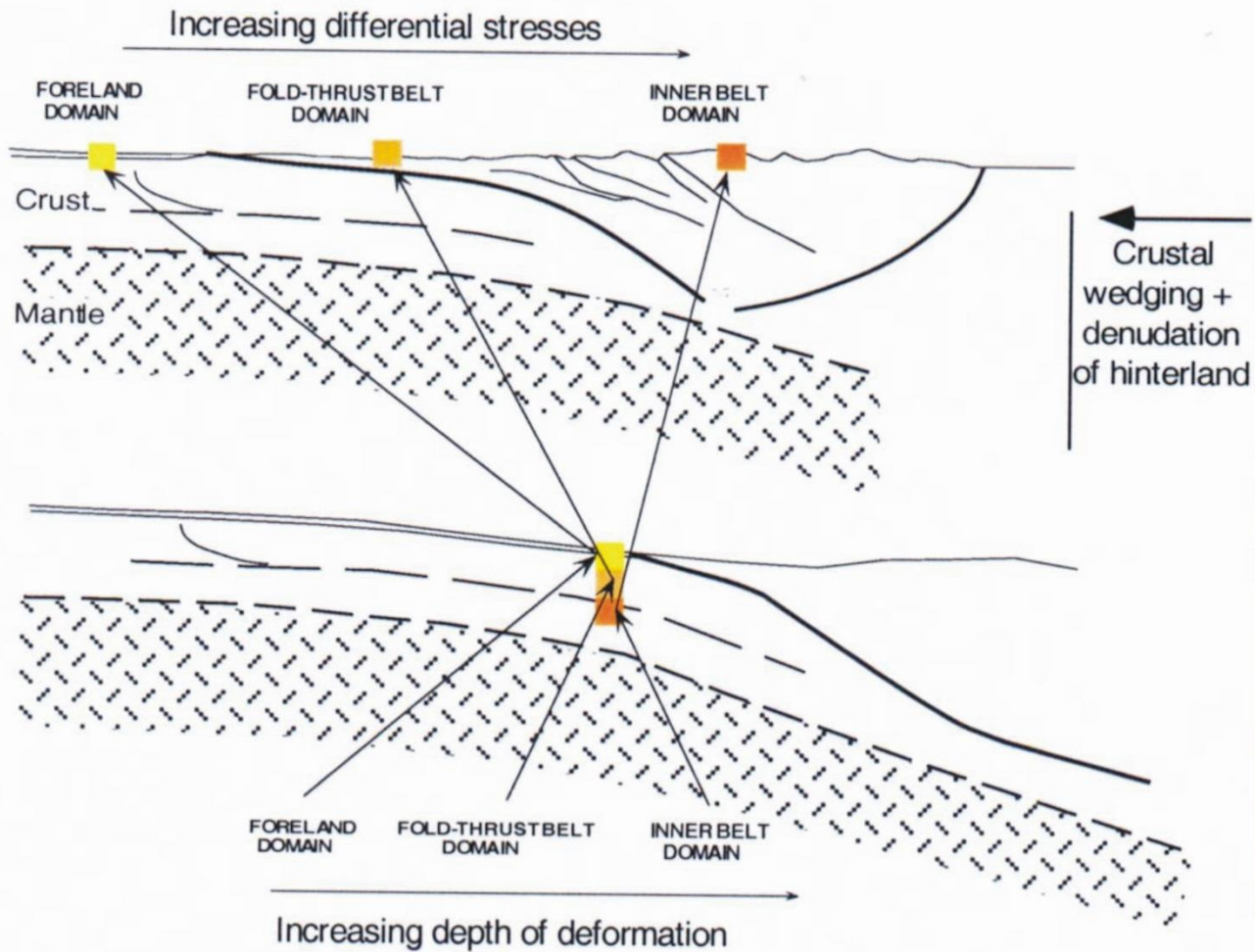
In drill holes, contemporary stresses are determined directly at a given depth, or at least in a narrow depth interval.

In contrast, paleopiezometers are generally sampled and analysed after they have reached the surface, i.e., after exhumation from an unknown depth, and establishing a differential stress versus depth relationship for paleostresses requires independent determination of differential stress and depth.

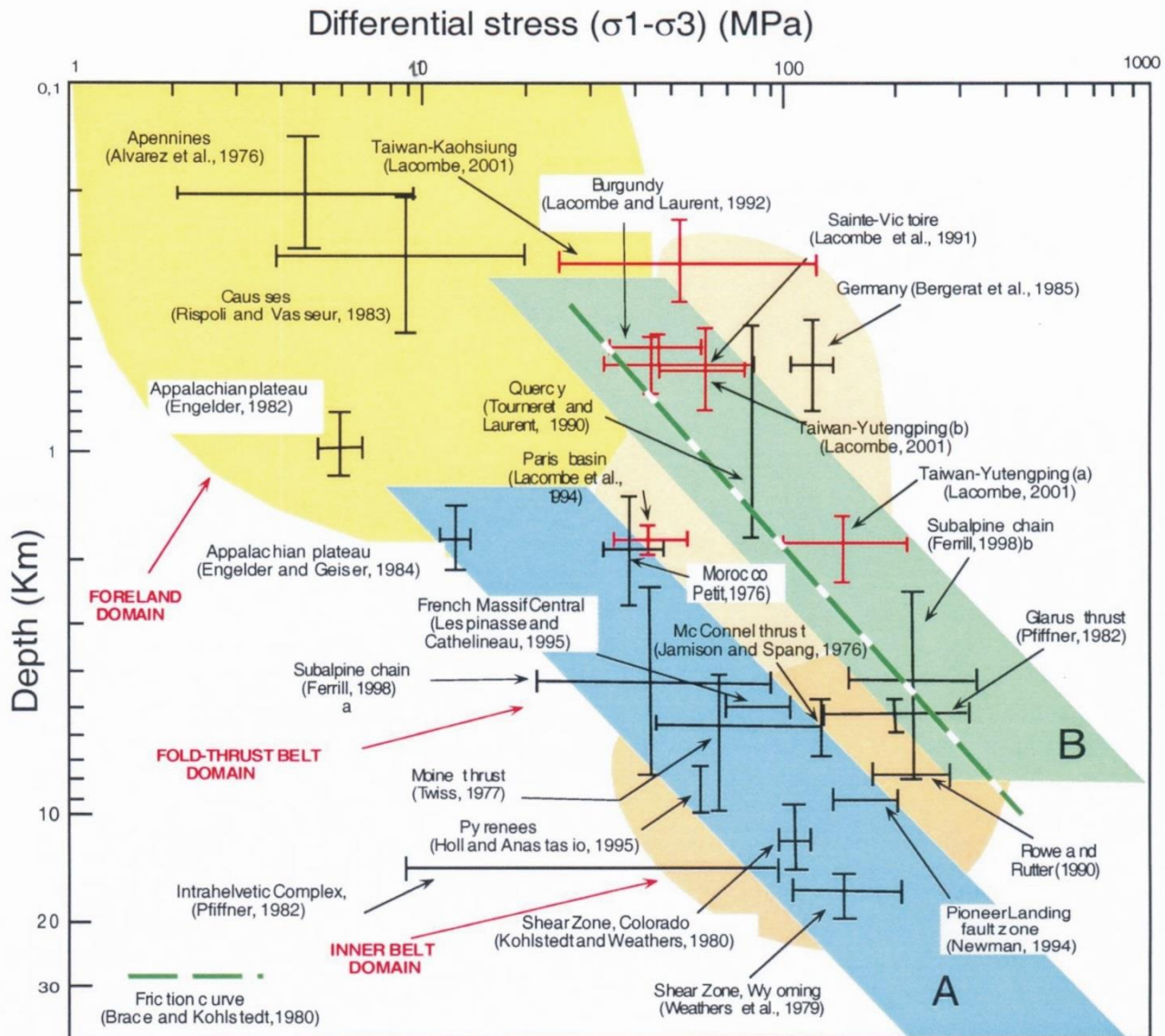
In addition, in case of polyphase tectonism, deciphering the stress/depth evolution requires to unambiguously relate a differential stress value to both a depth of deformation and a tectonic event.

Paleodepth estimates are usually derived from stratigraphic/sedimentological studies in forelands or even fold-thrust belts, from paleothermometry coupled with considerations on paleothermal gradient, recrystallisation accompanying ductile deformation or fabric development, or from metamorphism.

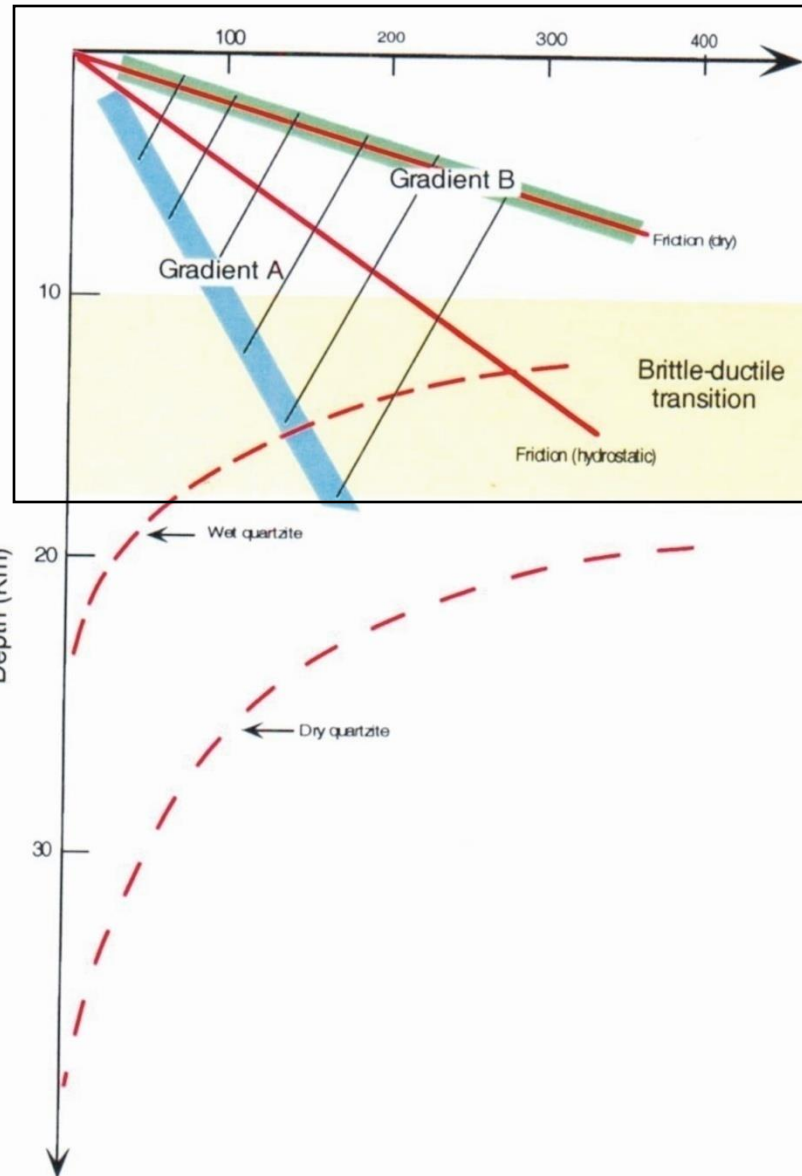
Uncertainties on the stress versus depth relationship of interest are partly due to uncertainties on depth estimates.



(Lacombe, *Tectonics*, 2001)



(Lacombe, 2001)



(Lacombe, 2001)

For a favourably oriented pre-existing cohesionless fault plane, the condition of reactivation, which therefore applies to a critically stressed crust, can be written as follows (Jaeger and Cook, 1969):

$$(\sigma_1 - P_f) / (\sigma_3 - P_f) = [(\mu^2 + 1)^{0.5} + \mu]^2$$

$$\sigma_1 - \sigma_3 = 2\rho g z (\lambda - 1) (1 - [(\mu^2 + 1)^{0.5} + \mu]^2) / (1 + [(\mu^2 + 1)^{0.5} + \mu]^2)$$

Strike-slip stress regime

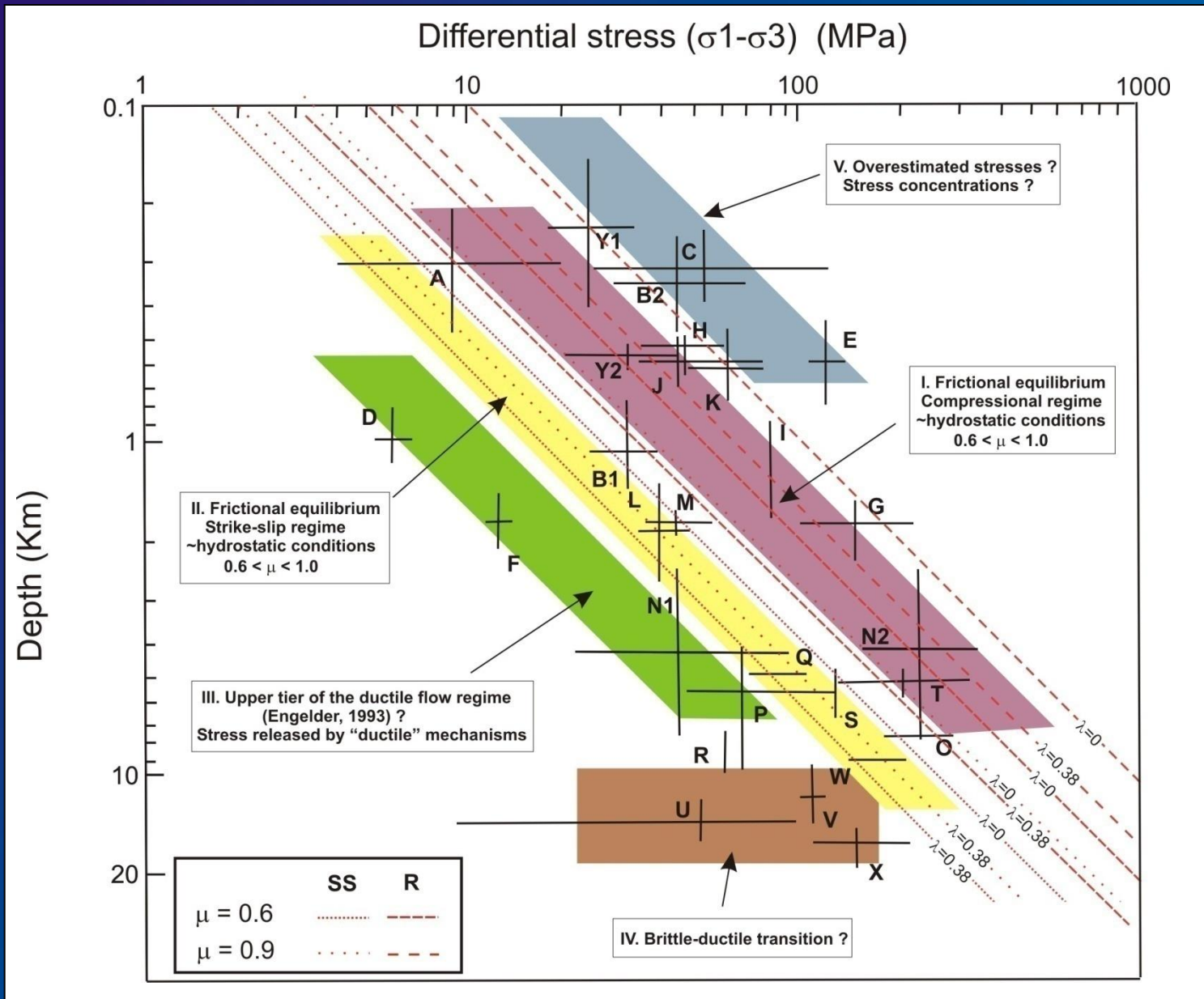
and

Reverse stress regime

$$\sigma_1 - \sigma_3 = \rho g z (\lambda - 1) (1 - [(\mu^2 + 1)^{0.5} + \mu]^2)$$

$$\text{with } \lambda = P_f / \rho g z$$

(Lacombe, 2007)



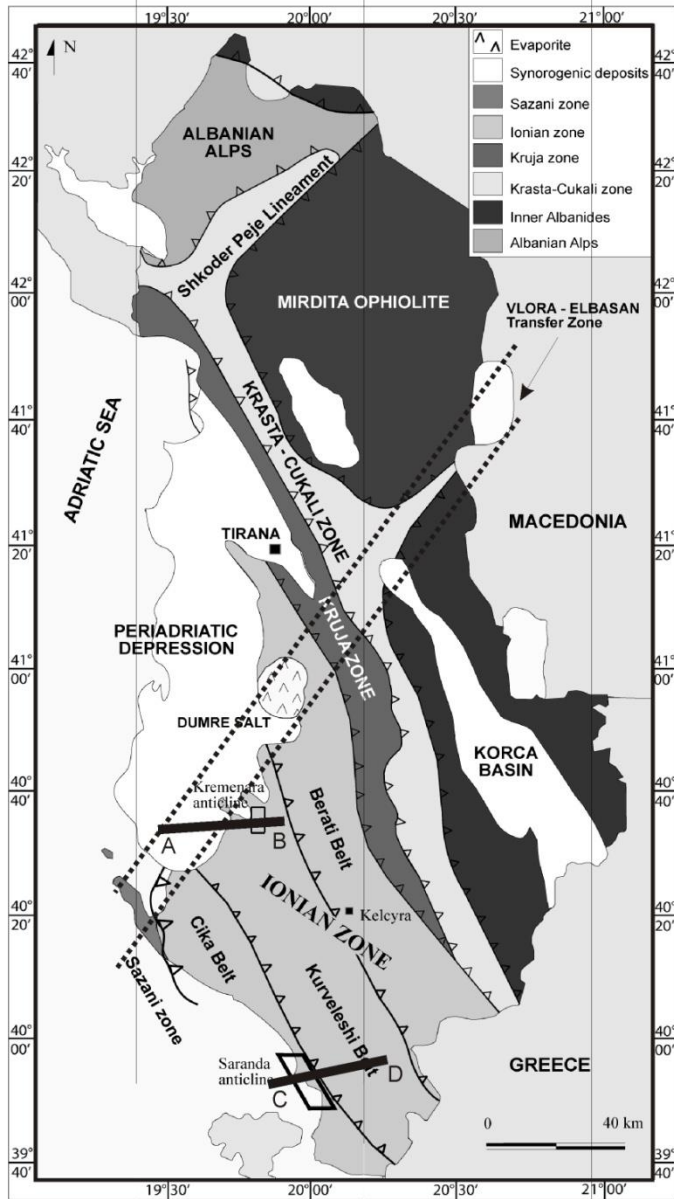
At the present-day state of our knowledge and with the available dataset, most contemporary stress and paleostress data support a first-order frictional behaviour of the upper continental crust.

The strength of the continental crust down to the brittle-ductile transition is generally controlled by frictional sliding on well-oriented pre-existing faults with frictional coefficients of 0.6-0.9 under hydrostatic fluid pressure (frictional stress equilibrium).

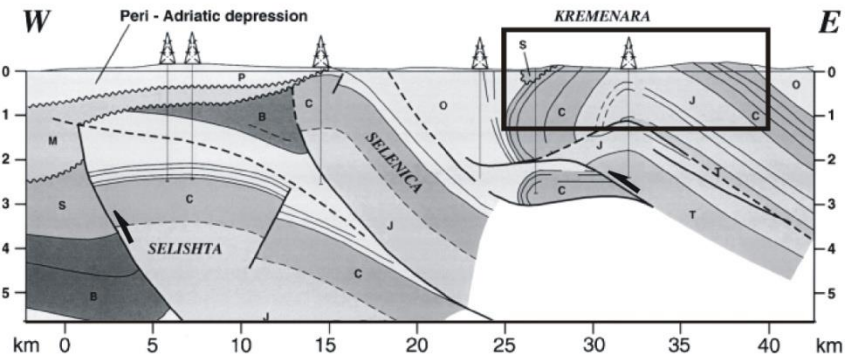
Some ductile mechanisms may, however, relieve stress and keep stress level beyond the frictional yield, as for instance in the detached cover of forelands.

The critically stressed upper continental crust is therefore able to sustain differential stresses as large as 150-200 MPa, so its strength makes it able to transmit a significant part of orogenic stresses from the plate boundary across the far foreland

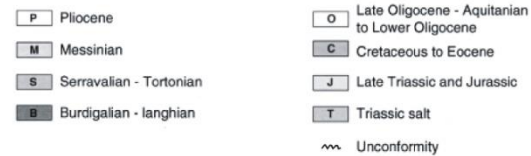
**From differential stress magnitudes to paleoburial
and exhumation path in fold-thrust belt :
The outer Albanides case**



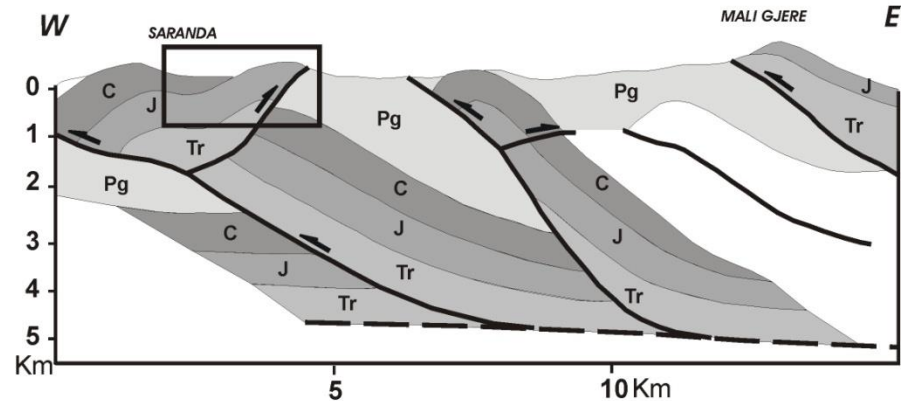
A



B



AB section

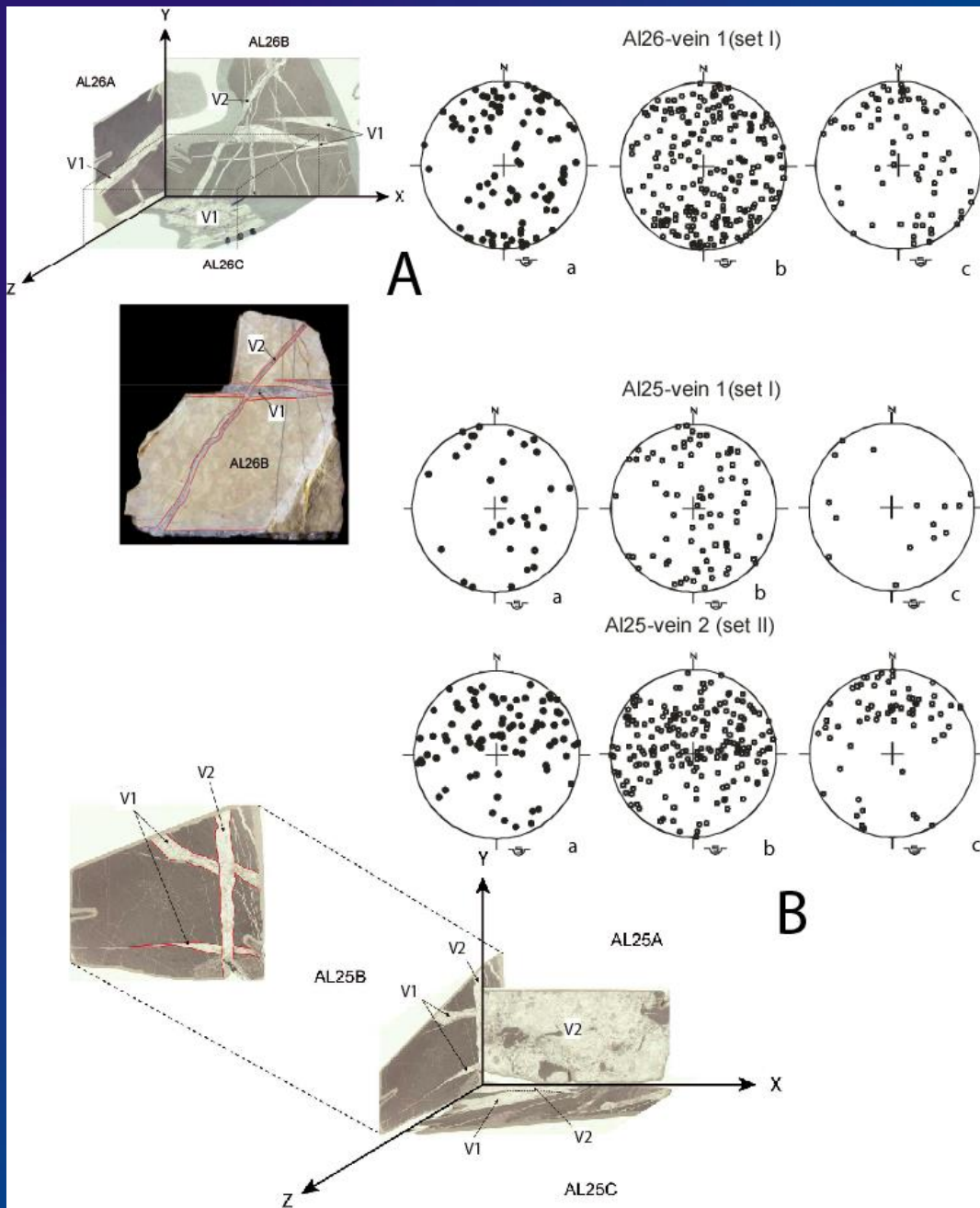


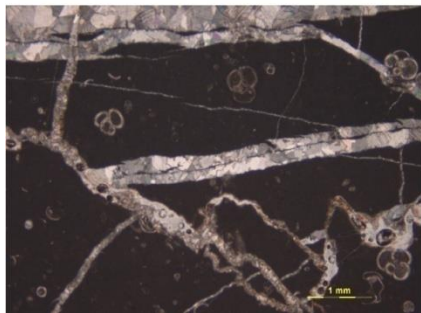
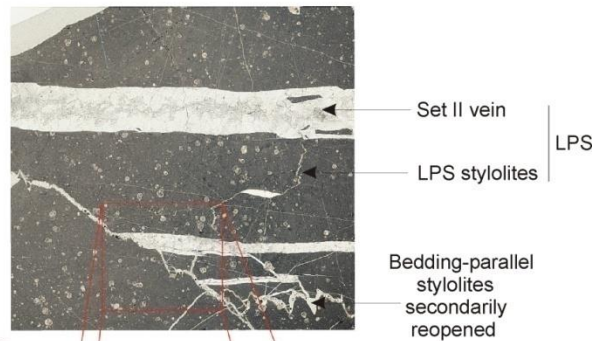
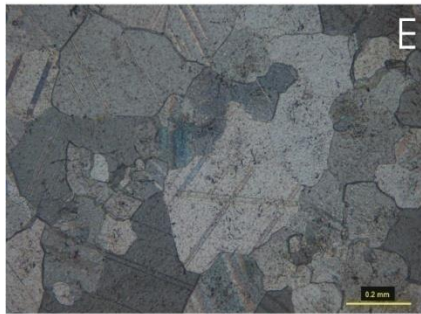
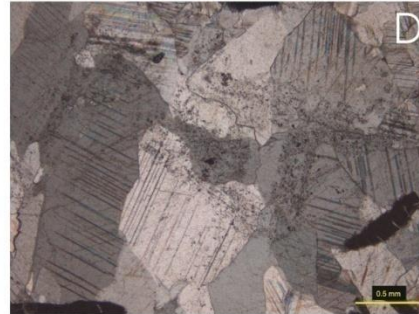
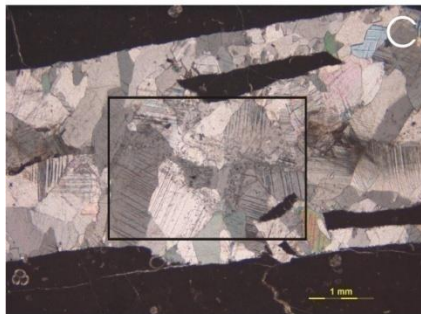
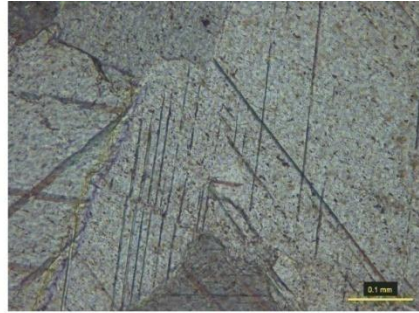
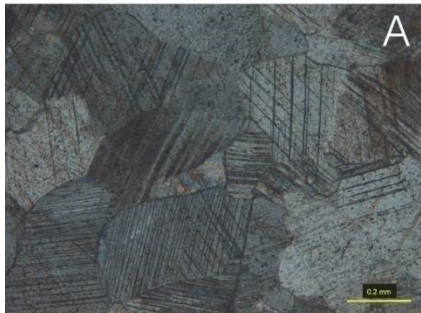
Tr, J, C : Triassic, Jurassic, Cretaceous
Pg : Paleogene

C

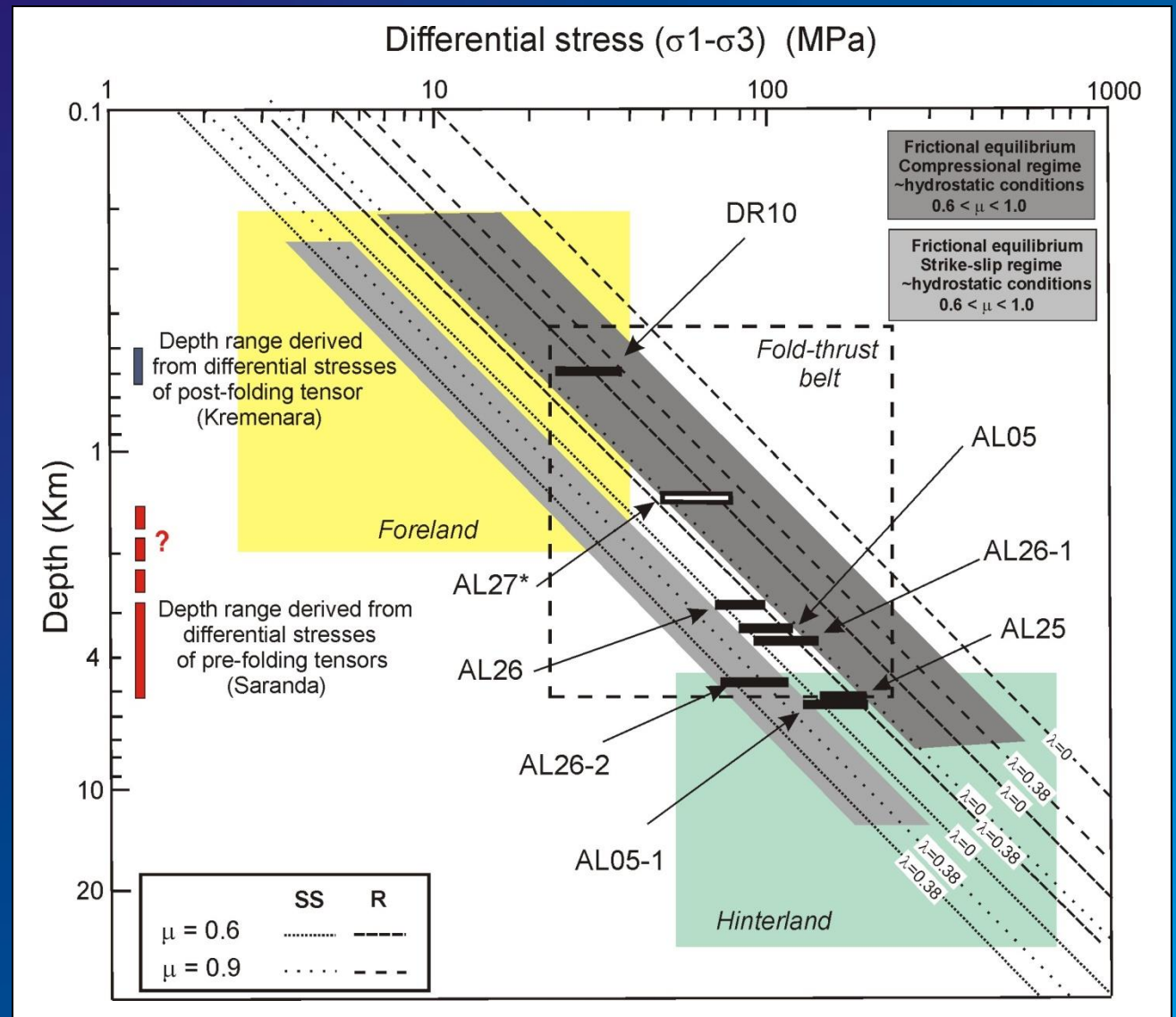
CD section

During the Alpine orogeny, the Albanian foothills formed as a consequence of the deformation of the former eastern passive margin of Apulia; the external zones were overthrust during the Neogene.

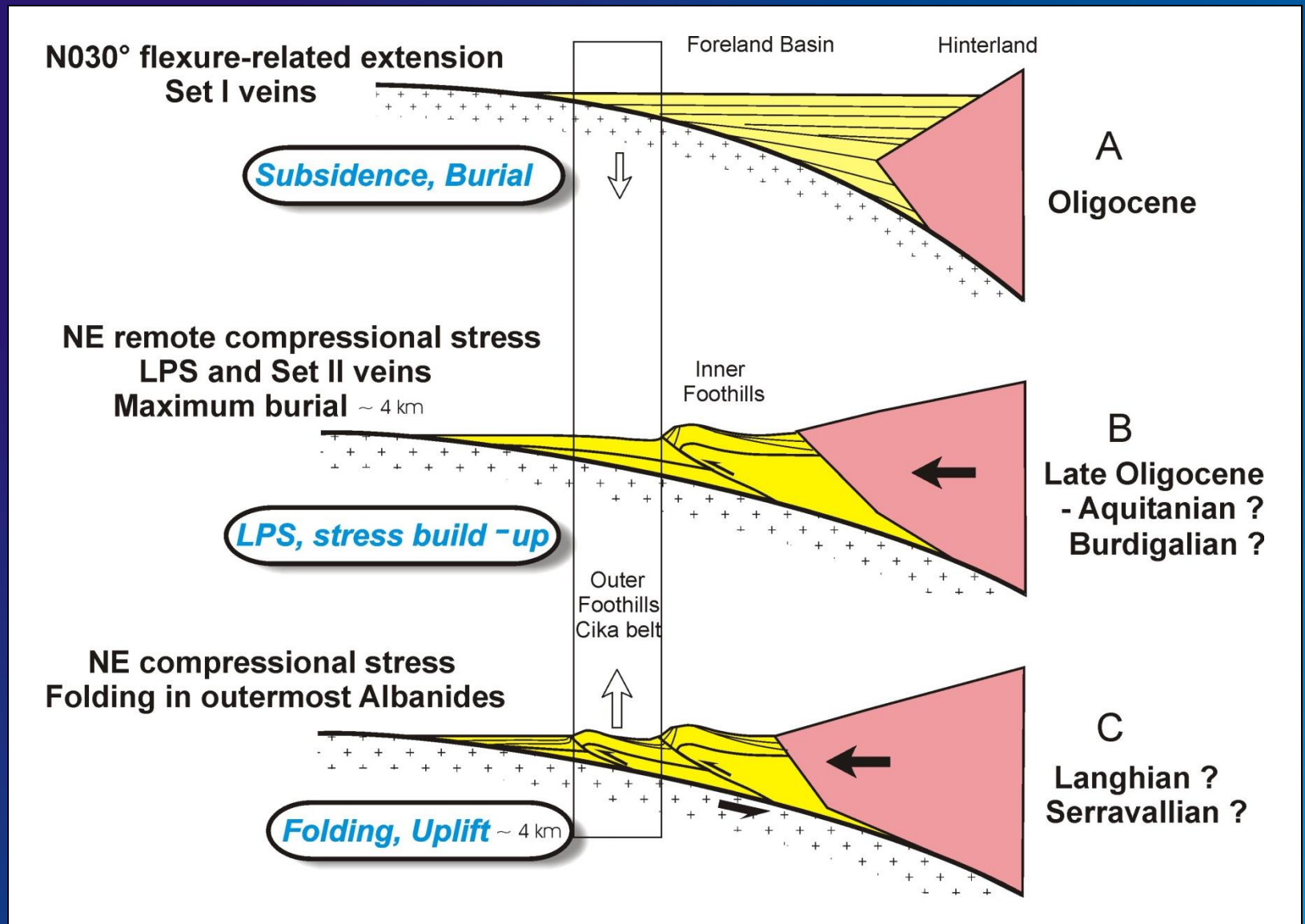




Calcite twins
 provide estimates
 of pre-folding
 paleoburial
 consistent with
 independent
 paleoburial
 estimates from
 micro-
 thermometry
 of fluid inclusions,
 maturity of organic
 matter and results
 of 1D thermal
 modeling.



(Lacombe et al., Tectonophysics, 2009)



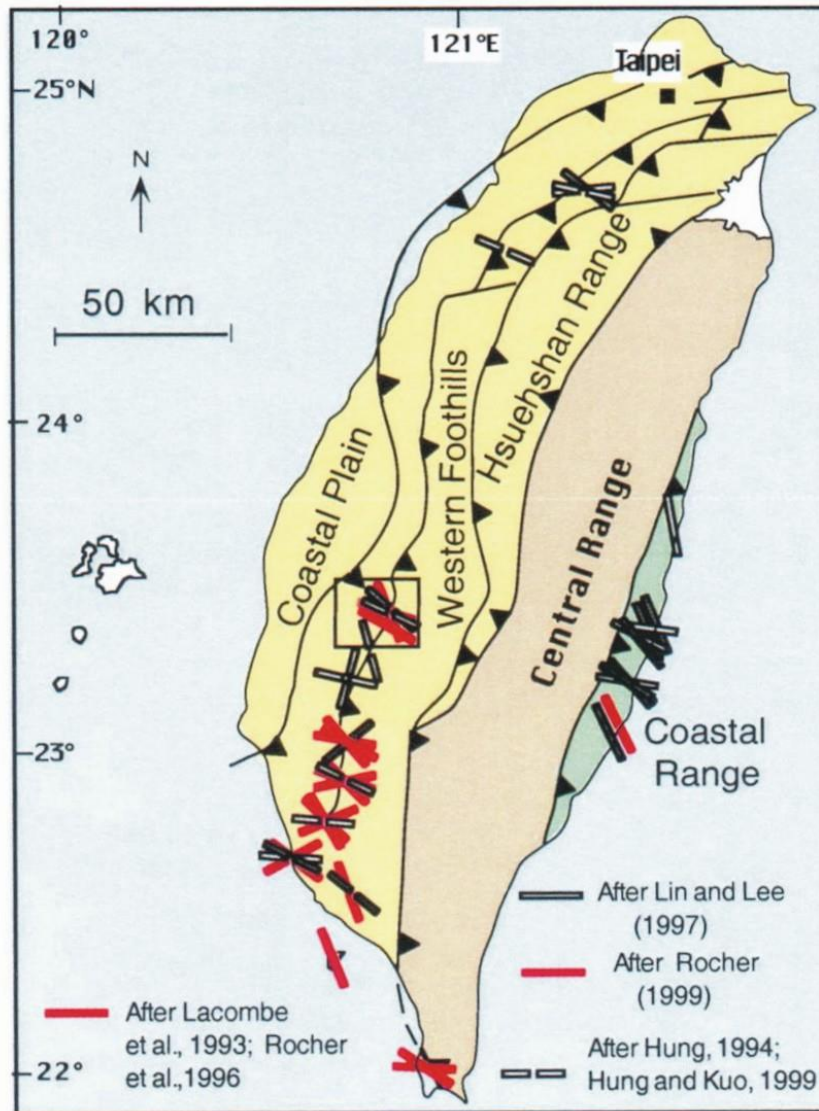
Calcite twins :
a powerful tool which may help constrain ...

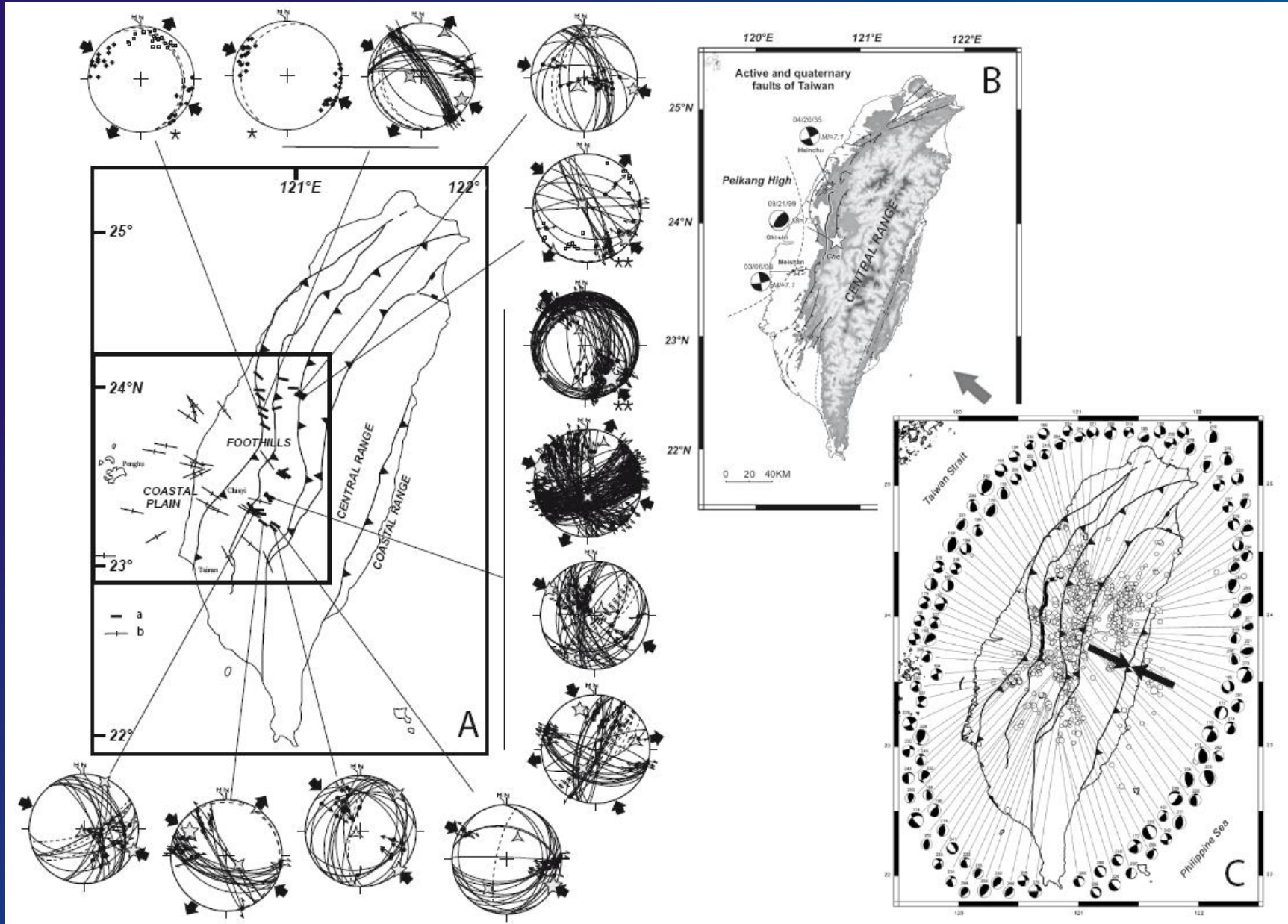
- stress orientations, regional structural/tectonic histories and geodynamic evolution;
 - values of tectonic (paleo)stress magnitudes;
 - upper crust mechanics;
- micro-mechanisms of internal deformation of carbonate rocks in folded/fractured reservoirs;
 - basin/thrust belt modelling

... among others...

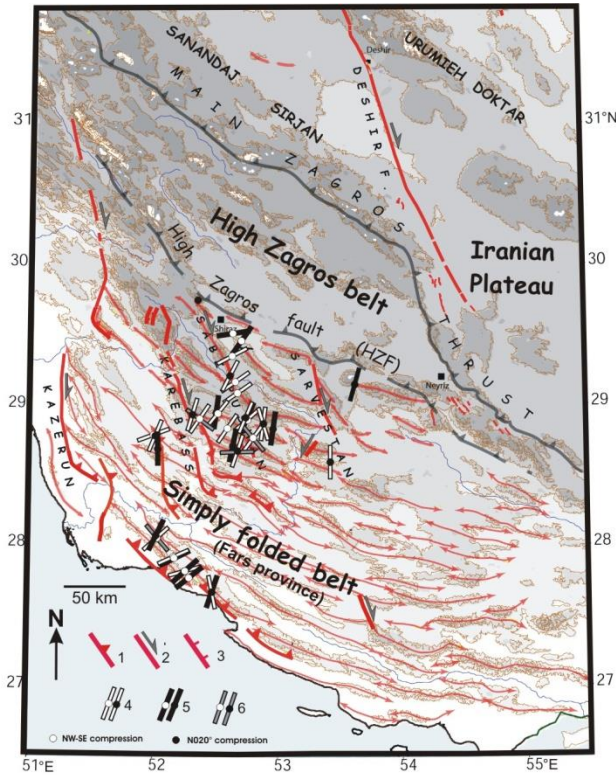
Comparison of paleostresses (from calcite twins, fault slips, ...) and contemporary stresses in terms of patterns and physical meaning

(Lacombe, 2001)

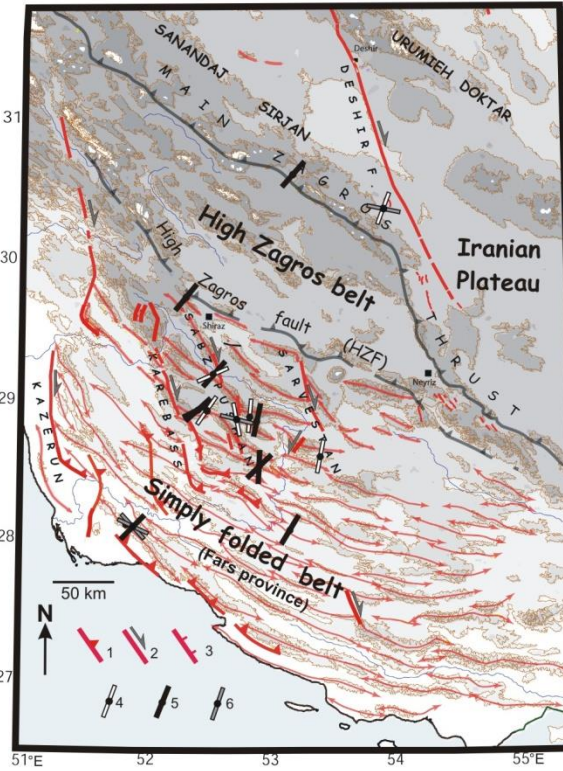




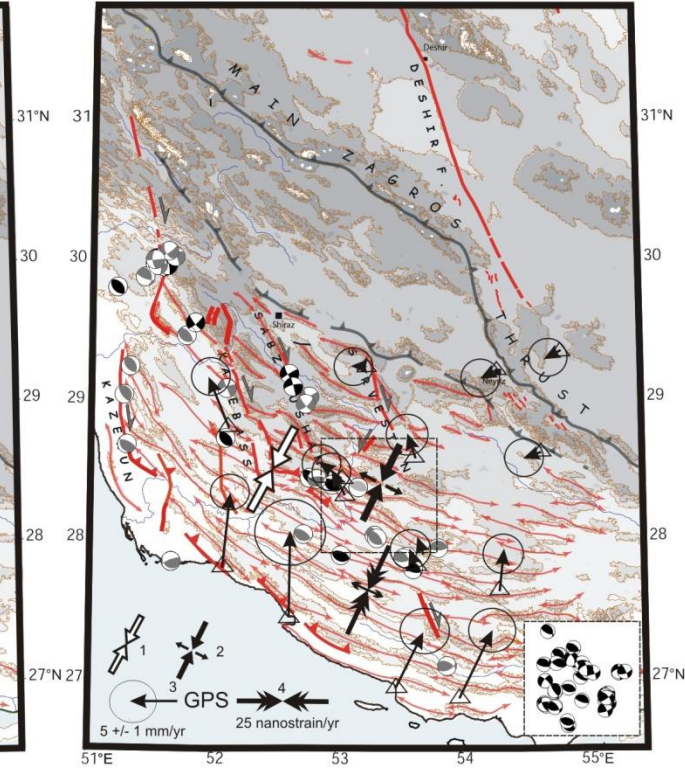
(Lacombe, 2012)



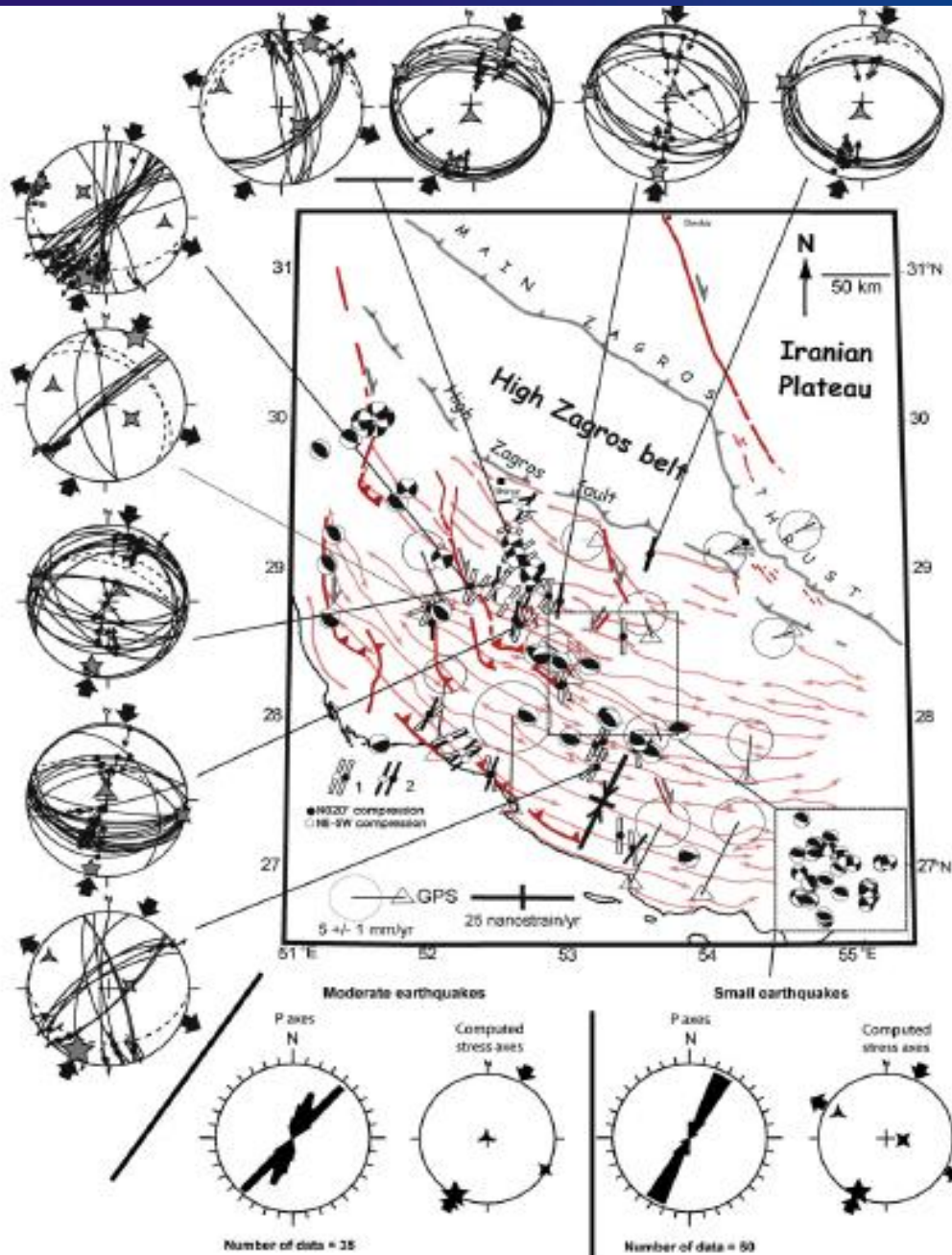
Neogene compressional trends from fault slip data in the cover (Lacombe et al., 2006)



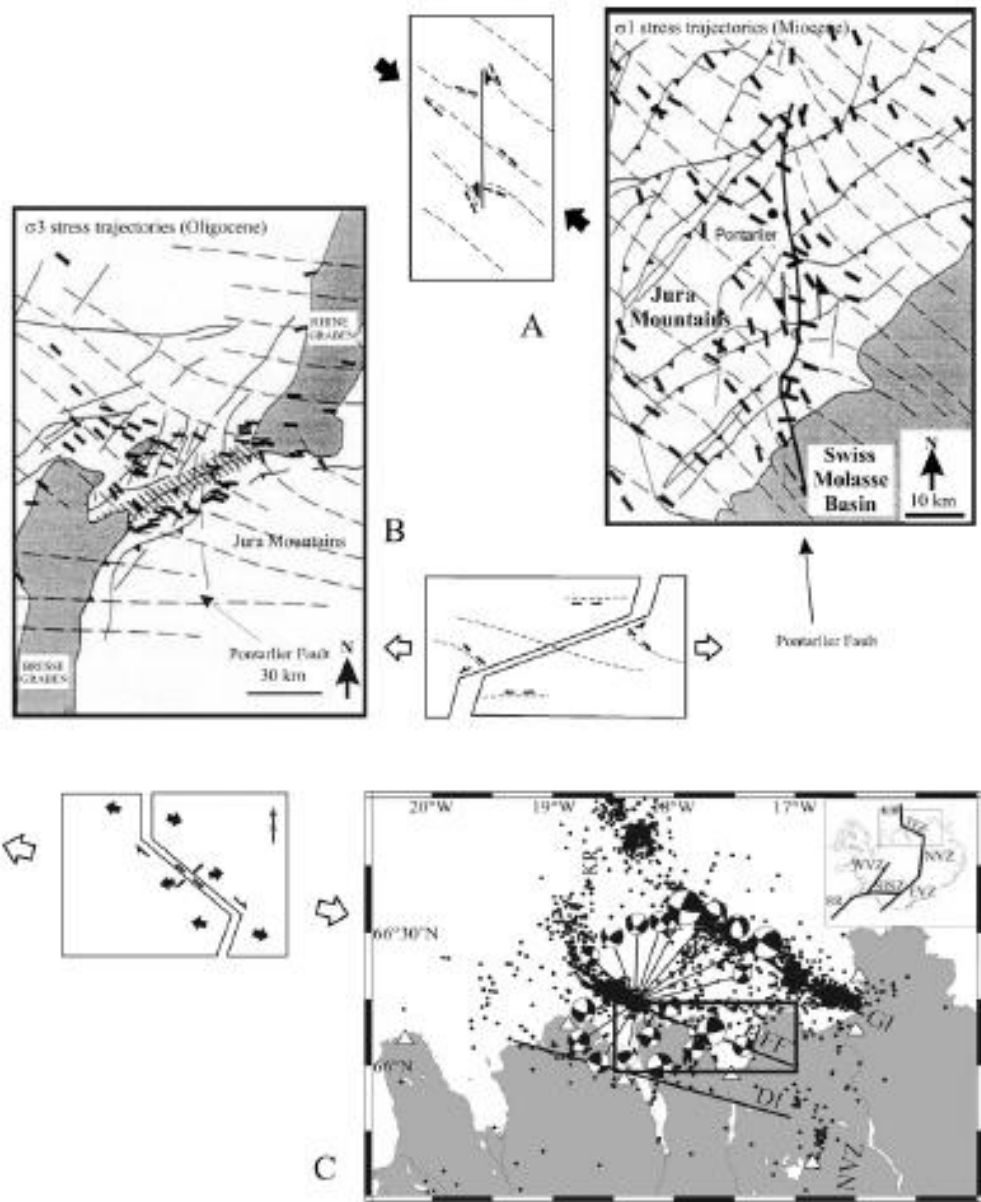
Neogene compressional trends from calcite twin data in the cover (Lacombe et al., 2007)



Current compressional trends from earthquake focal mechanisms in the basement (Lacombe et al., 2006) and GPS shortening rates (Walpersdorf et al., 2006)

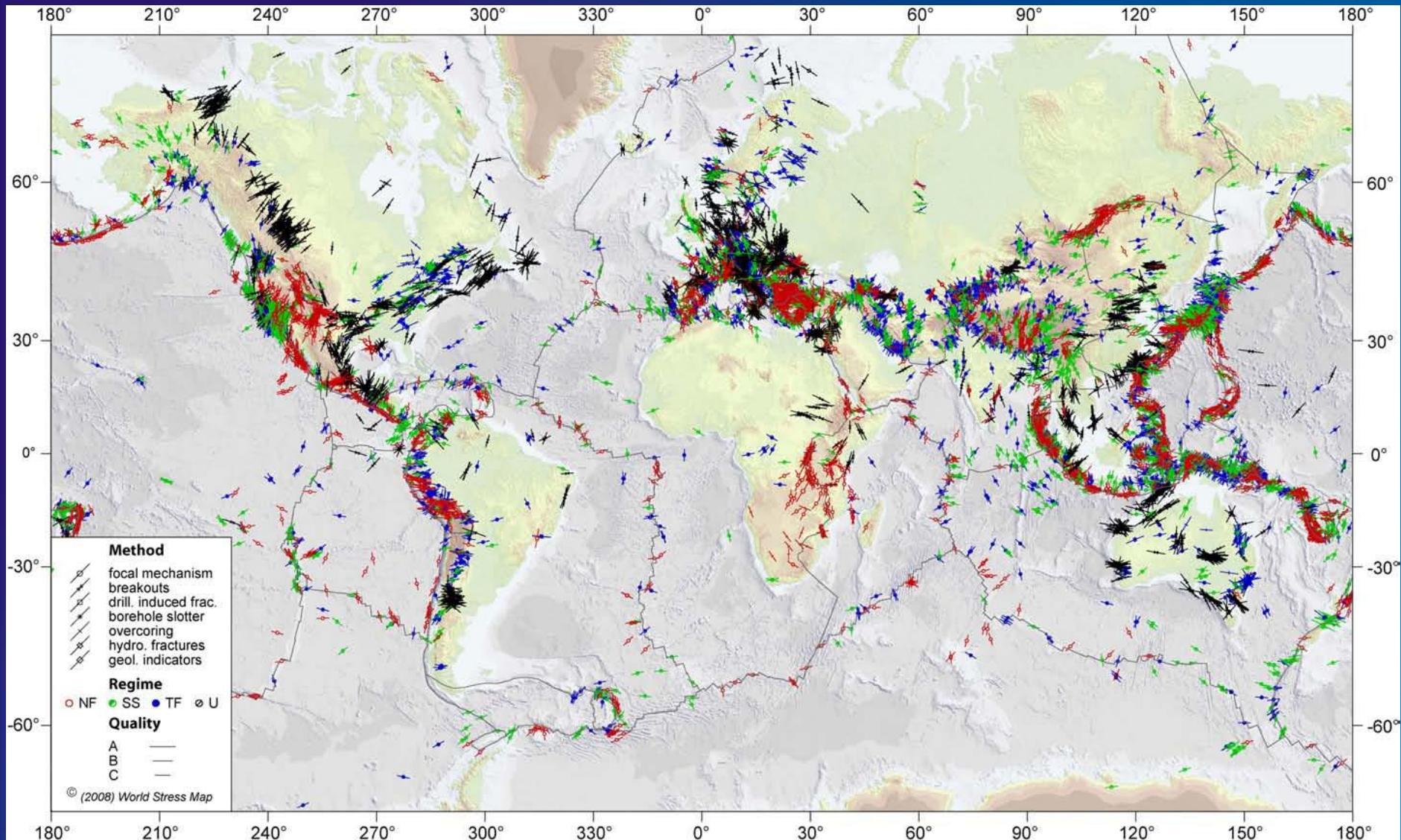


(Lacombe, 2012)



(Lacombe, 2012)

Global stress map based on the WSM database release 2008



Concepts and techniques underlying determinations of contemporary stresses and paleostresses are inherently different, and both types of stress data do not have strictly the same geological meaning.

Contemporary stresses measured *in situ* reflect local, instantaneous ambient crustal stresses, while reconstructed paleostresses reflect ancient crustal stresses at the particular time of tectonic deformation, averaged over the duration of a tectonic event and over a given rock volume.

Although to this respect contemporary stresses and paleostresses are not directly comparable, their analyses however rely on the same mechanics, and they constitute complementary stress data sets.

Paleostresses reflect stresses at the particular time of tectonic deformation, averaged over the duration of a tectonic event; both quantities can interestingly be compared in terms of patterns, at the scale of plate interiors or at more local scale.

Combination of both types of stress data provides new constraints on the differential stress gradients with depth, which are to date still poorly known.

Combining contemporary and paleostress data allows us to extend our stress/depth database in various settings, i.e., away horizontally from drill holes, and vertically by obtaining information on stress magnitudes at depth more or less continuously down to the brittle-ductile transition.

Finally, such a combination of stress data therefore brings useful information on the strength and mechanical behaviour of the upper continental crust over times scales of several tens of Ma, and should be taken into account in future modelling.

There may be more variability between different methods to infer contemporary stresses than between similar methods used to infer contemporary stresses and paleostresses in term of space.

Within contemporary stress methods, borehole or stress relief techniques are local whereas focal mechanism inversion may involve a very large volume.

Within paleostress stress methods, tension cracks or stylolites or calcite twinning are very local whereas fault slip inversion involves a volume that depends on the outcrop size.

The main issue is thus how to combine up or down scale results obtained from different methods, and this applies both to contemporary stresses and to paleostresses.

On a tectonic point of view, the similarity of stress and paleostress regimes may allow to go back into the past to determine over which time span the overall pattern of orogenic stresses has remained nearly unchanged, hence the regional tectonic regime and the plate kinematics remained more or less stable.

On a mechanical point of view, spatial and temporal stress/paleostress perturbations related to fault kinematics, when combined with mechanical modelling, may help constrain the rheological behaviour of the upper continental crust over time scales of up to tens of Ma.



Thank you for your attention...

Suggested readings :

Lacombe O. & Laurent P., 1992. Determination of principal stress magnitudes using calcite twins and rock mechanics data. **Tectonophysics**, 202, 83-93

Lacombe O. & Laurent P., 1996. Determination of deviatoric stress tensors based on inversion of calcite twin data from experimentally deformed monophase samples: preliminary results. **Tectonophysics**, 255, 189-202

Laurent P., Kern H. & Lacombe O., 2000. Determination of deviatoric stress tensors based on inversion of calcite twin data from experimentally deformed monophase samples. II : uniaxial and triaxial stress experiments. **Tectonophysics**, 327, 131-148

Lacombe O., 2001. Paleostress magnitudes associated with development of mountain belts : insights from tectonic analyses of calcite twins in the Taiwan Foothills. **Tectonics**, 20, 6, 834-849

Lacombe O., 2007, Comparison of paleostress magnitudes from calcite twins with contemporary stress magnitudes and frictional sliding criteria in the continental crust : Mechanical implications. **J. Struct. Geol.**, 29, 86-99

Lacombe O., Malandain J., Vilasi N., Amrouch K. & Roure F., 2009, From paleostresses to paleoburial in fold-thrust belts: preliminary results from calcite twin analysis in the outer Albanides. **Tectonophysics**, In “the Geology of Vertical Movements of the Lithosphere”, 475, 128-141

Lacombe O., 2010, Calcite twins, a tool for tectonic studies in thrust belts and stable orogenic forelands. **Oil and Gas Science and Technology**, 65, 6, 809-838

Lacombe O., 2012. Do fault slip data inversions actually yield ‘paleostresses’ that can be compared with contemporary stresses ? A critical discussion. **C.R. Geoscience**, 344, 159-173